Phytochemical characterization and biological activities of Stenomesson miniatum bulb extract, a medicinal plant of the Andes

Mariacaterina Lianza, Carmela Fimognari, Jean-Marc Nuzillard, Ferruccio Poli, Jean-Hugues Renault, Francesca Bonvicini, Giulia Greco, Eleonora Turrini

Phytochemical characterization and biological activities of *Stenomesson miniatum* bulb extract, a medicinal plant of the Andes.

Mariacaterina Lianza[a]*, Carmela Fimognari[a], Jean-Marc Nuzillard[b], Ferruccio Poli[c], Jean-Hugues Renault[b], Francesca Bonvicini[c], Giulia Greco[d], Eleonora Turrini[a]

[a]*Department for Life Quality Studies, University of Bologna, Rimini, Italy*

[b]*CNRS, ICMR UMR 7312, University of Reims Champagne-Ardenne, Reims, France*

[c] *Department of Pharmacy and Biotechnology, University of Bologna, Bologna, Italy*

[d] *Department of Chemistry, University of Bologna, Bologna, Italy*

*corresponding author: mariacaterina.lianz3@unibo.it

Phytochemical characterization and biological activities of *Stenomesson miniatum* bulb extract, a medicinal plant of the Andes.

Fresh bulbs of *Stenomesson miniatum*, a plant belonging to the Amaryllidaceae family with a poorly investigated phytochemical profile, were traditionally employed by Andean healers to treat tumors and abscesses. The aims of this study were to characterize the extract from the bulbs of *S. miniatum* and to test its cytotoxic and antibacterial potential. A previous structural study of the major extract constituents was extended to include the minor components by means of ^{13}C-NMR-based dereplication. Cytotoxic activities were evaluated on A431 human epidermoid carcinoma cells through a metabolic assay and on Jurkat human acute T-leukemia cells through a cell-impermeant fluorescent nuclear probe. Antibacterial assays were carried out against *Staphylococcus aureus*, *Staphylococcus epidermidis*, and *Streptococcus pyogenes* by using a standardized broth microdilution method. Eleven known Amaryllidaceae alkaloids were identified together with another compound determined as being an extraction artefact. The alkaloid-enriched extract showed good cytotoxic activity against both tumor cell lines, reaching an IC_{50} of 3.3 µg/mL against A431 cells and of 10.9 µg/mL against Jurkat cells. Biological assays carried out on single fractions showed that activity can be attributed to the presence of pretazettine and haemanthamine. Conversely, no antibacterial activities were recorded for any of the samples.

Keywords: *Stenomesson miniatum*; Amaryllidaceae alkaloids; *Urceolina peruviana*; ^{13}C-NMR-based dereplication; A431 human epidermoid carcinoma; Jurkat cells; artefact; Andean traditional medicine

1. Introduction

1.1 Stenomesson miniatum and the Amaryllidaceae alkaloids in Andean traditional medicine

The use of plants belonging to the Amaryllidaceae family is fairly widespread in the traditional medicines of the areas where these species are prominent, such as the

Mediterranean basin, South Africa, and Andean South America (Nair and van Staden 2013). The principal bioactive compounds produced by these plants are isoquinoline alkaloids, peculiar to the species of the subfamily Amaryllidoideae (Bastida et al. 2006). The Amaryllidaceae alkaloids were proved to be responsible for most of the medicinal properties exhibited by these plants, since they are endowed with several types of biological activities, including cytotoxic (Lianza et al. 2020), anticholinesterase (Ee et al. 2004), antiviral (Chen et al. 2020), and antibacterial activities (Nair et al. 2017). The genus *Stenomesson*, native to the Andean regions of South America, has been used for medicinal purposes since pre-Columbian times by the Incas and later by other indigenous populations (Bastien 1982; Lévi-Strauss 1952; Nair 2019) . However, many species of this genus remain unstudied in terms of their chemical and biological features. *Stenomesson miniatum* (Herb.) Ravenna is one of these. It was initially classified as belonging to the genus *Urceolina*, due to the urceolate appearance of the corolla and the ventricose perianth (Meerow 1985), for this reason it is widely known as *Urceolina peruviana* (C.Presl) J.F.Macbr. which is a synonym for this species (https://wfoplantlist.org/plant-list/ accessed on March 2023). *S. miniatum* is a bulbous perennial plant, which grows spontaneously in the Andean regions of Bolivia and Peru above 2,000 m and up to 3,500 m a.s.l. (Meerow et al. 2015). The itinerant healers of the Andes, named Kallawaya, employed the bulbs of *S. miniatum* to treat tumors and abscesses, administering an ointment for topical use made from fresh grated bulbs and llama or pig fat (Girault 2018). To the best of our knowledge, only one paper was published regarding the phytochemical characterization of *S. miniatum* bulbs. In 1957, Boit and Döpke analyzed the alkaloid composition of three-year old bulbs grown in Holland; they reported the identification of tazettine, haemanthamine, and lycorine, and two other alkaloids corresponding to the chemical structures of albomaculine and

67 nerinine (Boit and Döpke 1957). Hence, a more detailed characterization of this species
68 is presented in this study.

69 ***1.2 Dereplication approach for phytochemical characterization***

70 Obtaining pure compounds from a plant extract is difficult, time-consuming, and costly
71 due to the wide range of required experimental techniques. Hence, in recent years,
72 natural product chemists have accelerated drug discovery processes through the
73 development of dereplication approaches (Gaudêncio and Pereira 2015). The term
74 dereplication refers to a process of quick identification of known chemotypes (Hubert et
75 al. 2017), avoiding, at least in part, purification processes, thus reducing times, costs
76 and the generation of hazardous pollutants. Alkaloids from Amaryllidaceae plants have
77 been intensively studied in the last few decades and, to date, more than 600 compounds
78 have been isolated (Knolker 2020). Hence, Amaryllidoideae species are well suited for
79 this type of approach. Our method relied on the idea that dereplication of natural
80 products is best achieved by collecting taxonomic, structural, and spectroscopic data
81 altogether in a database. Unfortunately, such free databases do not exist. Our previous
82 publication explained the features and the construction of databases starting from the
83 KNApSAcK website, the Universal Natural Product Database (UNPD), and
84 COCONUT taking some of the alkaloids of *S. miniatum* as examples (Lianza et al.
85 2021). The complete characterization of the bulb extract is presented in this article. The
86 use of ^{13}C NMR spectroscopy as tool for dereplication brought up an issue concerning
87 the scarcity of freely available reference experimental spectroscopic data, a problem
88 solved by means of prediction software (e.g. ACD/Labs software). Tools that rely on
89 the matching of experimental data with predicted ones depend on the reproducibility of
90 the former. The NMR spectra of part of the identified alkaloids were recorded in
91 hexadeuterated dimethylsulfoxide (DMSO-d_6) and deuterated chloroform ($CDCl_3$) for

chemical shift comparison. Considering the interesting ethnobotanical usage and the poor phytochemical knowledge of this species, the aims of this study were to characterize the alkaloid-enriched bulb extract of *S. miniatum* and to determine if its medicinal properties could be ascribed to the presence of Amaryllidaceae alkaloids. The topical use of the ointment prepared by indigenous healers from fresh bulbs suggested a possible action against skin tumors and bacteria causing skin infections. Hence, cytotoxic activities against A431 human epidermoid carcinoma and, subsequently, against an in vitro model of a hematological tumor, i.e. Jurkat leukemia cells, as well as antibacterial activity against *Staphylococcus aureus*, *Staphylococcus epidermidis*, and *Streptococcus pyogenes* were assessed.

2. Materials and Methods

2.1 Plant material

Fresh bulbs of *S. miniatum* (Herb.) Ravenna (1090.3 g) were purchased in August 2019 at the plant nursery Quatro Estaciones in Cochabamba (Bolivia). For further verification some bulbs were grown, and the flowering plants were identified by Dr. Umberto Mossetti (Botanical Garden of the University of Bologna). A voucher specimen of these plants (BOLO0602041) is deposited in the Herbarium of the University of Bologna. The plant name was checked with http://www.worldfloraonline.org/ accessed in April 2022, which provides more up-to-date information than http://www.theplantlist.org/.

2.2 Chemicals

Acetonitrile (CH_3CN), methyl-tert-butyl ether (MtBE), triethylamine (TEA), methanol (MeOH), sulfuric acid (H_2SO_4), ethyl acetate (EtOAc) and chloroform ($CHCl_3$) were purchased from Carlo Erba Reactifs SDS (Val de Reuil, France). DMSO-d_6 and $CDCl_3$ were purchased from Eurisotop (Saclay, France).

2.3 Dereplication approach

The dereplication approach applied in this study was composed by several steps including different techniques. The crude extract was cleared from non-alkaloid compounds by acid-base liquid-liquid partition. The pre-purified extract was fractionated by Centrifugal Partition Chromatography (CPC) to obtain chemically simplified fractions which were analyzed by Ultra Performance Liquid Chromatography coupled with High Resolution Mass Spectrometry (UPLC-HRMS) and by 1D and 2D NMR spectroscopy. The matching between the ^{13}C NMR data and the molecular formula of the compound under investigation with those stored in databases (*e.g.* KnapsackSearch, CSEARCH) allowed the rapid identification of already reported alkaloids. The chemical structures were validated by the analysis of the NMR spectra.

2.3.1 Preparation of the alkaloid-enriched extract

The alkaloid-enriched extract was prepared according to the protocol proposed by Renault et al. (2009) with slight modifications. The freeze-dried crushed bulbs (220 g) were moistened with NH_4OH 2.5 M and macerated in 4 L of EtOAc for three days. The extractive solution was collected by lixiviation and a further 4 L of EtOAc were added for maceration for other two days, then the solution was concentrated to 1 L. Solid-liquid extraction by EtOAc instead of CH_2Cl_2 was chosen to avoid the known reaction of the latter with tertiary amine with halogenated solvents (Maltese et al. 2009). The EtOAc solution was extracted with 0.2 L (x3) and 0.1 L (x3) of H_2SO_4 0.6 M, the aqueous phase was basified with NH_4OH 7.5 M until pH 10 and extracted with 0.2 L (x3) and 0.1 L (x3) of $CHCl_3$. Finally, the organic phase was washed with water until pH 7 and the solvent evaporated under reduced pressure to leave 2.7 g of alkaloid extract.

142

143 ***2.3.2 Centrifugal Partition Chromatography***

144 Centrifugal partition chromatography (CPC) was carried out on 1 g of the bulb extract
145 as reported by Lianza et al. (2021) obtaining thirteen fractions (A1-A13), whose masses
146 and extraction yields are reported in Table S1 of Supplementary Information 2 (SI2).
147 Fraction 12 was further fractionated using a device adapted to its low mass (99.0 mg),
148 i.e. a FCPC-A200 column with 202 mL inner volume (Kromaton Technology, Angers,
149 France). The column was composed of 21 circular partition disks, each engraved with
150 40 twin-cells of 0.24 mL. The liquid phases were pumped by a preparative 1800 V7115
151 pump (Knauer, Berlin, Germany) and the sub-fractions collected by a Labocol Vario
152 4000 (Labomatic Instruments, All-schwil, Switzerland). The biphasic solvent system
153 was the same as the one used for extract fractionation, i.e. MtBE: CH_3CN: H_2O (5:2:3,
154 v/v/v). The concentration of the retainer (1.5 mM H_2SO_4), and of the displacer (2 mM
155 TEA), were adapted to the small sample mass.

156 ***2.3.3 UPLC-HRMS***

157 The Ultra Performance Liquid Chromatography coupled with High Resolution Mass
158 Spectrometry (UPLC-HRMS) analyses were performed as already reported by Lianza et
159 al. (2021).

160 ***2.3.4 NMR***

161 NMR analyses for spectra recording in DMSO-d_6 were performed according to Lianza
162 et al. (2021). For the analysis in $CDCl_3$, the central resonance (triplet) was set at δC
163 77.16 for ^{13}C NMR spectrum referencing and at δH 7.26 for ^{1}H NMR spectrum
164 referencing.

165 ***2.4 Cytotoxic activity***

166

2.4.1 Cell cultures

Authenticated A431 human epidermoid carcinoma cells and Jurkat cells (both provided by LGC Standards, Teddigton, Middlesex, UK) were propagated in RPMI 1640 medium supplemented with 10% heat-inactivated fetal bovine serum (FBS), 1% L-glutamine, and 1% penicillin/streptomycin solution (all purchased by Euroclone, Pero, Italy). Cells were grown at 37°C in a humidified incubator with 5% CO_2.

2.4.2 Cell viability assays

The alkaloid-enriched extract and its fractions (A2, A4, A6, A7, A8, A9, A10, A11, A12, and A13) were dissolved in DMSO at a final concentration of 50 mg/mL. Cells were treated with increasing concentrations of extract or its fractions (0.005 – 0.500 mg/mL) for 24, 48 and 72 h. The analysis of cell viability was performed using two different tests: the cell-impermeant fluorescent nuclear probe SytoxTM green (Thermo Fisher Scientific, Waltham, MA, USA) for the suspended Jurkat cells and a metabolic assay, using 4-methylumbelliferyl heptanoate (MUH, Merck, Darmstadt, Germany), for the adherent A431 cells. Fluorescence was measured with a Guava EasyCyte 6-2L flow cytometer (Merck) or Victor X3 microplate reader (Perkin Elmer, Walthman, MA, USA), respectively. The half maximal inhibitory concentration (IC_{50}) was calculated and normalized to the effect of the added DMSO. IC_{50} was calculated by interpolation from a dose-response curve [non-linear regression, log(inhibitor) vs normalized response].

2.4.3 Statistical analysis

Results are shown as means ± SEM of at least two different experiments. Significant differences among treatments were assessed by two-way analysis of variance (ANO-VA), using Dunnett as post-hoc test. GraphPad Prism 6 (Inc. La Jolla, CA, USA) was used for the statistical analysis and $p < 0.05$ was considered significant.

2.5 Antibacterial activity

2.5.1 Preparation of extract and fractions for antibacterial activity

For microbiological assays, the extracts were solubilized in DMSO at 20 mg/mL to obtain stock solutions, which were stored at 4°C until use.

2.5.2 Bacterial strains and antibacterial assay

Staphylococcus aureus ATCC 25293, *Staphylococcus epidermidis* (ATCC 12228), and *Streptococcus pyogenes* (ATCC 19615) were selected as representative strains to test the antibacterial properties of plant extracts by using a standardized microdilution broth method in a 96-well plate (Mandrone et al. 2019) according to the guidelines established by several international committees (Clinical and Laboratory Standards Institute, European Committee on Antimicrobial susceptibility testing). Bacterial strains were routinely cultured in 5% blood agar at 37°C. For experiments, the bacterial suspensions were prepared in PBS (phosphate buffer saline), adjusted at 0.5 McFarland, corresponding to 10^8 colony forming units (CFU)/mL, and subsequently diluted 1:200 in Brain Heart Infusion Broth (Sigma-Aldrich); they were incubated with the extract and its fractions at 200 µg/mL. A few wells were reserved in each microplate for negative (no inoculum added) and positive growth controls. The microplate was incubated at 37 °C and bacterial growth was monitored by measuring the optical density at 630 nm (Multiskan Ascent microplate reader, Thermo Fisher Scientific Inc., Waltham, USA). Percentage values of bacterial growth were determined relative to the positive control.

3. Results and Discussion

3.1 Phytochemical characterization by dereplication of S. miniatum bulb extract

Phytochemical characterization was conducted on chemically simplified fractions of the alkaloid-enriched extract, obtained from Centrifugal Partition Chromatography (CPC), by matching their ^{13}C NMR spectra and molecular formula with those found in databases (*e.g.* KnapsackSearch, CSEARCH), and validating the chemical structures by the analysis of ^{1}H NMR and 2D NMR spectra. The 2D NOESY spectra and the measurement of ^{1}H-^{1}H coupling constants provided data for the assessment of relative configurations of asymmetric centres and the tentative discrimination of inequivalent hydrogen atoms in methylene groups. Thirteen alkaloids (including two epimers) were identified (Figure 1), twelve of them being already known (compounds 1-10, 11A, 11B).

CPC in pH-zone refining mode is a chromatographic separation technique which allows the purification of compounds whose electric charge depends on pH, as in the case of alkaloids. The use of an acid retainer (*e.g.* H_2SO_4) in the aqueous stationary phase and a basic displacer (*e.g.* TEA) in the organic mobile phase enables the separation of the alkaloids by contiguous blocks arranged according their pK_a and partition coefficients (Renault et al. 1999). Collecting fractions in the centre of the blocks leads to the recovery of high-purity fractions (Kotland et al. 2016). A CPC run yielded i) purified alkaloids in fraction A4, A7 and A9, ii) highly chemically simplified fractions (*i.e.* mainly enriched in one alkaloid) A3, A5, and iii) mixtures in fractions A2, A6, A8, A10, A11, A12 and A13. Our previous publication (Lianza et al., 2021) reported the extraction, fractionation, and the detailed structure elucidation of compounds **1—3** namely tazettine, albomaculine and haemanthamine, isolated at a high purity level. Lianza et al. (2021) also reported the structure elucidation of crinine (compound 4) and trisphaeridine (compound **5**) identified in mixture fractions. The structures of compounds **6—12**, identified in mixture fractions, were not reported in our

241 previous work. UPLC-HRMS analysis provided the molecular formula of each alkaloid
242 (data reported in SI3), allowing the field of investigation to be narrowed down for ^{13}C
243 NMR-based dereplication. Table 1 indicates the fractions from which alkaloids were
244 identified, and the reference used for ^{13}C NMR-based dereplication. Among the extract
245 fractions, a complex and abundant one (A12) showed a compound with an NMR profile
246 that was not compatible with any of those previously reported, as attested by its absence
247 from the SciFinder^n database (https://scifinder-n.cas.org). Hence, it was subjected again
248 to CPC in order to obtain simpler fractions, among which A12_8 was the most useful
249 for compound identification. The ^1H NMR spectrum of compound **12** showed an
250 isolated doublet at 8.84 ppm for a hydrogen atom that was not bound to a carbon atom,
251 according to the HSQC spectrum. The exploration of the neighborhood of this hydrogen
252 atom by means of the HMBC spectrum indicated the presence of the acetamido group.
253 The COSY correlation of the NH signal provides the entry point into the nerinine
254 structure element via its position 6. The compound was identified as 6-dehydroxy-6-
255 acetamido-nerinine, which was hitherto never reported in the literature. Amaryllidaceae
256 alkaloids with two nitrogen atoms are rare; some examples are the plicamine and
257 secoplicamine type, together with some of those belonging to the group of
258 miscellaneous and unclassifiable compounds (Berkov et al. 2020; de Andrade et al.
259 2012). One of the most widely accepted hypotheses for the formation of dinitrogenous
260 alkaloids is the reaction between an intermediate of the biogenic pathway of an alkaloid
261 with one nitrogen atom, and an amino acid, which provides the second nitrogen atom.
262 For example, a key aminoaldehyde intermediate for the biogenesis of crinine and
263 tazettine type alkaloids probably reacts with tyramine for the formation of plicamine,
264 secoplicamine, and obliquine (Ünver et al., 1999). In the structure of compound **12**,
265 incorporation of an amino acid could not be detected; it is more likely, therefore, that a

reaction of the OH group at position 6 of nerinine with the reagents of the extraction process took place. The simultaneous presence of ammonium hydroxide (NH_4OH) and ethylacetate (EtOAc) for five days during extraction can explain the formation of compound **12** from nerinine according to Figure 2. Despite being a useful aqueous base for extraction of Amaryllidaceae alkaloids, NH_4OH reacts with carbonyl groups to give condensation products (Maltese et al., 2009); the typical hemiacetals in the structure of alkaloids or solvents with a carbonyl group, such as EtOAc, are therefore particularly susceptible. Thus, compound **12** was classified as an extraction artefact.

The description of the NMR spectra of all compounds is available from the zenodo.org archive in three forms. The first form is the traditional data table as published in chemistry journals, the second one is a text file that is structured according to the guidelines of the NMReDATA organization (Kuhn et al., 2021) for good human- and computer- readability, and the third one is a structure drawing, reproduced on a larger scale for a good readability by humans and with chemical shift values reported for each hydrogen and carbon atom. Accession details are reported in the Supplementary Information file 1 (SI1).

The spectra of all fractions obtained by CPC were analyzed by NMR using DMSO-*d6* as solvent. This choice was motivated by the systematic use of this solvent in the authors' laboratory as it has a strong dissolution ability for a very wide range of analytes. Moreover, DMSO-*d6* facilitates the detection of the ^{1}H NMR signal of exchangeable nuclei, thus allowing an efficient structural analysis. However, fractions A4, A7, A9, and A11 containing compounds **1—4** were also analyzed in $CDCl_3$, a solvent that is widely used for the analysis of Amaryllidaceae alkaloids. The ^{13}C NMR chemical shifts recorded using the two solvents is presented in Supplementary Information file 1 (SI1). Our experimental values were in good agreement with those

291 available in previously published reports (for all compounds except **7**, **11B,** and **12**).
292 The good reproducibility of NMR chemical shift values, regardless of the solvent used,
293 confirms the high reliability of compound search in databases from ^{13}C NMR data.
294
295 ***3.2 Biological activities of S. miniatum bulb extract***
296
297 The extract and some of the fractions were subjected to the fore-mentioned biological
298 assays. Among the 13 fractions obtained from CPC fractionation, A1 had a scarce mass
299 (4 mg); thus, the NMR analysis was difficult to interpret due to the low concentration of
300 alkaloids, while fractions A3 and A5 contained tazettine in a less pure form than the one
301 in fraction A4. Consequently, these fractions were not tested for biological activities.
302
303 ***3.2.1 Cytotoxic activities against A431 human epidermoid carcinoma cells***
304
305 The extract and part of the fractions were tested against human epidermoid A431
306 carcinoma cells by measuring cell viability after 24, 48 and 72 h of treatment. The
307 extract was slightly more potent than the other samples, with an IC_{50} of 3.3 μg/mL after
308 72 h. At the same time point, the IC_{50} calculated for fractions A8, A9, A10, A11, A12,
309 and A13 was in the range 3.7-8.2 μg/mL (Table 2).
310 The biological activity of a plant extract and of its fractions depends on synergism and
311 antagonism. Action additivity among the components of a mixture may depend on its
312 composition and on the relative concentrations of the individual components (Catanzaro
313 et al. 2018; Fimognari et al. 2012; Lenzi et al. 2018). This means that, even when both
314 the extraction and fractionation protocols are provided, if fractions with different
315 concentrations of individual components are obtained, different studies often yield

316 different results in their evaluation of biological activity. However, this approach allows
317 the identification of the most promising pool of molecules, discriminating them from
318 fractions that show no activity. The alkaloid-enriched extract was predominantly
319 composed of tazettine, haemanthamine, albomaculine, and crinine, with tazettine being
320 the most abundant (Table S1 of Supplementary Information file 2). Tazettine is not a
321 naturally occurring alkaloid, but an artefact formed under basic conditions by molecular
322 rearrangement of chemically labile pretazettine during extraction (de Andrade et al.
323 2012; Kobayashi et al. 1980). Consequently, the major alkaloid present in the fresh
324 bulbs of *S. miniatum*, used for medicinal purposes in ethnobotany, turned out to be
325 pretazettine. Pretazettine was successfully tested against A431 tumor cells, resulting in
326 an IC_{50} of 5.4 μM (Zupkó et al., 2009). Moreover, it exhibited cytotoxicity against
327 Rauscher leukemia, AKR lymphoblastic leukemia, HeLa cervical adenocarcinoma,
328 Lewis lung carcinoma and Ehrlich ascites carcinoma cells (Bastida et al., 2006). Among
329 the fractions showing inhibition of A431 cell viability, A11, A12, and A13 contained
330 pretazettine at various concentrations, mixed with other alkaloids, including crinine
331 (A11), and 6-dehydroxy-6-acetamido-nerinine (A12 and A13). Three pure alkaloids,
332 namely tazettine (A4), albumaculine (A7) and haemanthamine (A9), were also
333 investigated. In our experimental model, tazettine did not show any significant activity,
334 as previously reported (Masi et al., 2022). Albomaculine, tested for the first time against
335 the A431 tumor cell line, was not found to be active either. Conversely, haemanthamine
336 inhibited A431 cell viability with an IC_{50} of 3.7 μg/mL (12.3 μM) after a 72-h
337 treatment. This result does not match with the one published by Masi et al. (2022), who
338 found the compound to be inactive at 0.5-10 μM concentrations using the MTT cell
339 viability assay. The different cytotoxic effect is not surprising and can be due to the
340 higher concentrations of haemanthamine we tested in the present study compared to

341 those used by Masi et al. Fractions A8 and A10, containing haemanthamine in mixture,
342 were also effective. Considering that none of the other alkaloids identified in the
343 mixture, namely albomaculine and 6-hydroxybuphanisine in A8, and nerinine in A10,
344 exhibited significant cytotoxic activity in several tumor cell screenings (Nair et al. 2016;
345 Nair and Van Staden, 2021), haemanthamine is probably responsible for part or all the
346 effect of these fractions on A431 cell viability. Among the Amaryllidaceae alkaloids,
347 haemanthamine has been singled out for its promising anti-cancer properties; in fact, it
348 is a candidate lead for the development of drugs against several types of carcinomas and
349 leukemia (Cahlíková et al., 2021). Overall, the bulb extract of *S. miniatum* showed a
350 good cytotoxicity against A431 human epidermoid carcinoma cells. Conversion of the
351 original pretazettine to the inactive tazettine during the extraction procedure certainly
352 modified the cytotoxic potential of *S. miniatum* bulbs, which would be even higher
353 under natural conditions.
354
355 ***3.2.2 Cytotoxic activities against Jurkat human acute T-leukemia cells***
356
357 The alkaloid extract of *S. miniatum* and its fractions were tested against another type of
358 cancer, a blood tumor (Table 3).
359 On the whole, the cytotoxicity exhibited by the alkaloid-enriched extract of *S. miniatum*
360 and its fractions on blood tumor cells was lower than against A431 cells (Table 3). The
361 extract inhibited the viability of Jurkat cells with an IC_{50} of 10.9 µg/mL after a 72-h
362 treatment. The fraction consisting of pure haemanthamine (A9) was the most toxic, but
363 the IC_{50} value was higher than that recorded for A431 cells (14.9 µM *versus* 12.3 µM).
364 This alkaloid was already tested against Jurkat cells by Mc Nulty et al. who reported an
365 IC_{50} of 14.9 µM, matching the one found in our experiments (McNulty et al., 2007).

366 The same authors pointed out that the α 5-10b-ethano bridge and the hydroxyl group at
367 C-11 of the chemical structure of haemanthamine are key structural features for the
368 induction of selective apoptosis. The other haemanthamine-containing fractions were
369 less effective than the total extract. Conversely, the fractions containing pretazettine
370 (A11, A12, and A13) inhibited cell viability more than the extract. All experimental
371 results are shown in Supplementary Information file 2 (SI2).
372 *S. miniatum* bulbs proved to be a source of pretazettine and haemanthamine, two
373 Amaryllidaceae alkaloids endowed with potent cytotoxic activities, thus supporting
374 their anticancer ethnobotanical use.
375
376 ***3.2.3 Antibacterial activities***
377
378 The bulb extract of *S. miniatum* and the fractions were tested against bacteria triggering
379 skin abscesses, namely *Staphylococcus aureus*, *Staphylococcus epidermidis* and
380 *Streptococcus pyogenes*. No sample showed appreciable activity at the tested
381 concentration (200 µg/mL). Some of the alkaloids contained in the extract, namely
382 tazettine, haemanthamine and crinine, were already tested against *S. aureus* and *S.*
383 *epidermidis* without revealing antibacterial properties (Ločárek et al. 2015; Nair et al.
384 2017). The antibacterial action reported by the Kallawaya healers could be due to non-
385 alkaloid metabolites contained in whole fresh bulbs. Amaryllidaceae plants produce
386 other types of compounds, such as ceramides, which showed a moderate antibacterial
387 activity against *S. aureus* (Wu et al., 2009), besides polyphenols, whose antibacterial
388 action is widely recognized (Coppo and Marchese, 2014). Further studies could be
389 conducted on the analysis of non-alkaloid compounds produced by this species.
390

4. Conclusion

The dereplication approach for the characterization of *S. miniatum* bulb extract allowed the rapid identification of the twelve known Amaryllidaceae alkaloids and a new one artefact. The phytochemical profiling led to the detection of various cytotoxic alkaloids to which the cytotoxic activity against the tested tumor lines can be ascribed. Hence, the ethnobotanical use of *S. miniatum* bulb extract as skin cancer treatment was corroborated by this study. Additional research could be conducted on antibacterial activity, focusing on non-alkaloid compounds produced by this species.

Acknowledgements. Thanks to the Delle Piane-Encina family for their essential cooperation in finding the plant material, Prof. Stefania Biondi for revising the English and Prof. Fabiana Antognoni for valuable advice.
Conflicts of Interest: The authors declare no conflict of interest.
Funding: This research received no external funding.
Data Availability Statement: The data presented in this study are openly available at zenodo.org from https://doi.org/10.5281/zenodo.4574016 .

References

Ali, A.A., El Saved, H.M., Abdalliah, O.M., Steglich, W., 1986. Oxocrinine and other alkaloids from *Crinum americanum*. Phytochemistry 25, 2399–2401. https://doi.org/10.1016/S0031-9422(00)81704-5

Baldwin, S.W., Debenham, J.S., 2000. Total Syntheses of (−)-Haemanthidine, (+)-Pretazettine, and (+)-Tazettine. Org. Lett. 2, 99–102. https://doi.org/10.1021/ol9911472

Bastida, J., Lavilla, R., Viladomat, F., 2006. Chapter 3 Chemical and Biological Aspects of *Narcissus* Alkaloids, in: Cordell, G.A. (Ed.), The Alkaloids: Chemistry and Biology. Academic Press, pp. 87–179. https://doi.org/10.1016/S1099-4831(06)63003-4

Bastien, J.W., 1982. Herbal curing by Qollahuaya Andeans. J. Ethnopharmacol. 6, 13–28. https://doi.org/10.1016/0378-8741(82)90069-1

Berkov, S., Osorio, E., Viladomat, F., Bastida, J., 2020. Chemodiversity, chemotaxonomy and chemoecology of Amaryllidaceae alkaloids. Alkaloids Chem. Biol. 83, 113–185. https://doi.org/10.1016/bs.alkal.2019.10.002

Boit, H.-G., Döpke, W., 1957. Alkaloide aus *Urceolina-, Hymenocallis-, Elisena-, Calostemma-, Eustephia-* und *Hippeastrum*-Arten. Chem. Ber. 90, 1827–1830. https://doi.org/10.1002/cber.19570900920

Cahlíková, L., Kawano, I., Řezáčová, M., Blunden, G., Hulcová, D., Havelek, R., 2021. The Amaryllidaceae alkaloids haemanthamine, haemanthidine and their semisynthetic

derivatives as potential drugs. Phytochem. Rev. 20, 303–323. https://doi.org/10.1007/s11101-020-09675-8

Catanzaro, E., Greco, G., Potenza, L., Calcabrini, C., Fimognari, C., 2018. Natural Products to Fight Cancer: A Focus on Juglans regia. Toxins 10, 469. https://doi.org/10.3390/toxins10110469

Chen, H., Lao, Z., Xu, J., Li, Z., Long, H., Li, D., Lin, L., Liu, X., Yu, L., Liu, W., Li, G., Wu, J., 2020. Antiviral activity of lycorine against Zika virus in vivo and in vitro. Virology 546, 88–97. https://doi.org/10.1016/j.virol.2020.04.009

Coppo, E., Marchese, A., 2014. Antibacterial Activity of Polyphenols. Curr. Pharm. Biotechnol. 15, 380–390. https://doi.org/10.2174/1389201015041408251211 42

de Andrade, J.P., Guo, Y., Font-Bardia, M., Calvet, T., Dutilh, J., Viladomat, F., Codina, C., Nair, J.J., Zuanazzi, J.A.S., Bastida, J., 2014. Crinine-type alkaloids from *Hippeastrum aulicum* and *H. calyptratum*. Phytochemistry 103, 188–195. https://doi.org/10.1016/j.phytochem.2014.03.007

de Andrade, J.P., Pigni, N.B., Torras-Claveria, L., Berkov, S., Codina, C., Viladomat, F., Bastida, J., 2012. Bioactive alkaloid extracts from *Narcissus broussonetii*: Mass spectral studies. J. Pharm. Biomed. Anal. 70, 13–25. https://doi.org/10.1016/j.jpba.2012.05.009

Ee, E., Gi, S., J, V.S., 2004. Acetylcholinesterase enzyme inhibitory effects of Amaryllidaceae alkaloids. Planta Med. 70. https://doi.org/10.1055/s-2004-818919

Fimognari, C., Ferruzzi, L., Turrini, E., Carulli, G., Lenzi, M., Hrelia, P., Cantelli-Forti, G., 2012. Metabolic and toxicological considerations of botanicals in anticancer therapy. Expert Opin. Drug Metab. Toxicol. 8, 819–832. https://doi.org/10.1517/17425255.2012.685717

Frahm, A.W., Ali, A.A., Ramadan, M.A., 1985. 13C nuclear magnetic resonance spectra of amaryllidaceae alkaloids. I—alkaloids with the crinane skeleton. Magn. Reson. Chem. 23, 804–808. https://doi.org/10.1002/mrc.1260231004

Gaudêncio, S.P., Pereira, F., 2015. Dereplication: racing to speed up the natural products discovery process. Nat. Prod. Rep. 32, 779–810. https://doi.org/10.1039/C4NP00134F

Girault, L., 2018. Kallawaya, guérisseurs itinérants des Andes: Recherches sur les pratiques médicinales et magiques. IRD Éditions.

Hohmann, J., Forgo, P., Szabó, P., 2002. A new phenanthridine alkaloid from *Hymenocallis* × *festalis*. Fitoterapia 73, 749–751. https://doi.org/10.1016/S0367-326X(02)00240-X

Hubert, J., Nuzillard, J.-M., Renault, J.-H., 2017. Dereplication strategies in natural product research: How many tools and methodologies behind the same concept? Phytochem. Rev. 16, 55–95. https://doi.org/10.1007/s11101-015-9448-7

Jerald J. Nair, Johannes Van Staden, Jaume Bastida, 2016. Cytotoxic alkaloid constituents of the Amaryllidaceae.

Knolker, H., 2020. The Alkaloids. Elsevier.

Kobayashi, S., Kihara, M., Shingu, T., Shingu, K., 1980. Transformation of Tazettine to Pretazettine. Chem. Pharm. Bull. (Tokyo) 28, 2924–2932. https://doi.org/10.1248/cpb.28.2924

Kotland, A., Chollet, S., Diard, C., Autret, J.-M., Meucci, J., Renault, J.-H., Marchal, L., 2016. Industrial case study on alkaloids purification by pH-zone refining centrifugal partition chromatography. J. Chromatogr. A 1474, 59–70. https://doi.org/10.1016/j.chroma.2016.10.039

Kuhn, S., Wieske, L.H.E., Trevorrow, P., Schober, D., Schlörer, N.E., Nuzillard, J.-M., Kessler, P., Junker, J., Herráez, A., Farès, C., Erdélyi, M., Jeannerat, D., 2021. NMReDATA: Tools and applications. Magn. Reson. Chem. 59, 792–803. https://doi.org/10.1002/mrc.5146

Lenzi, M., Cocchi, V., Novaković, A., Karaman, M., Sakač, M., Mandić, A., Pojić, M., Barbalace, M.C., Angeloni, C., Hrelia, P., Malaguti, M., Hrelia, S., 2018. *Meripilus giganteus* ethanolic extract exhibits pro-apoptotic and anti-proliferative effects in leukemic cell lines. BMC Complement. Altern. Med. 18, 300. https://doi.org/10.1186/s12906-018-2366-7

Lévi-Strauss, C., 1952. The use of wild plants in tropical South America. Econ. Bot. 6, 252–270. https://doi.org/10.1007/BF02985068

Lianza, M., Leroy, R., Machado Rodrigues, C., Borie, N., Sayagh, C., Remy, S., Kuhn, S., Renault, J.-H., Nuzillard, J.-M., 2021. The Three Pillars of Natural Product Dereplication. Alkaloids from the Bulbs of *Urceolina peruviana* (C. Presl) J.F. Macbr. as a Preliminary Test Case. Molecules 26, 637. https://doi.org/10.3390/molecules26030637

Lianza, M., Verdan, M.H., de Andrade, J.P., Poli, F., de Almeida, L., Costa-Lotufo, L., Cunha Neto, Á., Oliveira, S., Bastida, J., Batista, A., Batista Jr., J., Borges, W., 2020. Isolation, Absolute Configuration and Cytotoxic Activities of Alkaloids from *Hippeastrum goianum* (Ravenna) Meerow (Amaryllidaceae). J. Braz. Chem. Soc. https://doi.org/10.21577/0103-5053.20200116

Ločárek, M., Nováková, J., Klouček, P., Hošťálková, A., Kokoška, L., Gábrlová, L., Šafratová, M., Opletal, L., Cahlíková, L., 2015. Antifungal and Antibacterial Activity of Extracts and Alkaloids of Selected Amaryllidaceae Species. Nat. Prod. Commun. 10, 1934578X1501000. https://doi.org/10.1177/1934578X1501000912

Maltese, F., van der Kooy, F., Verpoorte, R., 2009. Solvent Derived Artifacts in Natural Products Chemistry. Nat. Prod. Commun. 4, 1934578X0900400. https://doi.org/10.1177/1934578X0900400326

Mandrone, M., Bonvicini, F., Lianza, M., Sanna, C., Maxia, A., Gentilomi, G.A., Poli, F., 2019. Sardinian plants with antimicrobial potential. Biological screening with multivariate data treatment of thirty-six extracts. Ind. Crops Prod. 137, 557–565. https://doi.org/10.1016/j.indcrop.2019.05.069

Masi, M., Di Lecce, R., Mérindol, N., Girard, M.-P., Berthoux, L., Desgagné-Penix, I., Calabrò, V., Evidente, A., 2022. Cytotoxicity and Antiviral Properties of Alkaloids Isolated from *Pancratium maritimum*. Toxins 14, 262. https://doi.org/10.3390/toxins14040262

McNulty, J., Nair, J.J., Codina, C., Bastida, J., Pandey, S., Gerasimoff, J., Griffin, C., 2007. Selective apoptosis-inducing activity of crinum-type Amaryllidaceae alkaloids. Phytochemistry 68, 1068–1074. https://doi.org/10.1016/j.phytochem.2007.01.006

Meerow, A., Jost, L., Oleas, N., 2015. Two new species of endemic Ecuadorean Amaryllidaceae (Asparagales, Amaryllidaceae, Amarylloideae, Eucharideae). PhytoKeys 48, 1–9. https://doi.org/10.3897/phytokeys.48.4399

Meerow, A.W., 1985. A New Species of Eucrosia and a New Name in *Stenomesson* (Amaryllidaceae). Brittonia 37, 305. https://doi.org/10.2307/2806079

Nair, J.J., 2019. The Plant Family Amaryllidaceae: Special Collection Celebrating the 80th Birthday of Professor Johannes van Staden. Nat. Prod. Commun. 14, 1934578X1987293. https://doi.org/10.1177/1934578X19872932

Nair, J.J., Van Staden, J., 2021. Cytotoxic tazettine alkaloids of the plant family Amaryllidaceae. South Afr. J. Bot. 136, 147–156. https://doi.org/10.1016/j.sajb.2020.07.002

Nair, J.J., van Staden, J., 2013. Pharmacological and toxicological insights to the South African Amaryllidaceae. Food Chem. Toxicol. 62, 262–275. https://doi.org/10.1016/j.fct.2013.08.042

Nair, J. J., Van Staden, J., Bastida, J. 2016. Cytotoxic alkaloid constituents of the Amaryllidaceae. Stud. Nat. Prod. Chem. 49, 107-156. https://doi.org/10.1016/B978-0-444-63601-0.00003-X

Nair, J.J., Wilhelm, A., Bonnet, S.L., van Staden, J., 2017. Antibacterial constituents of the plant family Amaryllidaceae. Bioorg. Med. Chem. Lett. 27, 4943–4951. https://doi.org/10.1016/j.bmcl.2017.09.052

Renault, J.-H., Nuzillard, J.-M., Le Crouérour, G., Thépenier, P., Zèches-Hanrot, M., Le Men-Olivier, L., 1999. Isolation of indole alkaloids from *Catharanthus roseus* by centrifugal partition chromatography in the pH-zone refining mode. J. Chromatogr. A 849, 421–431. https://doi.org/10.1016/S0021-9673(99)00495-1

Renault, J.-H., Nuzillard, J.-M., Maciuk, A., Zeches-Hanrot, M., 2009. Use of centrifugal partition chromatography for purifying galanthamine. US20090216012A1.

Ünver, N., Gözler, T., Walch, N., Gözler, B., Hesse, M., 1999. Two novel dinitrogenous alkaloids from *Galanthus plicatus* subsp. *byzantinus* (Amaryllidaceae). Phytochemistry 50, 1255–1261. https://doi.org/10.1016/S0031-9422(98)00651-7

Viet Nguyen, K., Laidmäe, I., Kogermann, K., Lust, A., Meos, A., Viet Ho, D., Raal, A., Heinämäki, J., Thi Nguyen, H., 2019. Preformulation Study of Electrospun Haemanthamine-Loaded Amphiphilic Nanofibers Intended for a Solid Template for Self-Assembled Liposomes. Pharmaceutics 11, 499. https://doi.org/10.3390/pharmaceutics11100499

Viladomat, F., Bastida, J., Tribo, G., Codina, C., Rubiralta, M., 1990. Alkaloids from *Narcissus bicolor*. Phytochemistry 29, 1307–1310. https://doi.org/10.1016/0031-9422(90)85448-O

Viladomat, F., Codina, C., Bastida, J., Mathee, S., Campbell, W.E., 1995. Further alkaloids from Brunsvigia josephinae. Phytochemistry 40, 961–965. https://doi.org/10.1016/0031-9422(95)00375-H

Viladomat, F., Sellés, M., Cordina, C., Bastida, J., 1997. Alkaloids from *Narcissus asturiensis*. Planta Med. 63, 583–583. https://doi.org/10.1055/s-2006-957781

Wu, Z., Chen, Y., Xia, B., Wang, M., Dong, Y.-F., Feng, X., 2009. Two Novel Ceramides with a Phytosphingolipid and a Tertiary Amide Structure from *Zephyranthes candida*. Lipids 44, 63–70. https://doi.org/10.1007/s11745-008-3246-6

Zupkó, I., Réthy, B., Hohmann, J., Molnár, J., Ocsovszki, I., Falkay, G., 2009. Antitumor Activity of Alkaloids Derived from Amaryllidaceae Species. In Vivo 8.

Abbreviations

ANOVA	Analysis of variance
COCONUT	COlleCtion of Open Natural ProdUcTs
CPC	Centrifugal partition chromatography
KNApSAcK	Kurokawa Nakamura Asah personal Shinbo Altaf-Ul-Amin computer Kanaya
MtBE	Methyl tert-butyl ether
NMReDATA	NMR extracted data
RPMI	Roswell Park memorial institute
SEM	Standard error of the mean
TEA	Triethylamine
UNPD	Universal natural products database
UPLC	Ultra performance liquid chromatography

Table 1. Fraction composition, identified alkaloids in different fractions (first identification) of the *Stenomesson miniatum* bulb extract and bibliographic reference for ^{13}C NMR-based dereplication

FRACTION	Fraction composition	Identified Alkaloid	Reference for ^{13}C NMR-based dereplication
A1	-	-	-
A2	tazettine; trisphaeridine; 3-epimacronine; 3-methoxy-8,9-methylenedioxy-3,4-dihydrophenanthridine	Trisphaeridine **5**; 3-epimacronine **6**; 3-methoxy-8,9-methylenedioxy-3,4-dihydrophenanthridine **7**	(Viladomat et al. 1997) (Viladomat et al. 1990) (Hohmann et al. 2002)
A3	tazettine; trisphaeridine		
A4	tazettine	tazettine **1**	(Knolker 2020)
A5	tazettine; crinine acetate		
A6	crinine acetate; albomaculine	crinine acetate **8**	(Ali et al. 1986)
A7	albomaculine	albomaculine **2**	(de Andrade et al. 2014)
A8	albomaculine; 6α-hydroxybuphanisine; haemanthamine	6α-hydroxybuphanisine **9**	(Frahm et al. 1985)
A9	haemanthamine	haemanthamine **3**	(Viet Nguyen et al. 2019)
A10	haemanthamine; nerinine	nerinine **10**	(de Andrade et al. 2014)
A11	crinine; α-pretazettine	crinine **4**	(Viladomat et al. 1995)
A12	α-pretazettine; β-pretazettine; 6-dehydroxy-6-acetamido-nerinine	β-pretazettine **11A** α-pretazettine **11B** 6-dehydroxy-6-acetamido-nerinine **12**	(Baldwin and Debenham 2000) (Kobayashi et al. 1980) -
A13	β-pretazettine; α-pretazettine; 6-dehydroxy-6-acetamido-nerinine		

587 Table 2. IC_{50} values in µg/mL calculated after treatment of A431 cells with increasing
588 concentrations of the extract or its fractions for 24, 48 or 72 h.
589

Sample	**IC_{50} 24h**	**IC_{50} 48h**	**IC_{50} 72h**
extract	9.1	6.7	3.3
A2	347.1	297.5	232.1
A4 (tazettine)	901.3	1171.0	869.2
A6	394.0	419.0	412.9
A7 (albomaculine)	201.5	251.5	168.7
A8	10.1	7.1	5.1
A9 (haemanthamine)	7.6	5.4	3.7
A10	16.1	13.2	5.2
A11	9.9	10.3	8.2
A12	5.7	4.3	5.3
A13	6.4	4.9	3.8

590
591
592
593
594
595
596
597
598
599
600
601
602
603
604
605

606 Table 3. IC_{50} values in µg/mL calculated after treatment of Jurkat leukemia cells with

607 increasing concentrations of the extract or its fractions for 24, 48 or 72 h.

608

Sample	IC_{50} 24h	IC_{50} 48h	IC_{50} 72h
extract	124.6	31.4	10.9
A2	309.9	209.5	123.8
A4 (tazettine)	1373.0	857.8	881.9
A6	894.8	360.7	256.1
A7 (albomaculine)	1669.0	1073.0	446.1
A8	233.3	31.7	13.7
A9 (haemanthamine)	70.4	31.2	4.5
A10	292.3	53.7	13.9
A11	102.4	53.7	8.6
A12	119.3	16.4	5.1
A13	65.6	12.4	5.5

609

610

611

612

613

614

615

616

617

618

619

620

621

622

623

624

625

626

627

628

629

630

631 Figure 1. Chemical structures of the alkaloids identified in the *Stenomesson miniatum*
632 bulb extract: tazettine **1**, albomaculine **2**, haemanthamine **3**, crinine **4**, trisphaeridine **5**,
633 3-epimacronine **6,** 3-methoxy-8,9-methylenedioxy-3,4-dihydrophenanthridine **7**, crinine
634 acetate **8**, 6α-hydroxybuphanisine **9**, nerinine **10**, β-pretazettine **11A**, α-pretazettine
635 **11B**, 6-dehydroxy-6-acetamido-nerinine **12**
636
637 Figure 2. A likely mechanism for the formation of compound **12** from nerinine
638 (compound **10**) during the alkaloid extraction process.
639

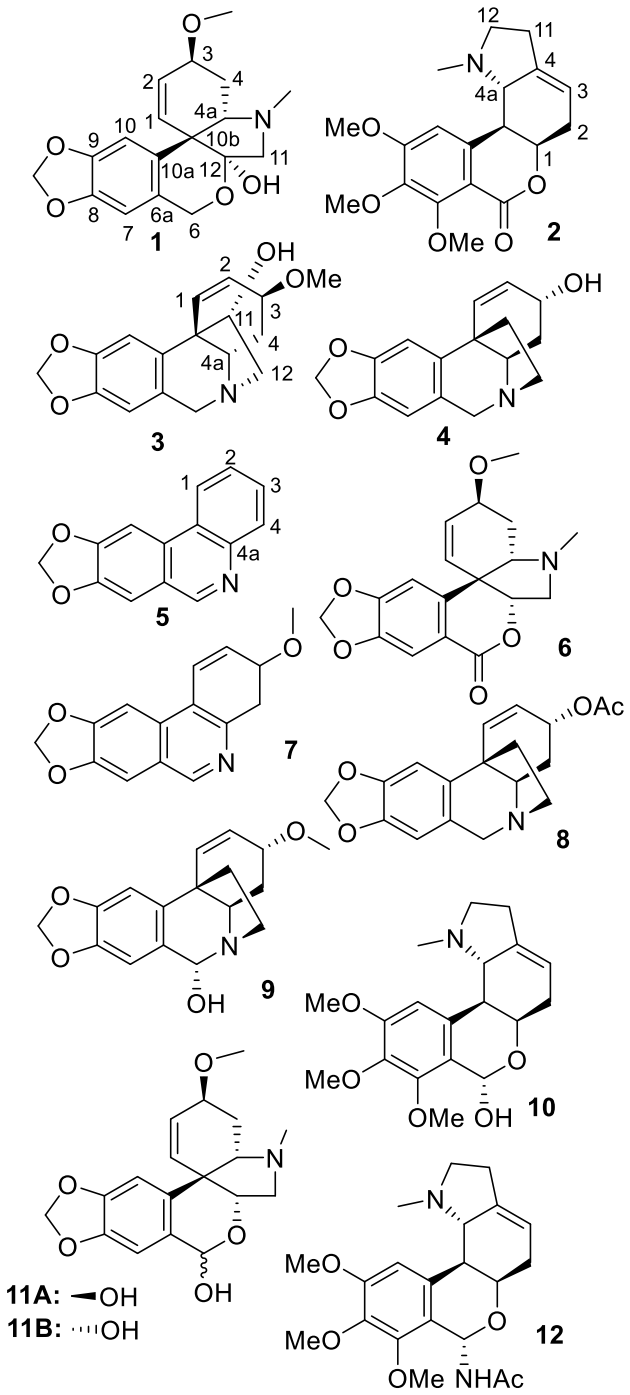

Figure 1.

644

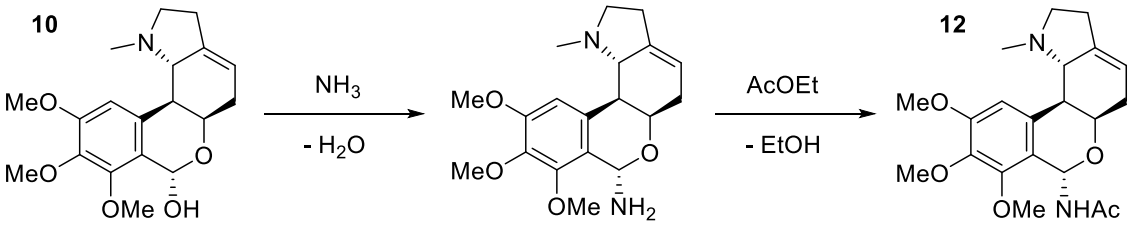

645

646 Figure 2

647

Supplementary Information SI1

Phytochemical characterization and biological activities of *Stenomesson miniatum* bulb extract, a medicinal plant of the Andes.

Mariacaterina Lianza[a]*, Carmela Fimognari[a], Jean-Marc Nuzillard[b], Ferruccio Poli[c], Jean-Hugues Renault[b], Francesca Bonvicini[c], Giulia Greco[d], Eleonora Turrini[a]

[a]Department for Life Quality Studies, University of Bologna, 47921 Rimini, Italy
[b] CNRS, ICMR UMR 7312, University of Reims Champagne-Ardenne, 51097 Reims, France
[c] Department of Pharmacy and Biotechnology, University of Bologna, 40138 Bologna, Italy
[d] Department of Chemistry, University of Bologna, 40126 Bologna, Italy

*Correspondence: mariacaterina.lianz3@unibo.it

The structures of the characterized compounds are reported in Figure 1. Table 1 connects each compound identifier, such as "compound1" with the compound name (tazettine) and with the reference of the fraction (A4) in which it is present and of the set of NMR spectra which was used to carry out structure determination. The raw NMR data, the corresponding spectra, and their interpretation are stored in a zenodo.org archive, https://doi.org/10.5281/zenodo.4574016. This archive contains four zipped directories named "Assignments", "NMReDATA", "$CDCl_3$", and "Tables".
The Assignments directory contains ChemDraw files, one per compound and a ChemDraw_PDF directory that shows them once exported as one-page PDF files. The all_compounds.cdx.pdf file shows them all in a single multi-page PDF file. Each ChemDraw file is named after the related compound identifier and shows the molecular structure of the compound, its name, and the identifier of the fraction from which it was characterized. The values of ^{13}C NMR chemical shifts are reported in the neighborhood of each carbon atom, as well as the ^{1}H NMR chemical shifts of the directly bound hydrogen atoms, if any. The NMR spectra recorded with DMSO-d_6 as solvent were referenced by means of residual solvent signals, set at 2.5 ppm for ^{1}H and 39.52 ppm for ^{13}C NMR spectra.
The NMReDATA directory contains zipped directories named NMReDATA records, one per compound, with nmredata.zip file extension. Each archive contains a directory and a file. For example, directory "compound1" contains an SDF file named "compound1.nmredata.sdf" and a directory named compound1_A4, after the identifiers of the compound and of the fraction. The compound1.nmredata.sdf file reports the features and their interpretation that were extracted from the spectra stored in the corresponding directory. Directory compound1_A4 contains NMR raw data and spectra produced by the TopSpin4 (TS4) software (Bruker, Rheinstetten, Germany) including 1D and 2D peak picking information. The nmredata.sdf files are text files formatted according to the computer readable NMReDATA template (https://nmredata.org/wiki).
Each NMReDATA file is an SDF file related to a single compound but contains two structures, a first one with 2D coordinates in the style of those usually published in Journals and a second one with 3D coordinates. The 2D structure section, enriched with chirality data at asymmetric centers, is followed by NMReDATA-specific key-value pairs for NMR spectra descriptions and for spectral assignment. An assignment is a triplet such as "c1, 129.1635, 4" that associates an atom name ("4" for the fourth atom in the list of atoms written in the atom block of the SDF file, an NMR signal label ("c1", for the ^{13}C NMR signal of the biogenetically numbered carbon atom C-1) and the corresponding chemical shift value (129.1635). The biogenetic atom numbering, the one displayed in Scheme 1, is incorporated in signal labels so that 1D NMR spectra descriptions are readily understandable. Assignment data make possible to describe 2D spectra as pairs of signal labels instead of pairs of chemical shift values, thus increasing data readability for humans. Atom numbering is consistent between the 2D and 3D structure descriptions and is standardized using the ALATIS software (Dashti et al., 2017). The 3D structures are produced by the ETKDGv3 procedure implemented in the RDKit library of cheminformatics tools (Wang et al., 2020). The 3D structure with the lowest Merck Molecular Force Field (MMFF) energy is retained as a reasonable guess of what the most stable molecular conformation could be, even this quick exploration procedure of the molecular conformational space is not intended to provide a definitive description of 3D structures. The 2D structures may be easily viewed with EdiSDF

(https://vpsolovev.ru/programs/edisdf/) and the 3D structures with Jmol (http://jmol.sourceforge.net/) but any alternative software selection is possible.
The $CDCl_3$ directory contains raw NMR data and the corresponding spectra for pure compounds **1**—**4** dissolved in $CDCl_3$, respectively from fractions A4, A7, A9, A11.
The Tables directory contains MS Excel files for compounds **1**—**4** and MS word files for the other ones. The tables are formatted in the style organic chemists expect to see for NMR spectra descriptions and assignments. They carry the same information as the nmredata.sdf files but the formers are hardly machine-readable.
The difference in the processing of compounds **1**—**4** for the writing of the NMR data tables was motivated considering that the fractions in which they were characterized, A4, A7, A9, A11 contain these compounds at a high purity state. The creation of nmredata.sdf files and of traditional data tables was partly automated while the creation of these files for the other fractions was a fully manual process, meaning that no computer script was involved. The manual peak picking in the 2D NMR spectra of compounds **1**—**4** relies on the peak integration tool of TopSpin while it relies on the peak annotation tool for the other compounds. This choice can be explained, at least in part, by the fact that it seemed complicated to exploit the highly crowded 2D spectra of complex mixtures by means of the integration tool.

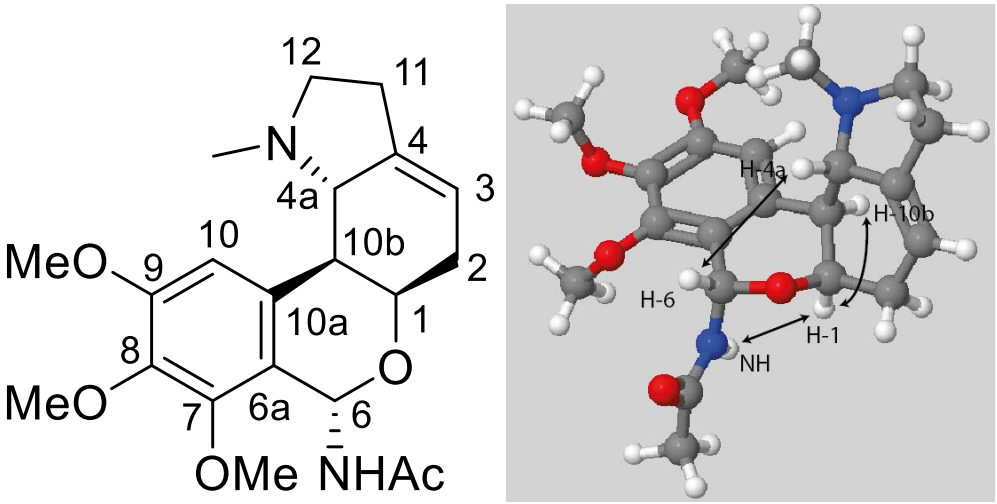

Structure of 6-dehydroxy-6-acetamido-nerinine: compound 12

Structure determination of compound 12. The planar structure was determined by the thorough analysis of 1D ^{1}H and ^{13}C NMR spectra and of 2D COSY, HSQC, and HMBC spectra. The *cis* ring junction at C-1 and C-10b, the α orientation of the acetamido group, and the *trans*-diaxial positions of H-4a and H-10b were deduced from the observation of the H-1/H-10b, NH/H-1, and H-6/H-4a ROESY correlations.

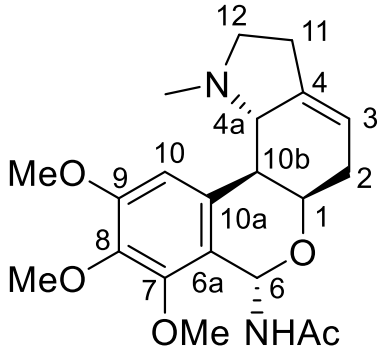

6-dehydroxy-6-acetamido-nerinine: ^{1}H NMR, ^{13}C NMR, COSY and HMBC NMR data (600 MHz, DMSO-*d*$_6$)

Position	**δ_H (*J* in Hz)**	**δ_C**	**COSY**	**HMBC**
1	4.153 *m*	65.57	H-2$_a$, H-2$_b$, H-6, H-10b	C-2, C-3, C-4a, C-6, C-10a
2$_a$	2.586 *m*	31.47	H-1, H-2$_b$, H-3	C-3, C-4, C-10b
2$_b$	2.042 *m*		H-2$_a$, H-3	C-1, C-3, C-4, C-10b
3	5.37 *ddd* (10.4, 1.9, 1.6)	114.93	H-2$_a$, H-2$_b$	C-4a
4		141.55		
4a	2.566 *m*	67.0	H-1, H-3	
6	6.248 *d* (8.7)	71.56	H-1, H-10, NH	C-1, C-6a, C-7, C-8, C-9, C-10a, CO(Ac)
6a		119.88		
7		150.13		
8		140.63		
9		152.25		
10	6.769 *s*	109.29	H-6, H-10b, 9-OMe	C-4a, C-6, C-6a, C-7, C-8, C-9, C-10a, C-10b
10a		133.34		
10b	2.274 *dd* (9.4, 2.2)	43.58	H-1, H-4a, H-10	C-4, C-4a, C-6a, C-10, C-10a
11$_a$	2.392 *m*		H-12$_a$, H-12$_b$	
11$_b$	2.289 *m*	28.16	H-12$_a$	
12$_a$	2.998 *ddd* (9.6, 7.6, 3.6)		H-11$_a$, H-11$_b$, H-12$_b$	C-4, C-4a, C-11, NMe
12$_b$	2.174 *m*	56.2	H-11$_a$, H-11$_b$, H-12$_a$	C-4, C-4a, C-11, NMe
NH	8.84 *d* (8.7)		H-6, Me(Ac)	C-6, C-6a, CO(Ac)
Me(Ac)	1.833 *s*	22.88	NH	CO(Ac)
CO(Ac)		168.45		
7-OMe	3.729 *s*	60.37		C-7
8-OMe	3.726 *s*	60.17		C-8
9-OMe	3.784 *s*	56.02	H-10	C-9
NMe	1.898 *s*	44.34		C-4a, C-12

ROESY (F_2--> F_1): H-1 --> H-2$_a$, H-10b, NH; H-2$_a$ --> H-1, H-3; H-2$_b$ --> H-1; H-3; H-4a --> NMe; H-10 --> NMe; H-10b --> H-1; H-12$_a$ --> H-12$_b$, NMe; H-12$_b$ --> H-12$_a$, NMe; NH --> H-1, Me(Ac), 7-OMe.

Descriptors for compounds **1**—**12**
Compound **1**
Tazettine $C_{18}H_{21}NO_5$ (Knolker 2020),

^{13}C NMR data reported from (Roberts et al. 1971)
InChI-Key: YLWAQARRNQVEHD-PBZHRCKQSA-N
InChI=1S/C18H21NO5/c1-19-9-18(20)17(4-3-12(21-2)6-16(17)19)13-7-15-14(22-10-23-15)5-11(13)8-24-18/h3-5,7,12,16,20H,6,8-10H2,1-2H3/t12-,16+,17+,18-/m1/s1
SMILES:
CN1[C@@H]2[C@@]3(C=C[C@@H](OC)C2)[C@](C1)(O)OCC4=C3C=C5C(OCO5)=C4

Compound **2**
Albomaculine $C_{19}H_{23}NO_5$(de Andrade et al. 2014)
InChI-Key: OXFLPPXWFHSXSK-XNRPHZJLSA-N
InChI=1S/C19H23NO5/c1-20-8-7-10-5-6-12-14(16(10)20)11-9-13(22-2)17(23-3)18(24-4)15(11)19(21)25-12/h5,9,12,14,16H,6-8H2,1-4H3/t12-,14-,16-/m1/s1
SMILES: CN1CCC2=CC[C@@H]3[C@H]([C@@H]21)C4=CC(=C(C(=C4C(=O)O3)OC)OC)OC

Compound **3**
Haemanthamine $C_{17}H_{19}NO_4$(Viet Nguyen et al. 2019)
InChI-Key: YGPRSGKVLATIHT-HSHDSVGOSA-N
InChI=1S/C17H19NO4/c1-20-11-2-3-17-12-6-14-13(21-9-22-14)4-10(12)7-18(8-16(17)19)15(17)5-11/h2-4,6,11,15-16,19H,5,7-9H2,1H3/t11-,15+,16+,17+/m1/s1
SMILES: CO[C@H]1C[C@H]2[C@@]3(C=C1)[C@H](CN2CC4=CC5=C(C=C34)OCO5)O

Compound **4**
Crinine $C_{16}H_{17}NO_3$(Viladomat et al. 1995)
InChI-Key: RPAORVSEYNOMBR-IUIKQTSFSA-N
InChI=1S/C16H17NO3/c18-11-1-2-16-3-4-17(15(16)6-11)8-10-5-13-14(7-12(10)16)20-9-19-13/h1-2,5,7,11,15,18H,3-4,6,8-9H2/t11-,15+,16+/m0/s1
SMILES: C1CN2CC3=CC4=C(C=C3[C@]15[C@H]2C[C@H](C=C5)O)OCO4

Compound **5**
Trisphaeridine $C_{14}H_9NO_2$(Viladomat et al. 1997)
RFILRSDHWIIIMN-UHFFFAOYSA-N
InChI=1S/C14H9NO2/c1-2-4-12-10(3-1)11-6-14-13(16-8-17-14)5-9(11)7-15-12/h1-7H,8H2
SMILES: C1OC2=C(O1)C=C3C4=CC=CC=C4N=CC3=C2

Compound **6**
3-Epimacronine $C_{18}H_{19}NO_5$(Viladomat et al. 1990)
InChI-Key: YEISBJOTHHFANE-NJVUAGGXSA-N
InChI=1S/C18H19NO5/c1-19-8-16-18(4-3-10(21-2)5-15(18)19)12-7-14-13(22-9-23-14)6-11(12)17(20)24-16/h3-4,6-7,10,15-16H,5,8-9H2,1-2H3/t10-,15+,16+,18+/m1/s1
SMILES:
CN1C[C@H]2[C@]3([C@@H]1C[C@@H](C=C3)OC)C4=CC5=C(C=C4C(=O)O2)OCO5

Compound **7**
3-methoxy-8,9-methylenedioxy-3,4-dihydrophenanthridine $C_{15}H_{13}NO_3$(Hohmann et al., 2002)
InChI-Key: OIOVDHXEPUXTQZ-UHFFFAOYSA-N
InChI=1S/C15H13NO3/c1-17-10-2-3-11-12-6-15-14(18-8-19-15)4-9(12)7-16-13(11)5-10/h2-4,6-7,10H,5,8H2,1H3
SMILES: COC1CC2=C(C=C1)C3=CC4=C(C=C3C=N2)OCO4

Compound **8**
Crinine-3-acetate $C_{18}H_{19}NO_4$(Ali et al. 1986)
InChI-Key: YEIGSYFTXGPBIB-MORSLUCNSA-N
InChI=1S/C18H19NO4/c1-11(20)23-13-2-3-18-4-5-19(17(18)7-13)9-12-6-15-16(8-14(12)18)22-10-21-15/h2-3,6,8,13,17H,4-5,7,9-10H2,1H3/t13-,17+,18+/m0/s1

SMILES: CC(O[C@@H](C=C[C@]12CC3)C[C@H]1N3CC4=C2C=C5C(OCO5)=C4)=O

Compound **9**
6α-Hydroxybuphanisine $C_{17}H_{19}NO_4$ (Frahm et al. 1985)
InChI-Key: VCFGXYUXSWZFDE-CNFIPTJHSA-N
InChI=1S/C17H19NO4/c1-20-10-2-3-17-4-5-18(15(17)6-10)16(19)11-7-13-14(8-12(11)17)22-9-21-13/h2-3,7-8,10,15-16,19H,4-6,9H2,1H3/t10-,15+,16+,17+/m0/s1
SMILES:
CO[C@@H]1C[C@@H]2[C@@]3(CCN2[C@@H](C4=CC5=C(C=C43)OCO5)O)C=C1Co

Compound **10**
Nerinine $C_{19}H_{25}NO_5$(de Andrade et al. 2014)
InChI-Key: MNAREALDHXFRFJ-QNDNMDDASA-N
InChI=1S/C19H25NO5/c1-20-8-7-10-5-6-12-14(16(10)20)11-9-13(22-2)17(23-3)18(24-4)15(11)19(21)25-12/h5,9,12,14,16,19,21H,6-8H2,1-4H3/t12-,14-,16-,19+/m1/s1
SMILES:
CN1CCC2=CC[C@@H]3[C@H]([C@@H]21)C4=CC(=C(C(=C4[C@H](O3)O)OC)OC)OC

Compound **11A**
Pretazettine (major epimer, 6β-pretazattine) $C_{18}H_{21}NO_5$(Baldwin and Debenham 2000; Kobayashi et al. 1980)
InChI-Key: KLJOYDMUWKSYBP-YNBLHMCPSA-N
InChI=1S/C18H21NO5/c1-19-8-16-18(4-3-10(21-2)5-15(18)19)12-7-14-13(22-9-23-14)6-11(12)17(20)24-16/h3-4,6-7,10,15-17,20H,5,8-9H2,1-2H3/t10-,15+,16+,17-,18+/m1/s1
SMILES:
CN1C[C@H]2[C@]3([C@@H]1C[C@@H](C=C3)OC)C4=CC5=C(C=C4[C@@H](O2)O)OCO5

Compound **11B**
Pretazettine (minor epimer, 6α-pretazettine) $C_{18}H_{21}NO_5$(Kobayashi et al. 1980)
InChI-Key: KLJOYDMUWKSYBP-GTQNRYLJSA-N
InChI=1S/C18H21NO5/c1-19-8-16-18(4-3-10(21-2)5-15(18)19)12-7-14-13(22-9-23-14)6-11(12)17(20)24-16/h3-4,6-7,10,15-17,20H,5,8-9H2,1-2H3/t10-,15+,16+,17+,18+/m1/s1
SMILES:
CN1C[C@H]2[C@@]3(C4=CC5=C(OCO5)C=C4[C@@H](O)O2)[C@@H]1C[C@H](OC)C=C3

Compound **12**
6-dehydroxy-6-acetamido-nerinine $C_{21}H_{28}N_2O_5$
InChI-Key: JPSHDRAJDZKEJG-OQBJRAFVSA-N
InChI=1S/C21H28N2O5/c1-11(24)22-21-17-13(10-15(25-3)19(26-4)20(17)27-5)16-14(28-21)7-6-12-8-9-23(2)18(12)16/h6,10,14,16,18,21H,7-9H2,1-5H3,(H,22,24)/t14-,16-,18-,21+/m1/s1
SMILES:
CN1CCC2=CC[C@H]([C@@H]3[C@@H]21)O[C@H](NC(C)=O)C4=C3C=C(OC)C(OC)=C4OC

Comparison of the data recorded by the authors with those from literature, when available

Tazettine **1**			Albomaculine **2**			Haemanthamine **3**			Crinine **4**		
Our data $CDCl_3$	Literature $CDCl_3$	Our data DMSO-*d6*	Our data $CDCl_3$	Literature $CDCl_3$	Our data DMSO-*d6*	Our data $CDCl_3$	Literature $CDCl_3$	Our data DMSO-*d6*	Our data $CDCl_3$	Literature $CDCl_3$	Our data DMSO-*d6*
146.75	146.60	145.74	162.39	162.40	161.30	146.60	146.50	145.80	146.25	146.10	145.58
146.54	146.40	145.67	157.15	157.20	156.55	146.30	146.20	145.29	145.84	145.70	145.10
130.74	130.60	129.56	156.25	156.30	155.03	135.25	135.40	136.59	138.25	138.40	138.82
128.74	128.60	129.16	142.57	142.70	141.81	132.25	132.00	129.52	131.87	132.20	130.79
127.94	128.00	127.97	140.77	140.80	141.13	127.30	127.40	128.74	127.83	127.40	128.47
125.60	125.50	126.36	140.42	140.60	140.68	126.62	126.90	127.35	126.02	126.50	126.96
109.48	109.30	108.38	115.62	115.60	115.01	106.97	106.90	106.81	107.06	106.90	106.88
104.13	104.00	104.16	111.44	111.60	110.96	103.45	103.30	103.28	102.98	102.70	103.15
102.10	102.10	101.06	107.30	107.40	108.20	100.98	100.80	100.52	100.91	100.60	100.46
101.09	100.90	100.81	76.29	76.30	75.71	80.13	80.20	80.09	63.86	64.10	62.46
72.94	72.90	72.60	65.95	66.00	65.83	72.81	72.80	72.41	62.92	62.80	62.40
70.22	70.00	69.40	62.08	62.10	61.67	63.54	63.60	63.71	62.16	62.40	61.93
65.54	65.60	65.20	61.30	61.30	60.72	62.79	62.70	62.47	53.57	53.60	53.01
62.18	62.10	60.75	56.57	56.60	56.34	61.35	61.40	60.71	44.34	44.20	44.20
56.30	56.20	55.36	56.45	56.50	55.72	56.78	56.70	55.65	44.09	44.20	43.87
49.98	49.90	49.48	45.35	45.50	43.93	50.23	50.10	49.90	32.76	32.70	32.71
42.22	41.90	41.86	43.68	43.70	43.22	28.23	28.30	28.18			
26.72	26.70	25.93	30.97	31.00	30.40						
			27.98	28.10	27.59						

Literature

Tazettine **1** (Pham et al. 1999)
Albomaculine **2** (de Andrade et al. 2014)
Haemanthamine **3** (Viet Nguyen et al. 2019)
Crinine **4** (Frahm et al. 1985)

Trisphaeridine **5**		3-epimacronine **6**		Crinine acetate **8**		6α-hydroxybuphanisine **9**		Nerinine **10**	
Our data DMSO-*d6*	Literature $CDCl_3$	Our data DMSO-*d6*	Literature $CDCl_3$	Our data DMSO-*d6*	Literature $CDCl_3$	Our data DMSO-*d6*	Literature $CDCl_3$	Our data DMSO-*d6*	Literature $CDCl_3$

151.85	151.80	164.89	168.50	169.93	170.00	146.59	147.30	152.00	153.10
151.51	148.20	152.18	152.30	145.67	146.20	145.05	145.80	150.80	151.30
148.14	148.10	146.83	147.10	145.31	145.90	139.15	138.50	141.62	141.20
143.74	143.80	142.11	142.20	138.07	138.20	132.95	131.80	140.71	141.10
129.57	130.30	131.76	131.30	135.25	134.50	129.13	127.40	132.92	133.60
129.51	129.90	125.94	126.00	126.85	126.40	125.35	125.70	122.42	121.20
128.04	128.10	118.07	118.60	123.15	123.70	109.42	109.30	115.06	115.80
126.72	126.70	109.91	111.00	106.99	107.00	102.54	102.30	109.20	109.10
124.02	124.30	104.06	103.80	103.09	102.00	100.63	100.70	88.04	89.80
123.07	122.00	102.41	102.10	100.54	100.00	88.05	88.70	66.90	67.50
122.87	123.10	79.29	80.10	66.33	66.60	72.03	72.10	63.98	66.30
105.39	105.50	72.37	72.70	62.86	63.30	56.49	56.40	60.81	61.40
102.25	101.90	62.50	63.30	61.66	62.40	55.69	56.20	60.36	61.00
100.35	99.90	55.37	56.20	52.95	53.60	47.87	47.60	56.19	57.10
		52.98	53.50	44.03	44.30	43.97	44.20	55.86	56.30
		45.68	46.20	43.94	44.10	40.76	40.60	44.32	44.60
		42.53	42.80	29.28	29.90	28.29	27.70	43.72	44.50
		28.95	29.80	20.97	21.20			31.39	31.90
								28.14	28.40

Literature

Trisphaeridine **5** (Viladomat et al. 1997)
3-Epimacronine **6** (Viladomat et al. 1990)
Crinine acetate **8** (Ali et al. 1986)
6α-OH-Buphanisine **9** (Frahm et al. 1985)
Nerinine **10** (de Andrade et al. 2014)

Pretazettine **11A**		Compound **7**	Pretazettine **11B**	Compound **12**
Our data DMSO-*d6*	Literature $CDCl_3$	Our data DMSO-*d6*	Our data DMSO-*d6*	Our data DMSO-*d6*
146.77	147.70	151.35	146.62	168.45
145.76	146.50	148.21	145.92	152.24
134.80	135.30	147.40	134.98	150.13

129.43	129.10		147.07		130.80		141.55
129.41	128.80		130.02		130.37		140.63
128.60	127.40		128.36		128.02		133.34
108.28	108.10		124.81		107.65		119.88
104.11	104.80		124.15		104.30		114.93
101.02	101.20		120.53		101.02		109.29
92.64	93.90		103.20		95.78		71.56
73.08	73.80		101.94		77.24		67.00
72.69	73.10		98.06		72.69		65.57
63.48	64.10		72.01		63.86		60.37
55.25	56.10		54.94		55.25		60.17
53.81	54.00		35.93		54.09		56.20
45.80	46.20				45.52		56.02
43.02	43.30				42.95		44.34
29.65	30.20				29.68		43.58
							31.47
							28.16
							22.88

Literature

3-methoxy-8,9-methylenedioxy-3,4-dihydrophenanthridine **7**	(Hohmann et al. 2002)
Pretazettine (major epimer) **11A**	(Baldwin and Debenham 2000)
Pretazettine (major epimer) **11B**	no reference found
6-dehydroxy-6-acetamido-Nerinine **12**	

References

Ali, A.A., El Saved, H.M., Abdalliah, O.M., Steglich, W., 1986. Oxocrinine and other alkaloids from *Crinum americanum*. Phytochemistry 25, 2399–2401. https://doi.org/10.1016/S0031-9422(00)81704-5

Baldwin, S.W., Debenham, J.S., 2000. Total Syntheses of (−)-Haemanthidine, (+)-Pretazettine, and (+)-Tazettine. Org. Lett. 2, 99–102. https://doi.org/10.1021/ol9911472

Dashti, H., Westler, W.M., Markley, J.L., Eghbalnia, H.R., 2017. Unique identifiers for small molecules enable rigorous labeling of their atoms. Sci. Data 4, 170073. https://doi.org/10.1038/sdata.2017.73

de Andrade, J.P., Guo, Y., Font-Bardia, M., Calvet, T., Dutilh, J., Viladomat, F., Codina, C., Nair, J.J., Zuanazzi, J.A.S., Bastida, J., 2014. Crinine-type alkaloids from *Hippeastrum aulicum* and *H. calyptratum*. Phytochemistry 103, 188–195. https://doi.org/10.1016/j.phytochem.2014.03.007

Frahm, A.W., Ali, A.A., Ramadan, M.A., 1985. 13C nuclear magnetic resonance spectra of amaryllidaceae alkaloids. I—alkaloids with the crinane skeleton. Magn. Reson. Chem. 23, 804–808. https://doi.org/10.1002/mrc.1260231004

Hohmann, J., Forgo, P., Szabó, P., 2002. A new phenanthridine alkaloid from *Hymenocallis* × *festalis*. Fitoterapia 73, 749–751. https://doi.org/10.1016/S0367-326X(02)00240-X

Knolker, H., 2020. The Alkaloids. Elsevier.

Kobayashi, S., Kihara, M., Shingu, T., Shingu, K., 1980. Transformation of Tazettine to Pretazettine. Chem. Pharm. Bull. (Tokyo) 28, 2924–2932. https://doi.org/10.1248/cpb.28.2924

Pham, L.H., Gründemann, E., Wagner, J., Bartoszek, M., Döpke, W., 1999. Two novel Amaryllidaceae alkaloids from *Hippeastrum equestre* Herb.: 3-O-demethyltazettine and egonine. Phytochemistry 51, 327–332. https://doi.org/10.1016/S0031-9422(98)00743-2

Roberts, J.D., Crain, W.O., Wildman, W.C., 1971. Nuclear magnetic resonance spectroscopy. Carbon-13 spectra of nicotine, quinine, and some Amaryllidaceae alkaloids. J. Am. Chem. Soc. 93, 990–994. https://doi.org/10.1021/ja00733a035

Viet Nguyen, K., Laidmäe, I., Kogermann, K., Lust, A., Meos, A., Viet Ho, D., Raal, A., Heinämäki, J., Thi Nguyen, H., 2019. Preformulation Study of Electrospun Haemanthamine-Loaded Amphiphilic Nanofibers Intended for a Solid Template for Self-Assembled Liposomes. Pharmaceutics 11, 499. https://doi.org/10.3390/pharmaceutics11100499

Viladomat, F., Bastida, J., Tribo, G., Codina, C., Rubiralta, M., 1990. Alkaloids from *Narcissus bicolor*. Phytochemistry 29, 1307–1310. https://doi.org/10.1016/0031-9422(90)85448-O

Viladomat, F., Codina, C., Bastida, J., Mathee, S., Campbell, W.E., 1995. Further alkaloids from *Brunsvigia josephinae*. Phytochemistry 40, 961–965. https://doi.org/10.1016/0031-9422(95)00375-H

Viladomat, F., Sellés, M., Cordina, C., Bastida, J., 1997. Alkaloids from *Narcissus asturiensis*. Planta Med. 63, 583–583. https://doi.org/10.1055/s-2006-957781

Wang, S., Witek, J., Landrum, G.A., Riniker, S., 2020. Improving Conformer Generation for Small Rings and Macrocycles Based on Distance Geometry and Experimental Torsional-Angle Preferences. J. Chem. Inf. Model. 60, 2044–2058. https://doi.org/10.1021/acs.jcim.0c00025

Supplementary Information SI2

Phytochemical characterization by dereplication and biological activities of *Stenomesson miniatum* bulb extract, a medicinal plant of the Andes.

Mariacaterina Lianza[a]*, Carmela Fimognari[a], Jean-Marc Nuzillard[b], Ferruccio Poli[c], Jean-Hugues Renault[b], Francesca Bonvicini[c], Giulia Greco[d], Eleonora Turrini[a]

[a]Department for Life Quality Studies, University of Bologna, 47921 Rimini, Italy
[b] CNRS, ICMR UMR 7312, University of Reims Champagne-Ardenne, 51097 Reims, France
[c] Department of Pharmacy and Biotechnology, University of Bologna, 40138 Bologna, Italy
[d] Department of Chemistry, University of Bologna, 40126 Bologna, Italy

*Correspondence: mariacaterina.lianz3@unibo.it

The results of cytotoxicity activities are shown as the means ± SEM of at least two different experiments. Significant differences among treatments were assessed by two-way analysis of variance (ANOVA), using Dunnett as post-hoc-test. GraphPad Prism 6 (Inc. La Jolla, CA, USA) was used for the statistical analysis and $p < 0.05$ was considered significant.

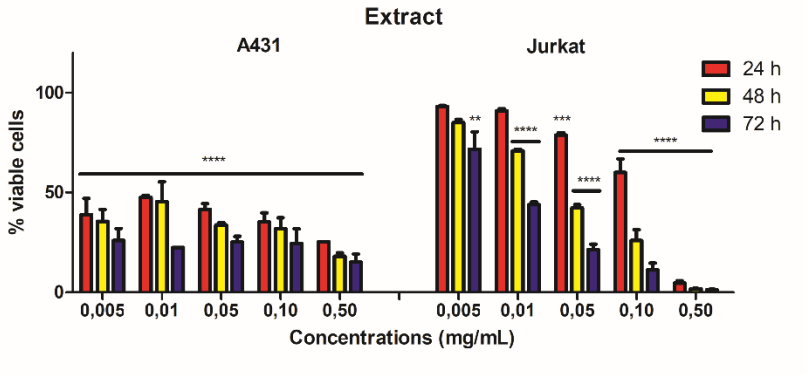

Figure 1. Cytotoxic effects of the alkaloids enriched extract after 24, 48 or 72 h from treatment of A431 and Jurkat cells. Statistical significance was calculated by two-way ANOVA followed by Dunnett as post-hoc test. ** $p < 0.01$; *** $p < 0.001$; **** $p < 0.0001$ compared to control (100% viability).

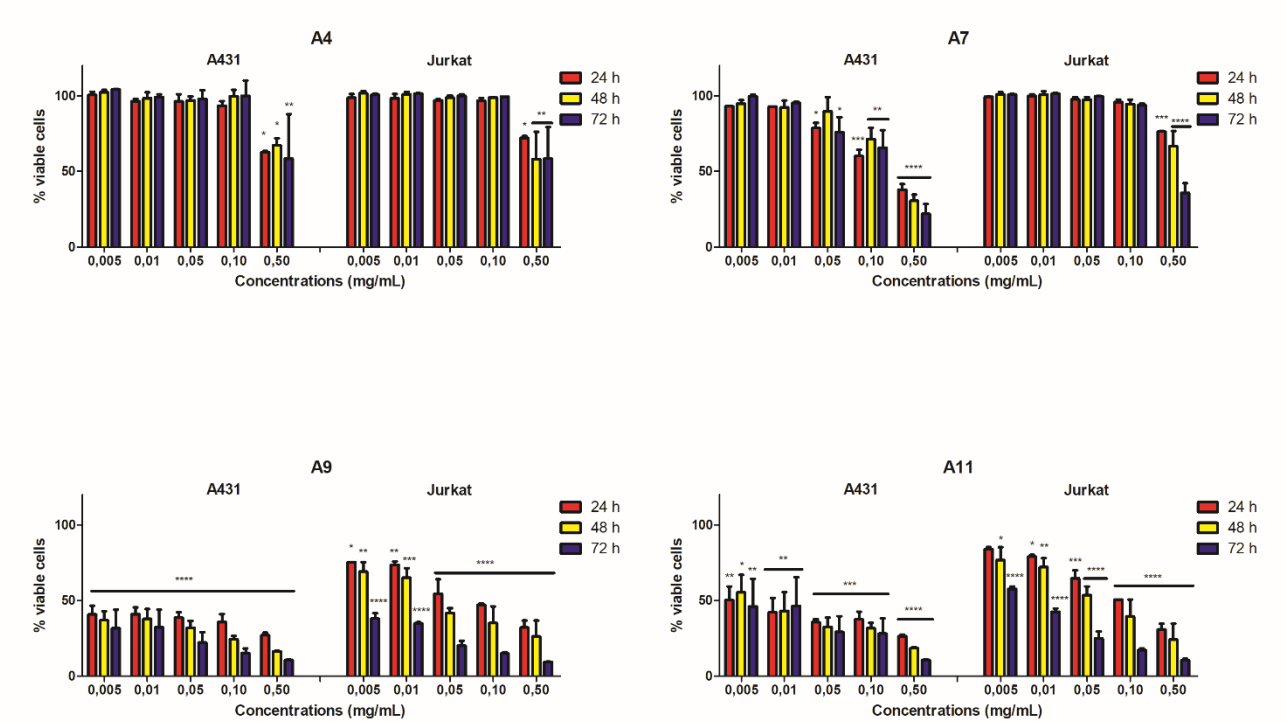

Figure 2. Cytotoxic effects of the pure or semi-pure fractions of the major alkaloids of the extract tazettine (A4), albomaculine (A7), haemanthamine (A9) and crinine (A11) after 24, 48 or 72 h from treatment of A431 and Jurkat cells. Statistical significance was calculated by two-way ANOVA followed by Dunnett as post-hoc test. * $p < 0.05$; ** $p < 0.01$; *** $p < 0.001$; **** $p < 0.0001$ compared to control (100% viability).

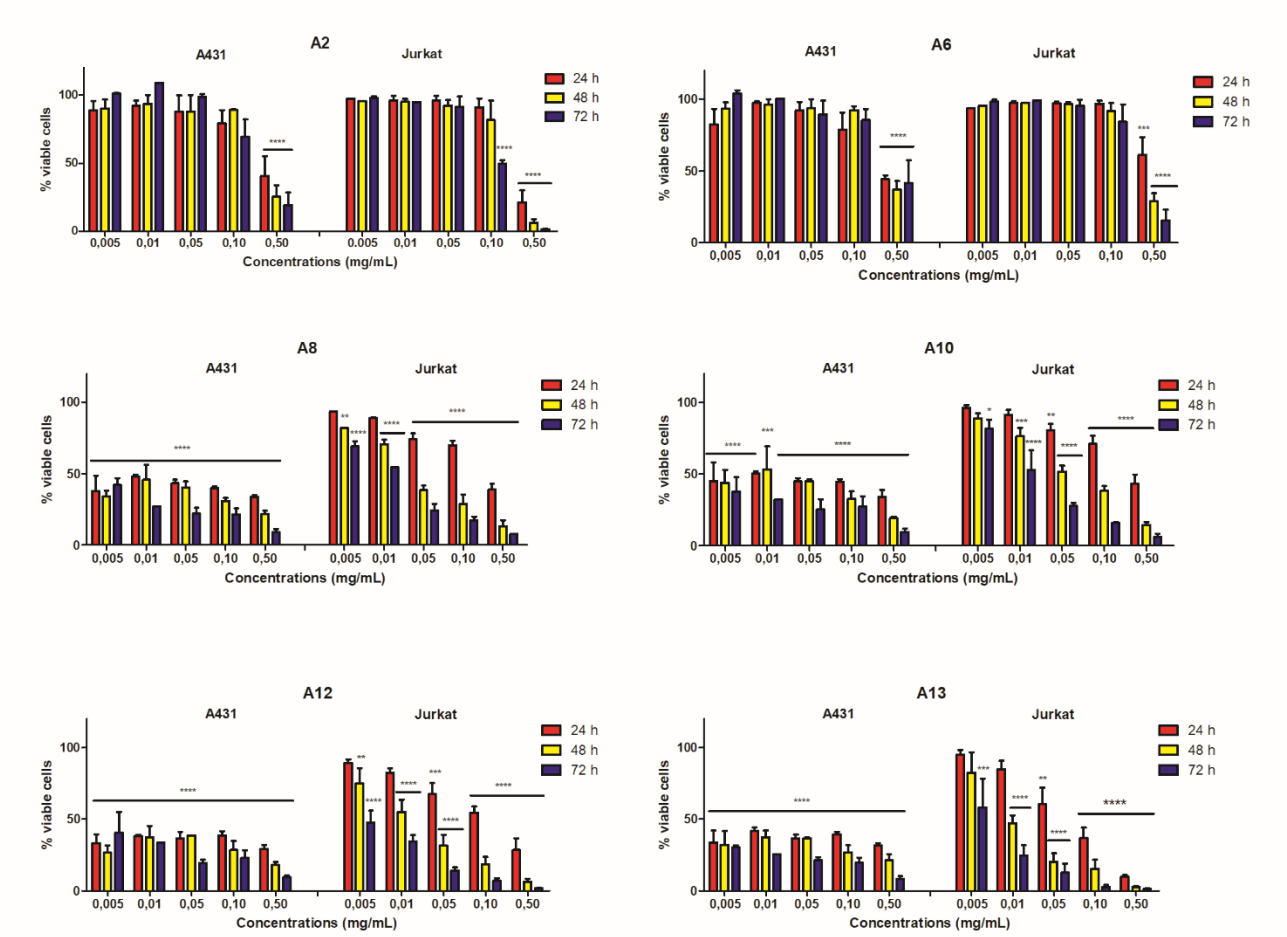

Figure 3: Cytotoxic effects of the mixed alkaloids fractions of the extract A2, A6, A8, A10, A12 and A13 after 24, 48 or 72 h from treatment of A431 and Jurkat cells. Statistical significance was calculated by two-way ANOVA followed by Dunnett as post-hoc test. * $p < 0.05$; ** $p < 0.01$; *** $p < 0.001$; **** $p < 0.0001$ compared to control (100% viability).

Table S1: Identified alkaloids in the fractions, mass of the fractions obtained by CPC fractionation and extractive yields.

FRACTION	Identified alkaloids	MASS (g) from CPC fractionation of 1 g of alkaloid extract	Extractive Yield [%]
A1	-	0,004	0,005
A2	tazettine; trisphaeridine; 3-epimacronine; 3-methoxy-8,9-methylenedioxy-3,4-dihydrophenanthridine	0,024	0,029
A3	tazettine; trisphaeridine	0,028	0,034
A4	tazettine	0,122	0,150
A5	tazettine; crinine acetate	0,069	0,085
A6	crinine acetate; albomaculine	0,082	0,101
A7	albomaculine	0,053	0,065
A8	albomaculine; 6α-hydroxybuphanisine; haemanthamine	0,089	0,109
A9	haemanthamine	0,151	0,185
A10	haemanthamine; nerinine	0,09	0,110
A11	crinine; pretazettine	0,158	0,194
A12	pretazettine; 6-dehydroxy-6-acetamido-nerinine	0,099	0,122
A13	pretazettine; 6-dehydroxy-6-acetamido-nerinine	0,028	0,034

Supplementary Information SI3

Phytochemical characterization and biological activities of *Stenomesson miniatum* bulb extract, a medicinal plant of the Andes.

Mariacaterina Lianza[a]*, Carmela Fimognari[a], Jean-Marc Nuzillard[b], Ferruccio Poli[c], Jean-Hugues Renault[b], Francesca Bonvicini[c], Giulia Greco[d], Eleonora Turrini[a]

[a]Department for Life Quality Studies, University of Bologna, 47921 Rimini, Italy
[b] CNRS, ICMR UMR 7312, University of Reims Champagne-Ardenne, 51097 Reims, France
[c] Department of Pharmacy and Biotechnology, University of Bologna, 40138 Bologna, Italy
[d] Department of Chemistry, University of Bologna, 40126 Bologna, Italy

*Correspondence: mariacaterina.lianz3@unibo.it

UPLC-HRMS DATA

Table SI3~~2~~: Calculated molecular formulas of alkaloids detected in the fractions.

FRACTION	CALCULATED MOLECULAR FORMULA	RETENTION TIME [min]
A1	-----	----
A2	$C_{18}H_{19}NO_5$, $C_{15}H_{13}NO_3$	7.00, 10.09,
	$C_{18}H_{21}NO_5$, $C_{14}H_9NO_2$	12.59, 14.06
A3	$C_{18}H_{18}N_2O_4$, $C_{18}H_{21}NO_5$, $C_{14}H_9NO_2$	11.82, 12.59, 14.06
A4	$C_{18}H_{21}NO_5$	12.59
A5	$C_{18}H_{21}NO_5$	12.59
A6	$C_{19}H_{23}NO_5$, $C_{18}H_{21}NO_5$	9.56, 12.59
A7	$C_{19}H_{23}NO_5$	9.58
A8	$C_{17}H_{19}NO_4$, $C_{19}H_{23}NO_5$,	7.01, 9.62,
	$C_{16}H_{17}NO_4$	10.02
A9	$C_{17}H_{19}NO_4$	6.99
A10	$C_{19}H_{25}NO_5$, $C_{16}H_{17}NO_3$,	4.92, 6.19,
	$C_{17}H_{19}NO_4$	7.02
A11	$C_{18}H_{21}NO_5$, $C_{16}H_{17}NO_3$	5.03, 6.19
A12	$C_{18}H_{21}NO_5$, $C_{19}H_{25}NO_5$	4.56, 4.93
	$C_{21}H_{28}N_2O_5$, $C_{16}H_{17}NO_3$	5.16, 6.20
A13	$C_{18}H_{21}NO_5$, $C_{17}H_{19}NO_5$	5.02, 5.67,
	$C_{16}H_{17}NO_3$	6.19

UPLC-HRMS analysis of extract. a) Blank determination b) BPI chromatograms of *S. miniatum* bulb extract

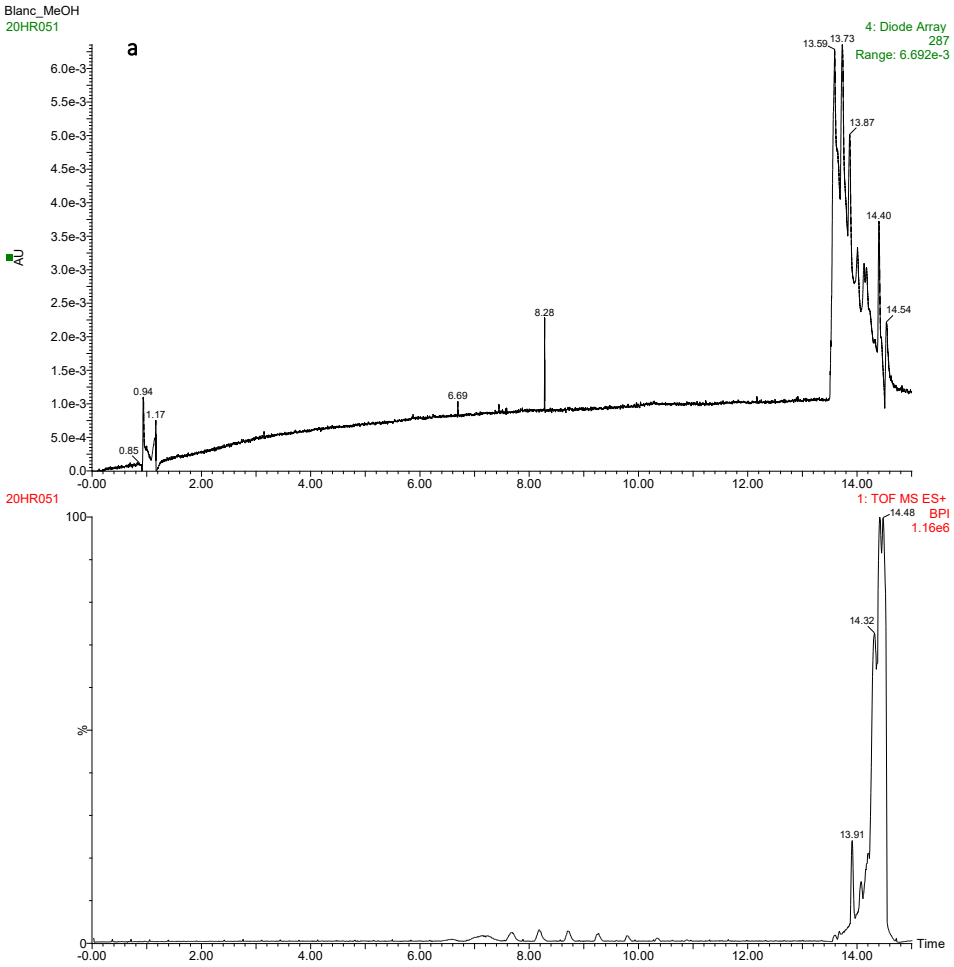

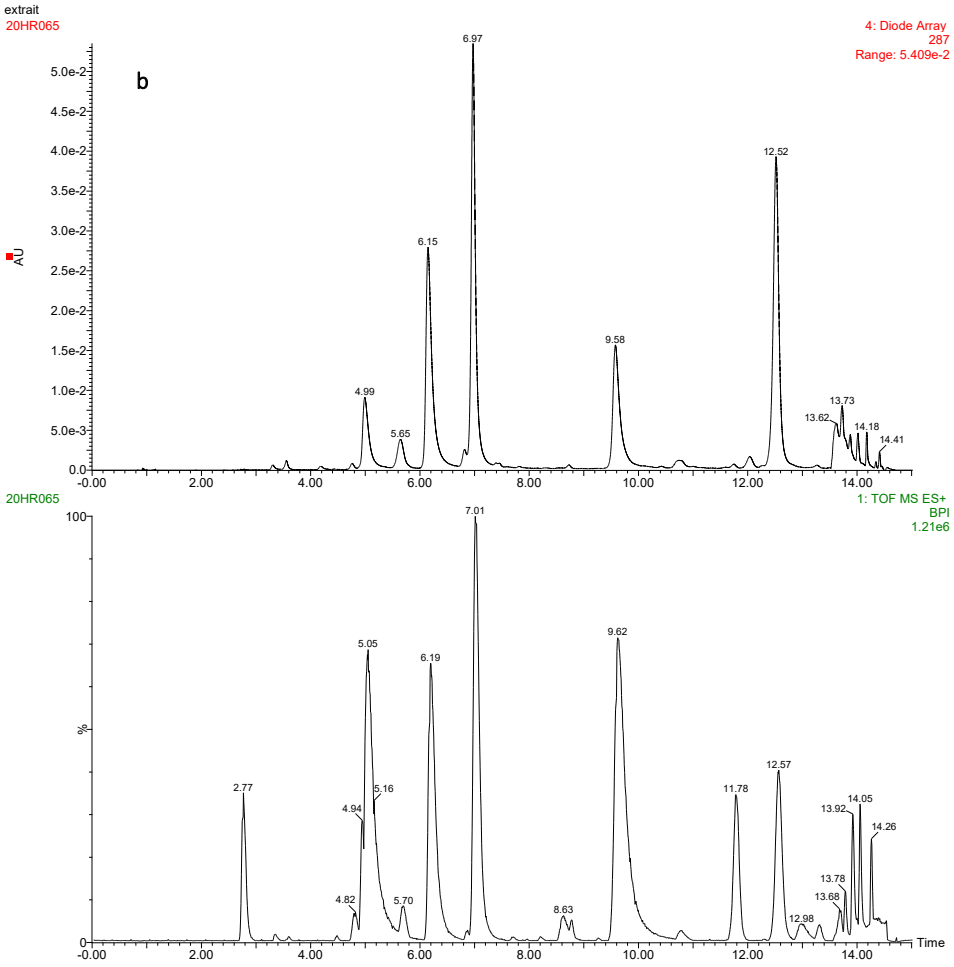
extrait
20HR065
4: Diode Array
287
Range: 5.409e-2
b
AU
6.97
12.52
6.15
9.58
4.99
5.65
13.73
13.62
14.18
14.41
20HR065
1: TOF MS ES+
BPI
1.21e6
%
7.01
5.05
6.19
9.62
12.57
2.77
5.16
4.94
11.78
14.05
13.92
14.26
13.78
13.68
4.82
5.70
8.63
12.98
Time

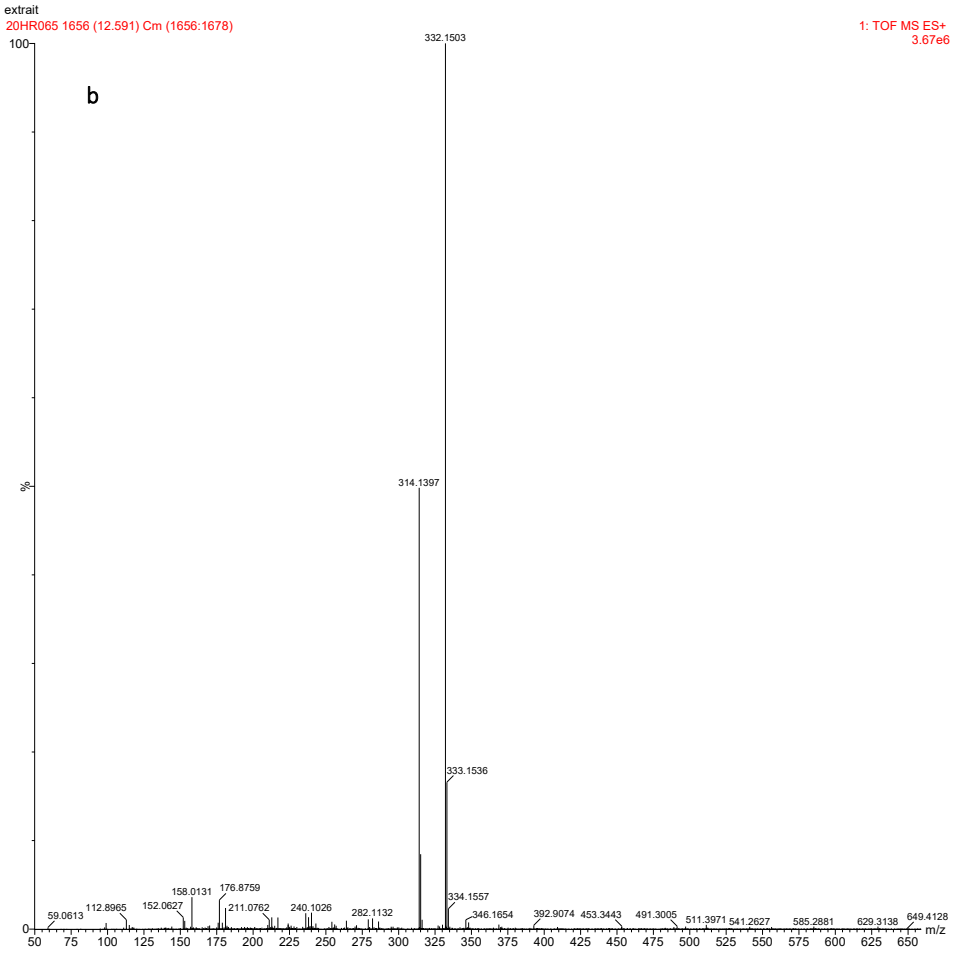

Extract, RT = 12.59 min

Elemental Composition Report

Mass	Calc. Mass	mDa	PPM	DBE	i-FIT	Norm	Conf(%)	Formula
332.1503	332.1498	0.5	1.5	8.5	2030.0	n/a	n/a	C18 H22 N O5

Mass	Calc. Mass	mDa	PPM	DBE	i-FIT	Norm	Conf(%)	Formula
314.1397	314.1392	0.5	1.6	9.5	1836.3	n/a	n/a	C18 H20 N O4

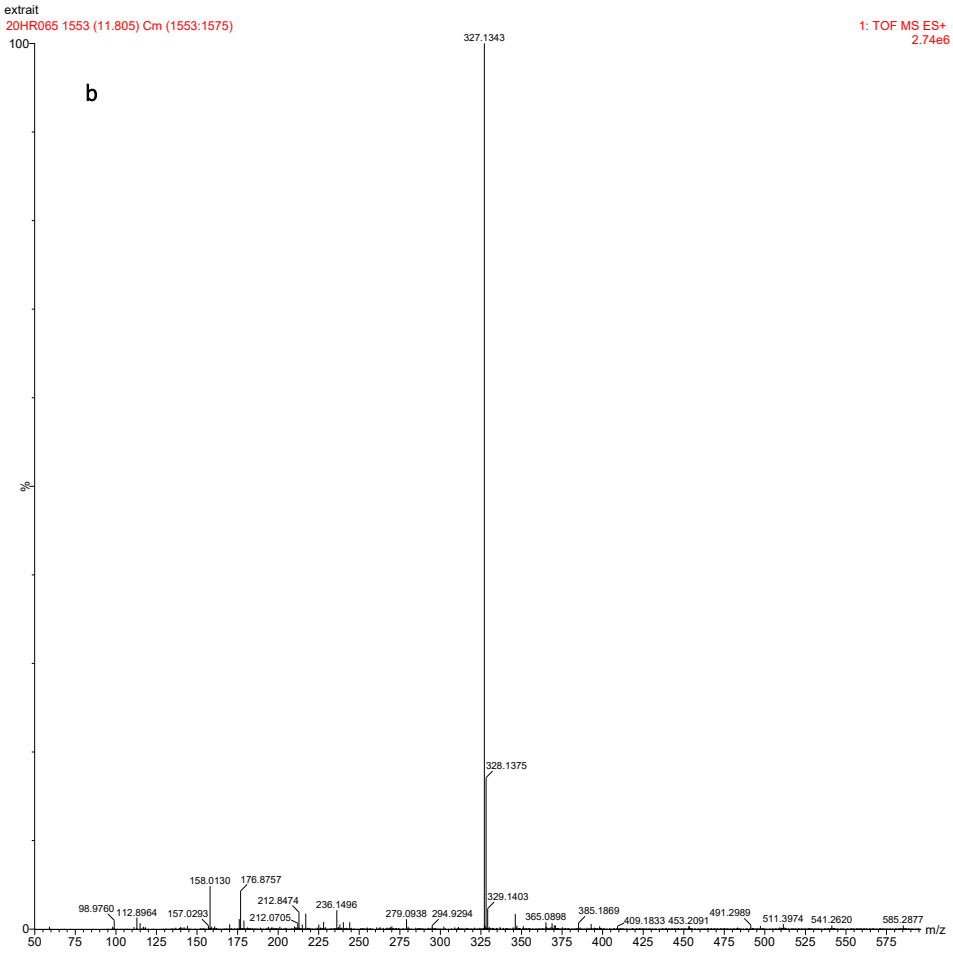

Extract, RT=11.81 min

Mass	Calc. Mass	mDa	PPM	DBE	i-FIT	Norm	Conf(%)	Formula
327.1343	327.1345	-0.2	-0.6	10.5	1904.5	n/a	n/a	C18 H19 N2 O4

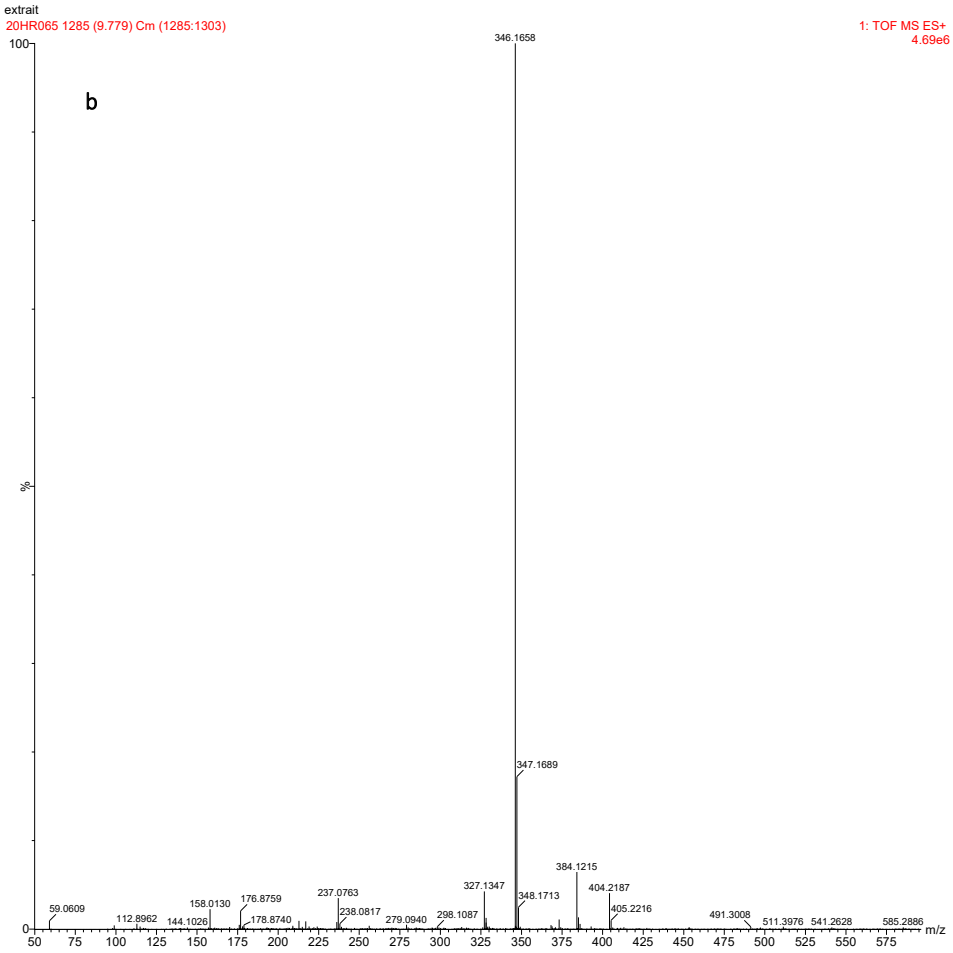

Extract, RT = 9.81 min

Elemental Composition Report

Single Mass Analysis

Tolerance = 5.0 PPM / DBE: min = -1.5, max = 50.0 / Element prediction: Off

Number of isotope peaks used for i-FIT = 3

Monoisotopic Mass, Even Electron Ions

Mass	Calc. Mass	mDa	PPM	DBE	i-FIT	Norm	Conf(%)	Formula
346.1658	346.1654	0.4	1.2	8.5	2035.4	n/a	n/a	C19 H24 N O5

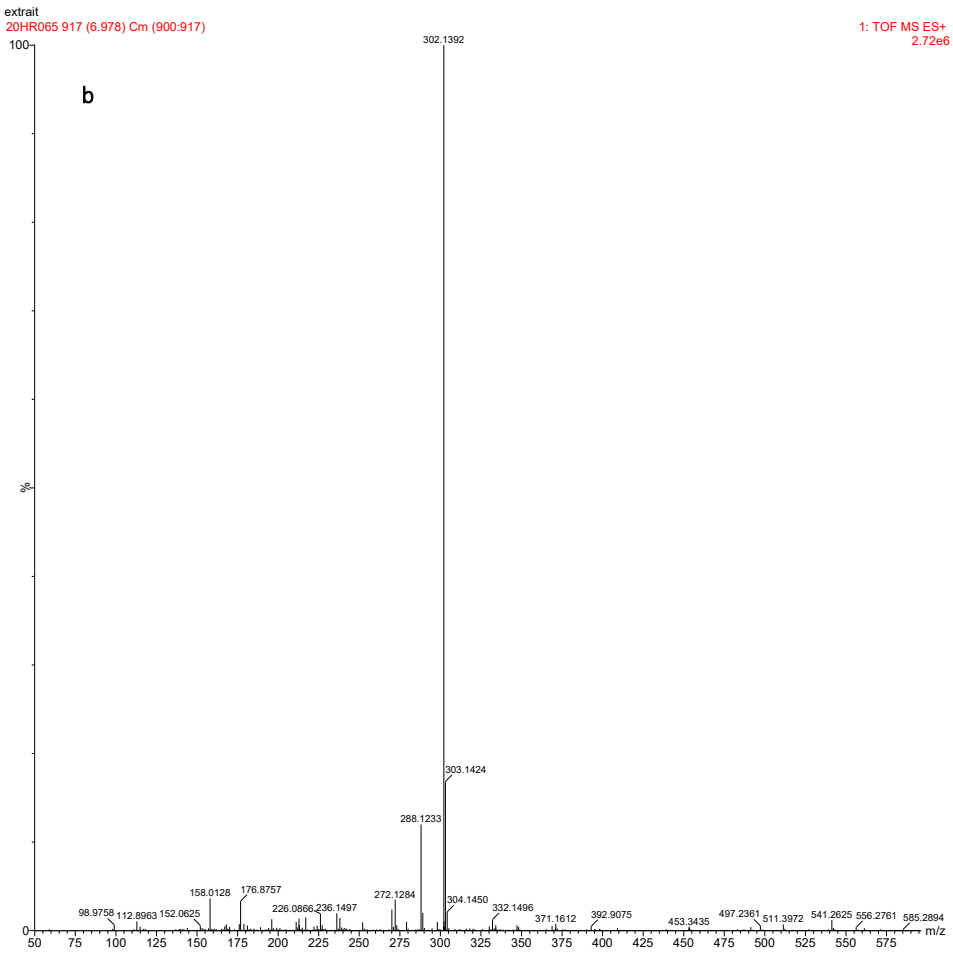

Extract, RT = 6.98 min

Mass	Calc. Mass	mDa	PPM	DBE	i-FIT	Norm	Conf(%)	Formula
302.1393	302.1392	0.1	0.3	8.5	2085.3	n/a	n/a	C17 H20 N O4

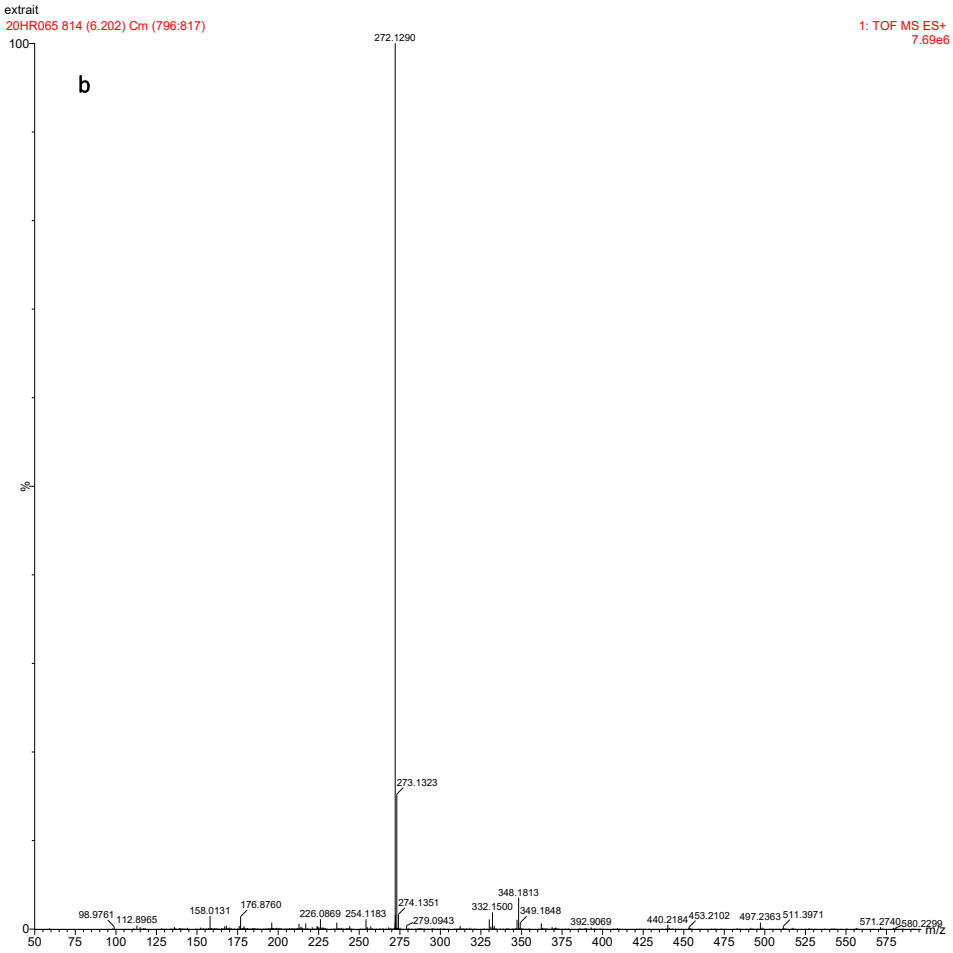

Extract, RT = 6.20 min

Mass	Calc. Mass	mDa	PPM	DBE	i-FIT	Norm	Conf(%)	Formula
272.1290	272.1287	0.3	1.1	8.5	2113.0	n/a	n/a	C16 H18 N O3

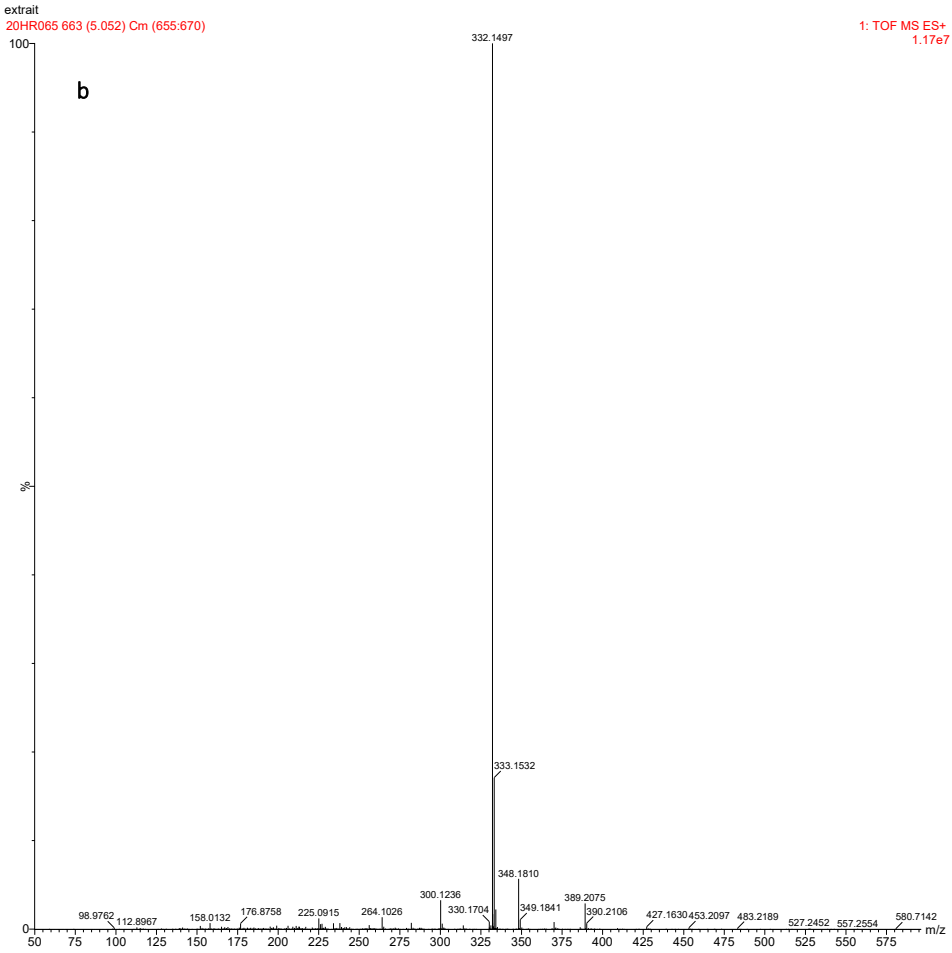

RT = 5.05 min

Mass	Calc. Mass	mDa	PPM	DBE	i-FIT	Norm	Conf(%)	Formula
332.1497	332.1498	-0.1	-0.3	8.5	2250.6	n/a	n/a	C18 H22 N O5

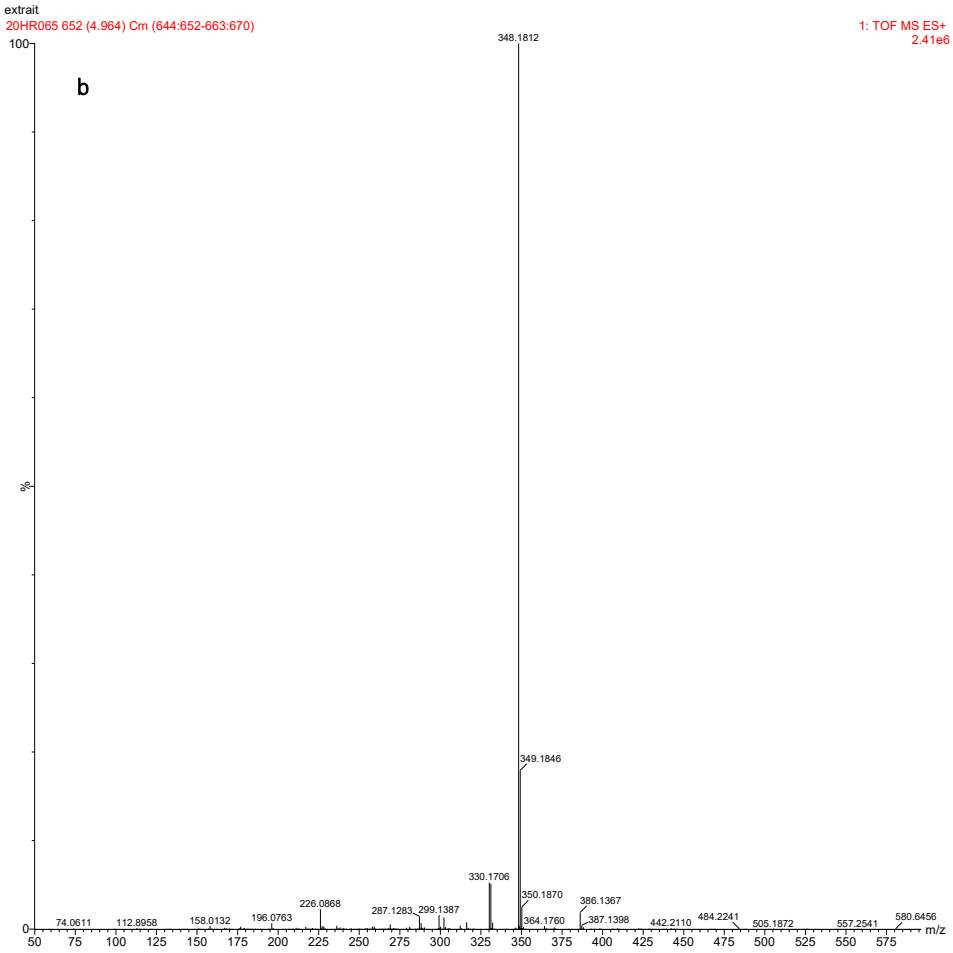

Extract, RT = 4.96 min

Mass	Calc. Mass	mDa	PPM	DBE	i-FIT	Norm	Conf(%)	Formula
348.1812	348.1811	0.1	0.3	7.5	1775.8	n/a	n/a	C19 H26 N O5

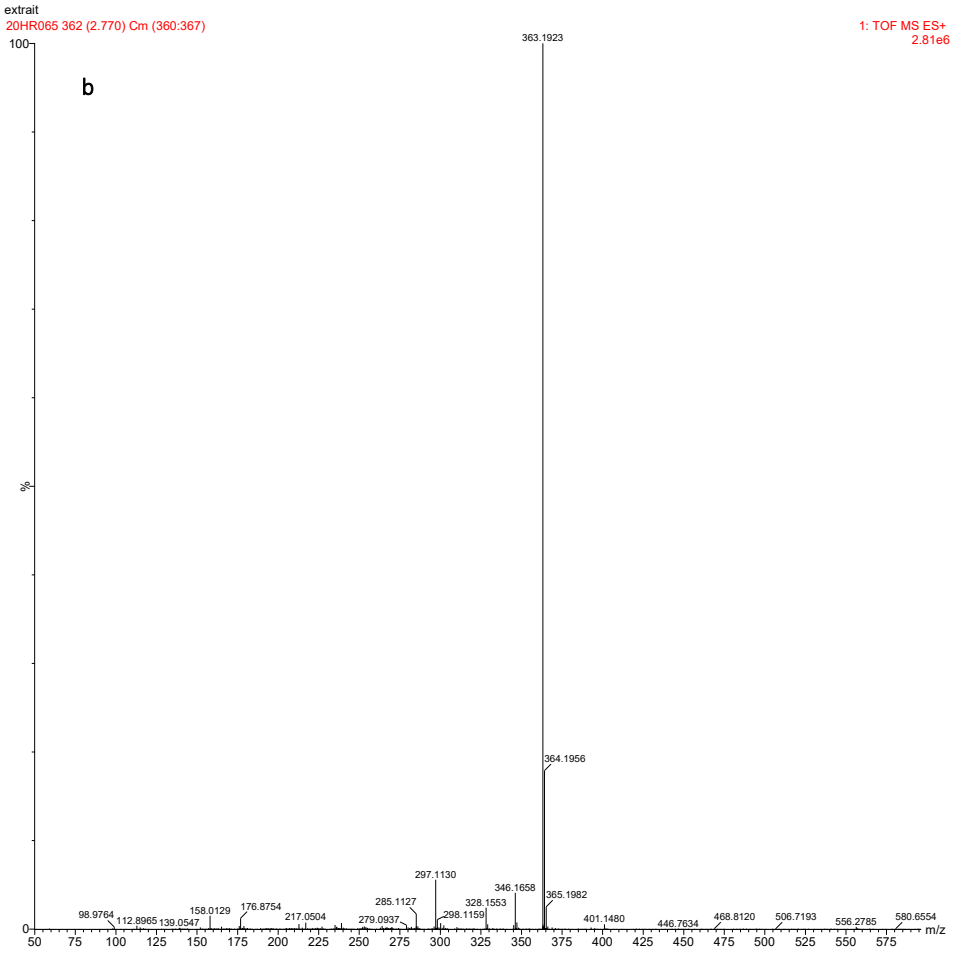

Extract, RT = 2.77 min

Mass	Calc. Mass	mDa	PPM	DBE	i-FIT	Norm	Conf(%)	Formula
363.1923	363.1920	0.3	0.8	7.5	1909.2	0.017	98.33	C19 H27 N2 O5
	363.1936	-1.3	-3.6	8.5	1913.3	4.090	1.67	C22 H28 O3 Na

UPLC-HRMS analysis of fractions

Fraction A1

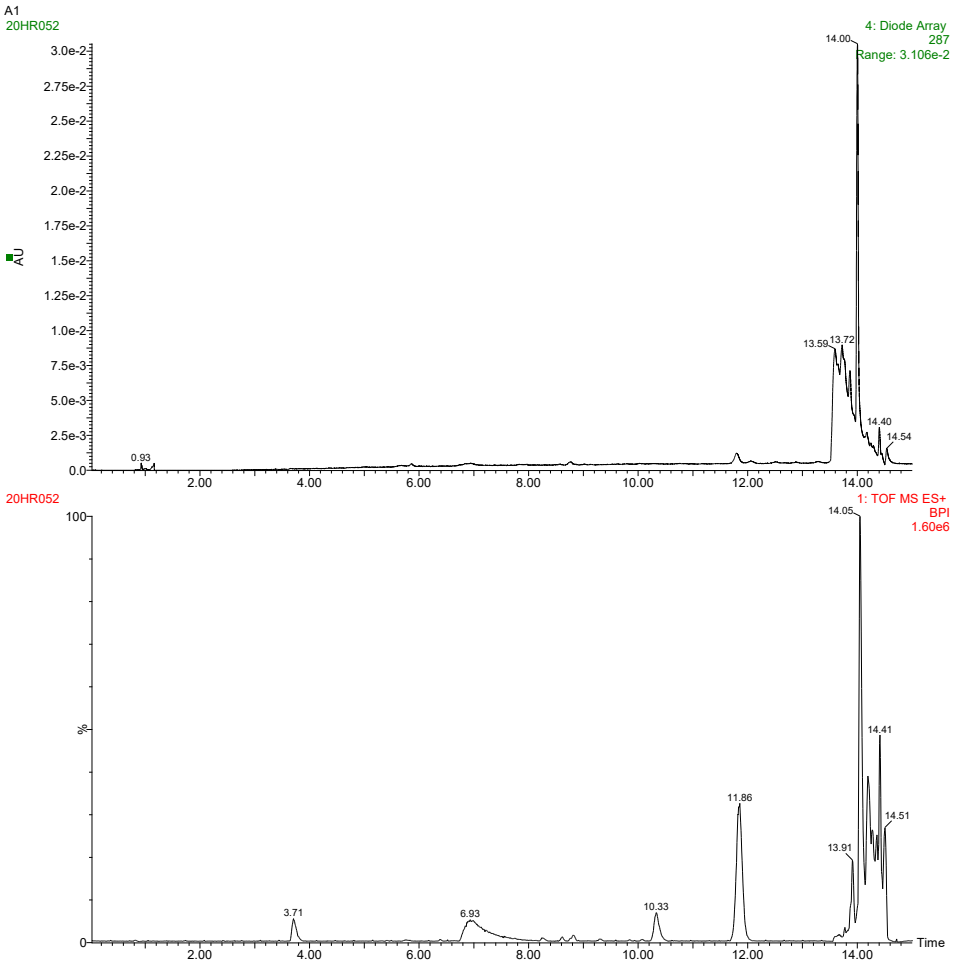

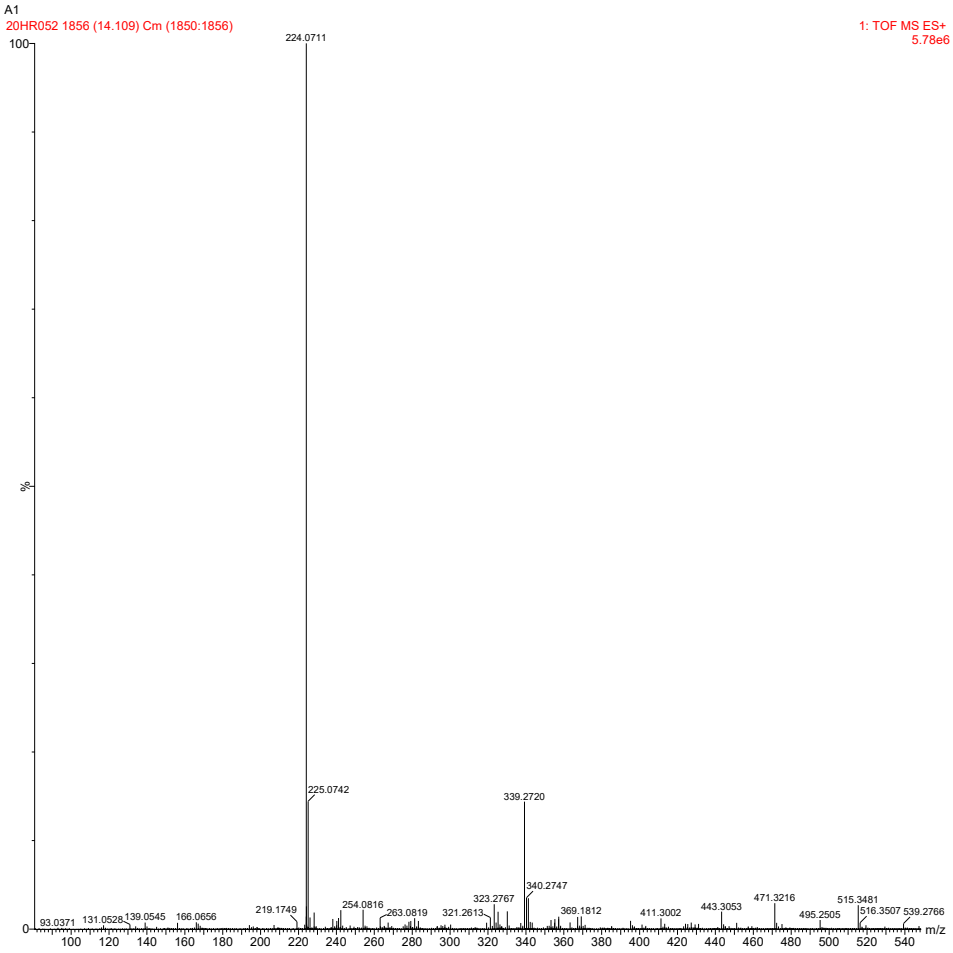

Fraction A1, RT = 14.11 min

Mass	Calc. Mass	mDa	PPM	DBE	i-FIT	Norm	Conf(%)	Formula
224.0711	224.0712	-0.1	-0.4	10.5	2054.8	n/a	n/a	C14 H10 N O2

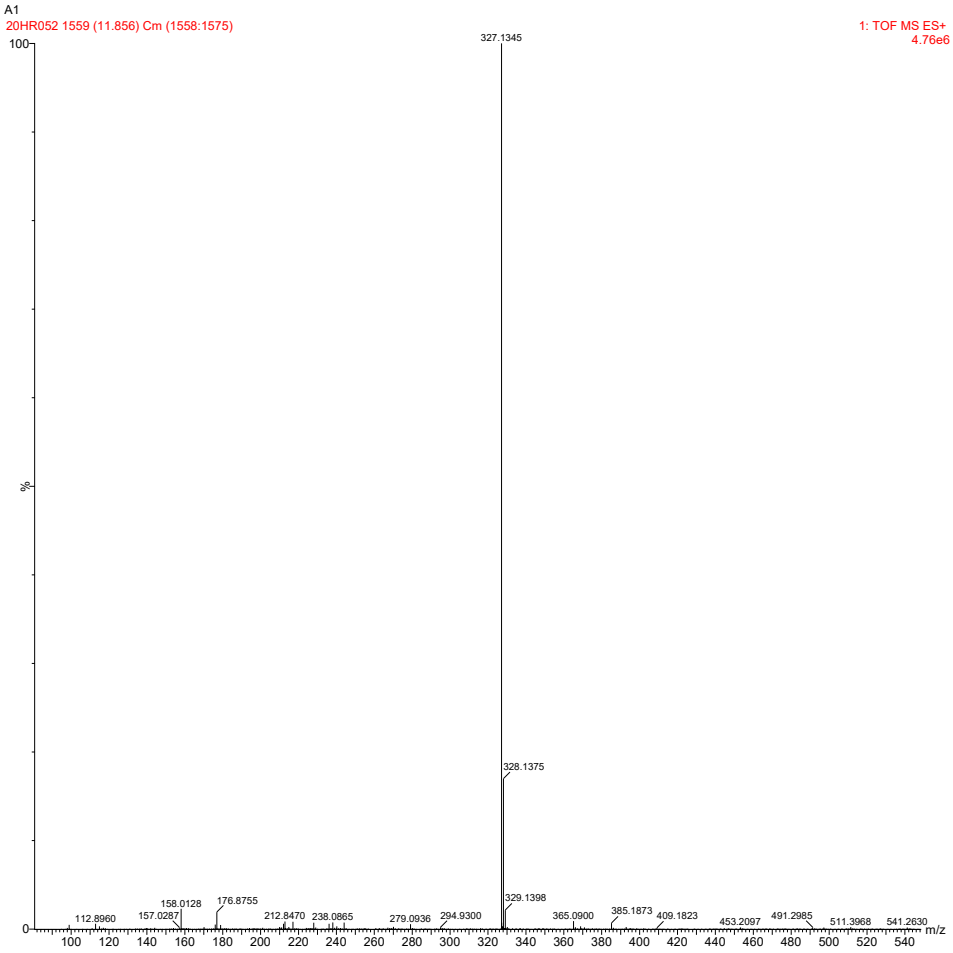

Fraction A1, RT = 11.86 min

Mass	Calc. Mass	mDa	PPM	DBE	i-FIT	Norm	Conf(%)	Formula
327.1345	327.1345	0.0	0.0	10.5	2097.4	0.002	99.81	C18 H19 N2 O4
	327.1361	-1.6	-4.9	11.5	2103.7	6.272	0.19	C21 H20 O2 Na

Fraction A1, RT = 10.34 min

Mass	Calc. Mass	mDa	PPM	DBE	i-FIT	Norm	Conf(%)	Formula
447.1925	447.1920	0.5	1.1	14.5	1799.0	0.013	98.74	C26 H27 N2 O5
	447.1936	-1.1	-2.5	15.5	1803.3	4.375	1.26	C29 H28 O3 Na

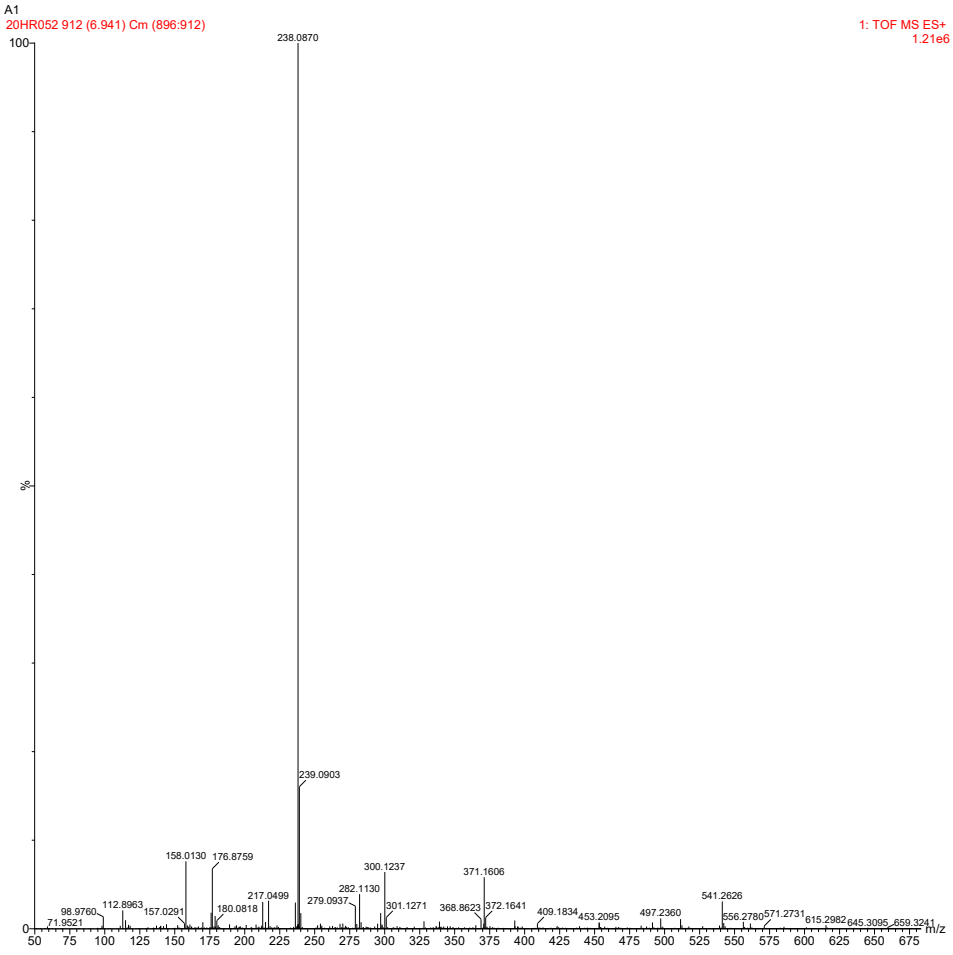

Fraction A1, RT = 6.94 min

Mass	Calc. Mass	mDa	PPM	DBE	i-FIT	Norm	Conf(%)	Formula
238.0870	238.0868	0.2	0.8	10.5	1567.5	n/a	n/a	C15 H12 N O2

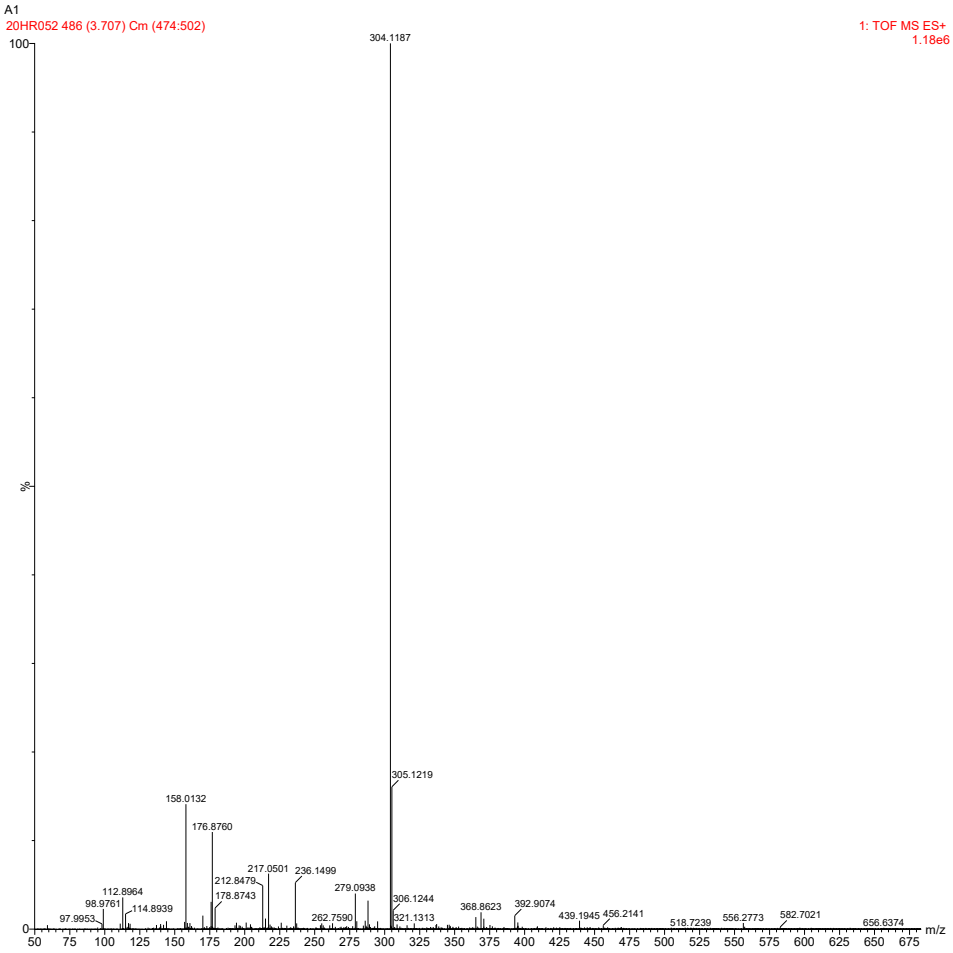

Fraction A1, RT = 3.71 min

Mass	Calc. Mass	mDa	PPM	DBE	i-FIT	Norm	Conf(%)	Formula
304.1187	304.1185	0.2	0.7	8.5	1698.8	n/a	n/a	C16 H18 N O5

Fraction A2

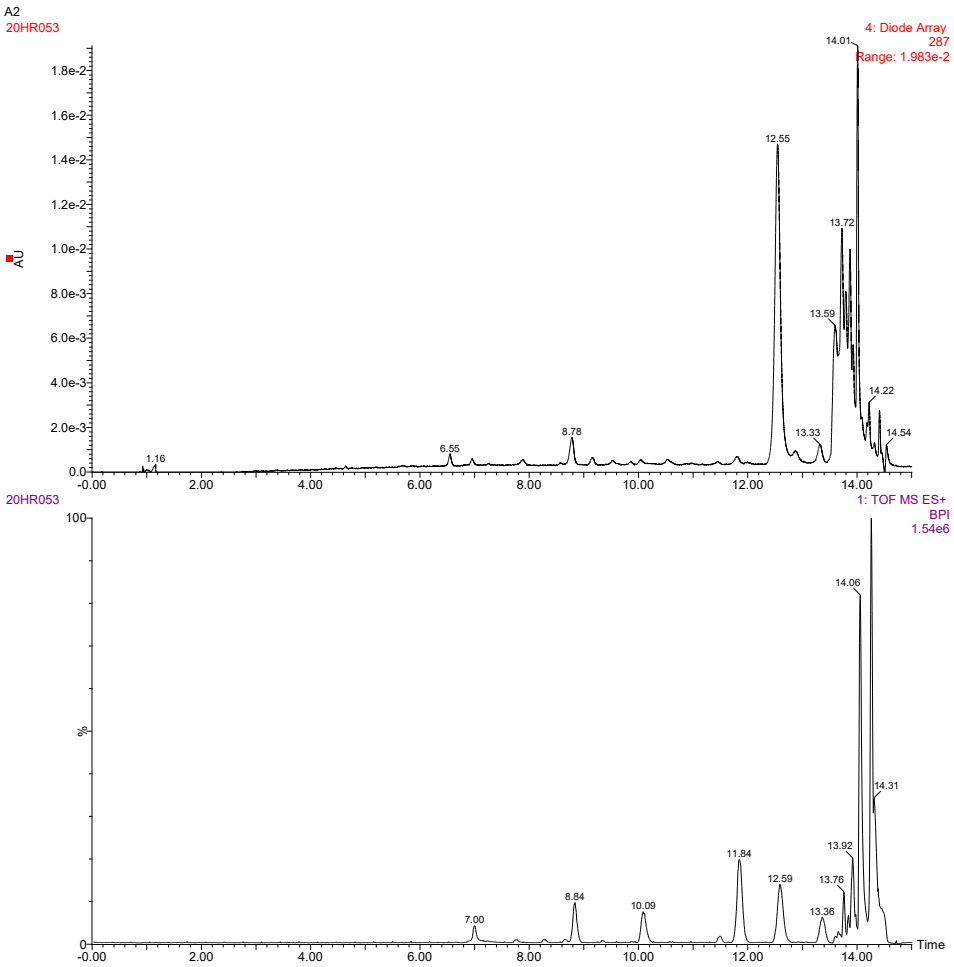
A2
20HR053
4: Diode Array
287
Range: 1.983e-2
AU
1.8e-2
1.6e-2
1.4e-2
1.2e-2
1.0e-2
8.0e-3
6.0e-3
4.0e-3
2.0e-3
0.0
1.16
6.55
8.78
12.55
13.33
13.59
13.72
14.01
14.22
14.54
-0.00
2.00
4.00
6.00
8.00
10.00
12.00
14.00
20HR053
1: TOF MS ES+
BPI
1.54e6
100
%
0
7.00
8.84
10.09
11.84
12.59
13.36
13.76
13.92
14.06
14.31
Time

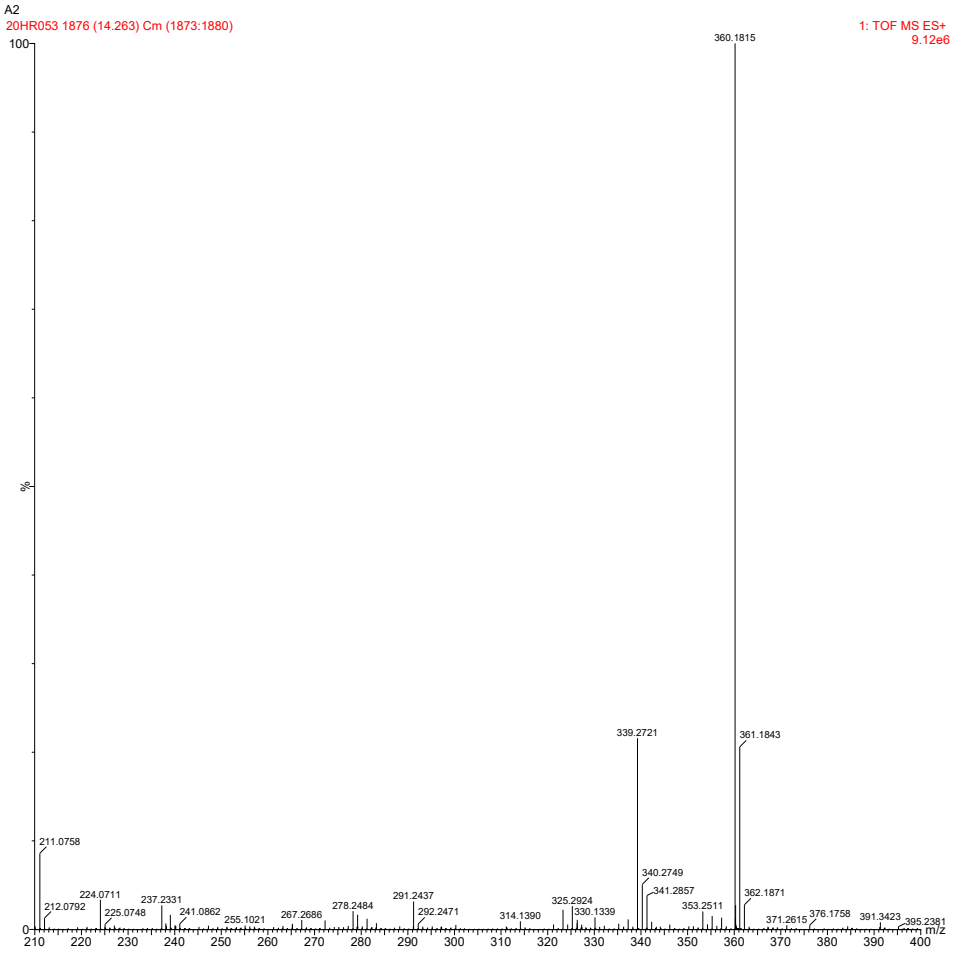

Fraction A2, RT = 14.26 min

Mass	Calc. Mass	mDa	PPM	DBE	i-FIT	Norm	Conf(%)	Formula
360.1815	360.1811	0.4	1.1	8.5	2245.7	n/a	n/a	C20 H26 N O5

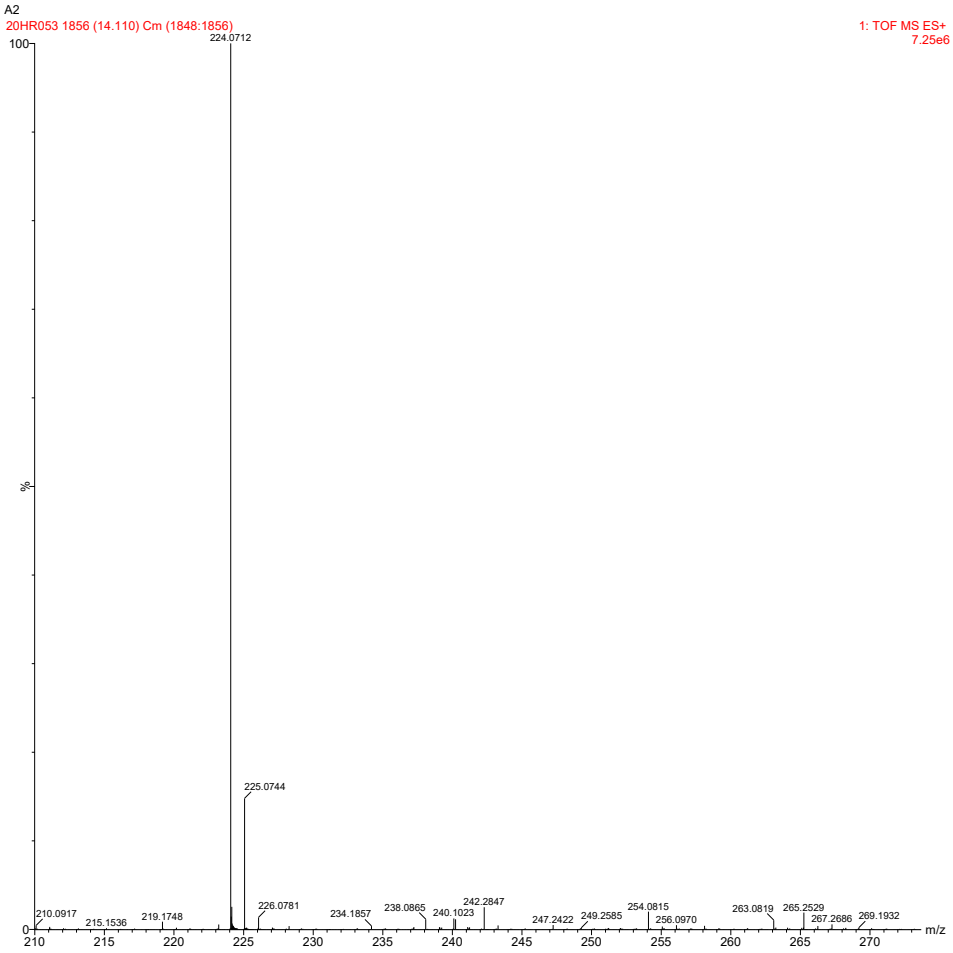

Fraction A2, RT = 14.11 min

Mass	Calc. Mass	mDa	PPM	DBE	i-FIT	Norm	Conf(%)	Formula
224.0712	224.0712	0.0	0.0	10.5	2165.7	n/a	n/a	C14 H10 N O2

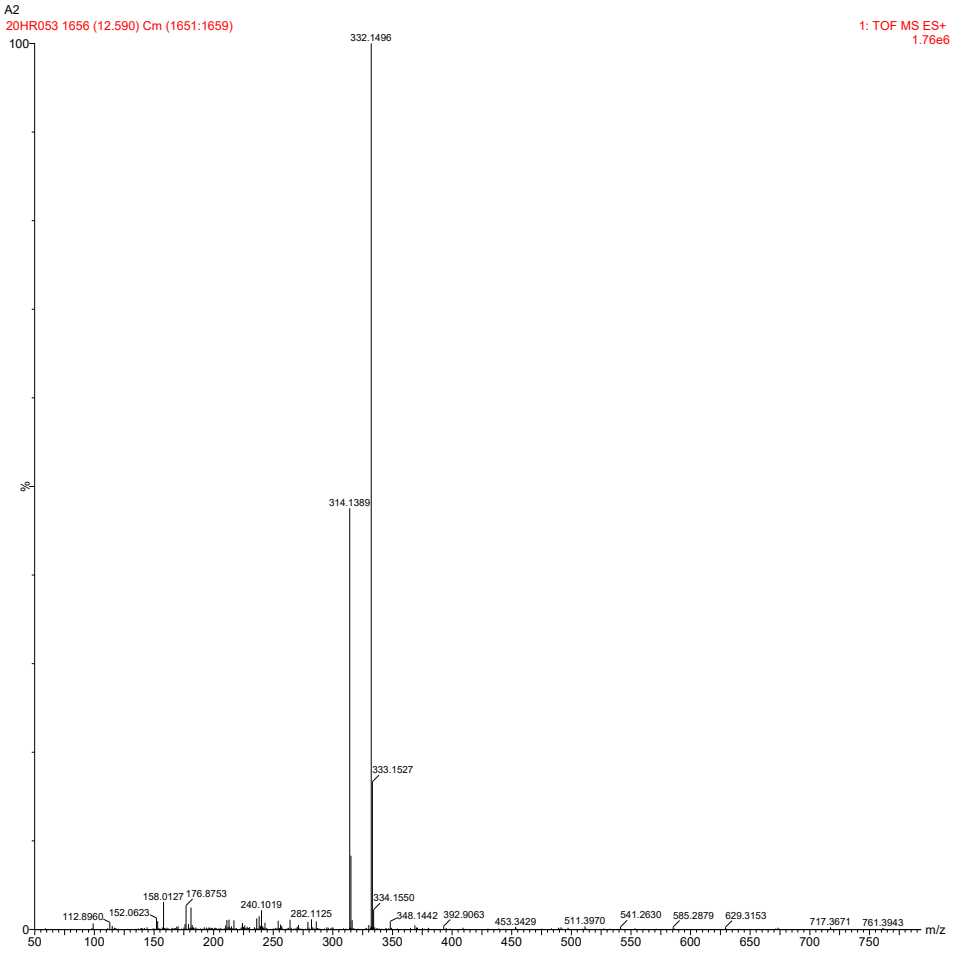

Fraction A2, RT = 12.59 min

Mass	Calc. Mass	mDa	PPM	DBE	i-FIT	Norm	Conf(%)	Formula
332.1496	332.1498	-0.2	-0.6	8.5	1708.1	n/a	n/a	C18 H22 N O5

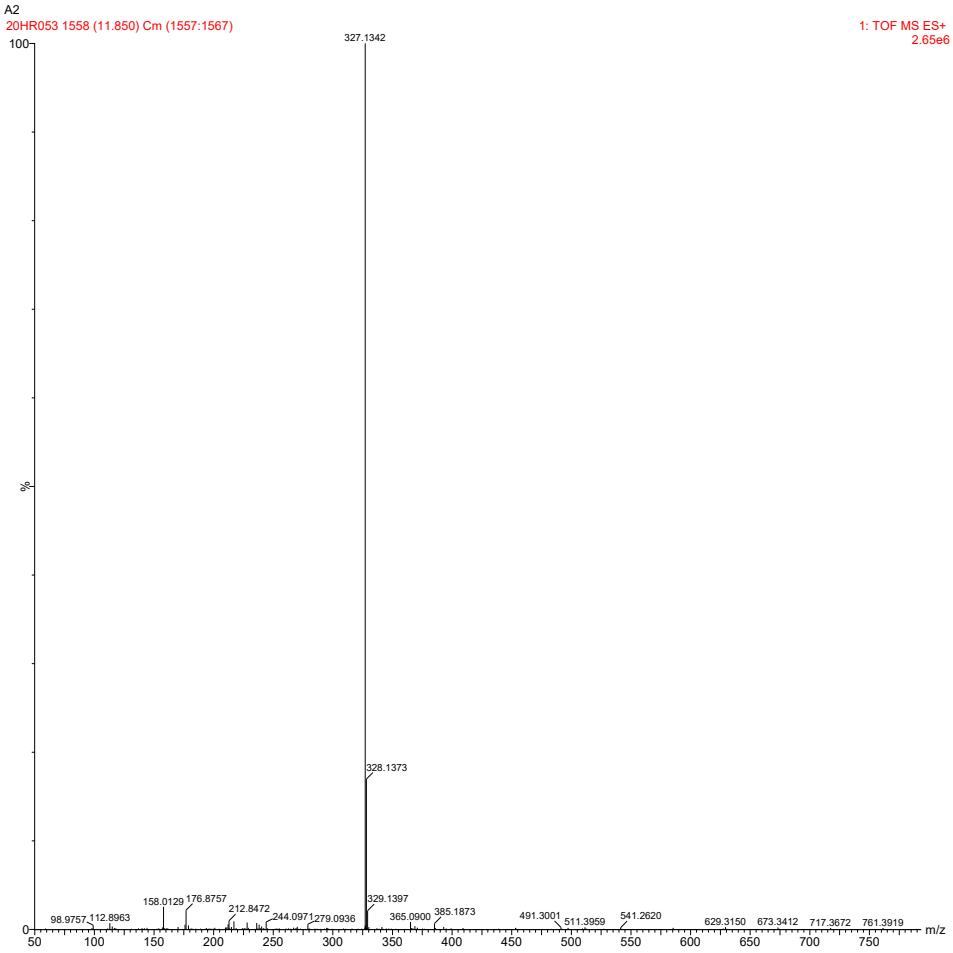

Fraction A2, RT = 11.85 min

Mass	Calc. Mass	mDa	PPM	DBE	i-FIT	Norm	Conf(%)	Formula
327.1342	327.1345	-0.3	-0.9	10.5	1896.4	n/a	n/a	C18 H19 N2 O4

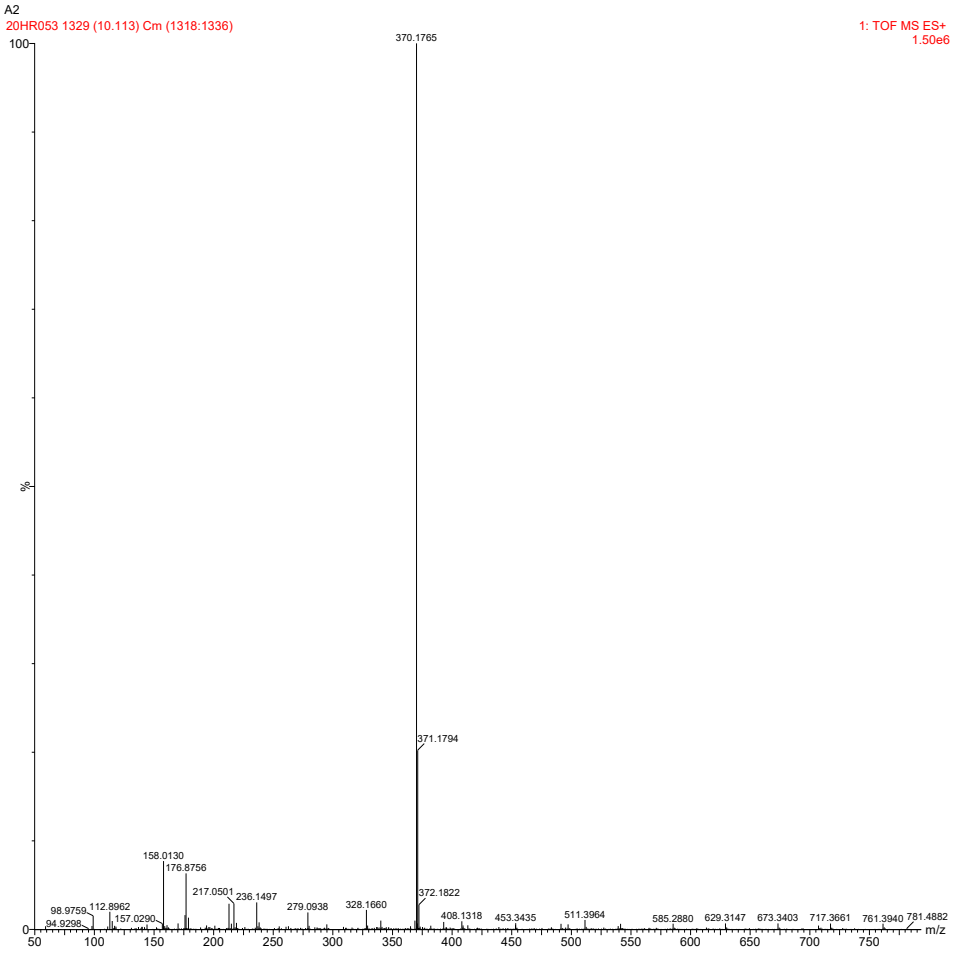

Fraction A2, RT = 13.29 min

Mass	Calc. Mass	mDa	PPM	DBE	i-FIT	Norm	Conf(%)	Formula
370.1765	370.1783	-1.8	-4.9	11.5	1812.6	n/a	n/a	C23 H25 N O2 Na

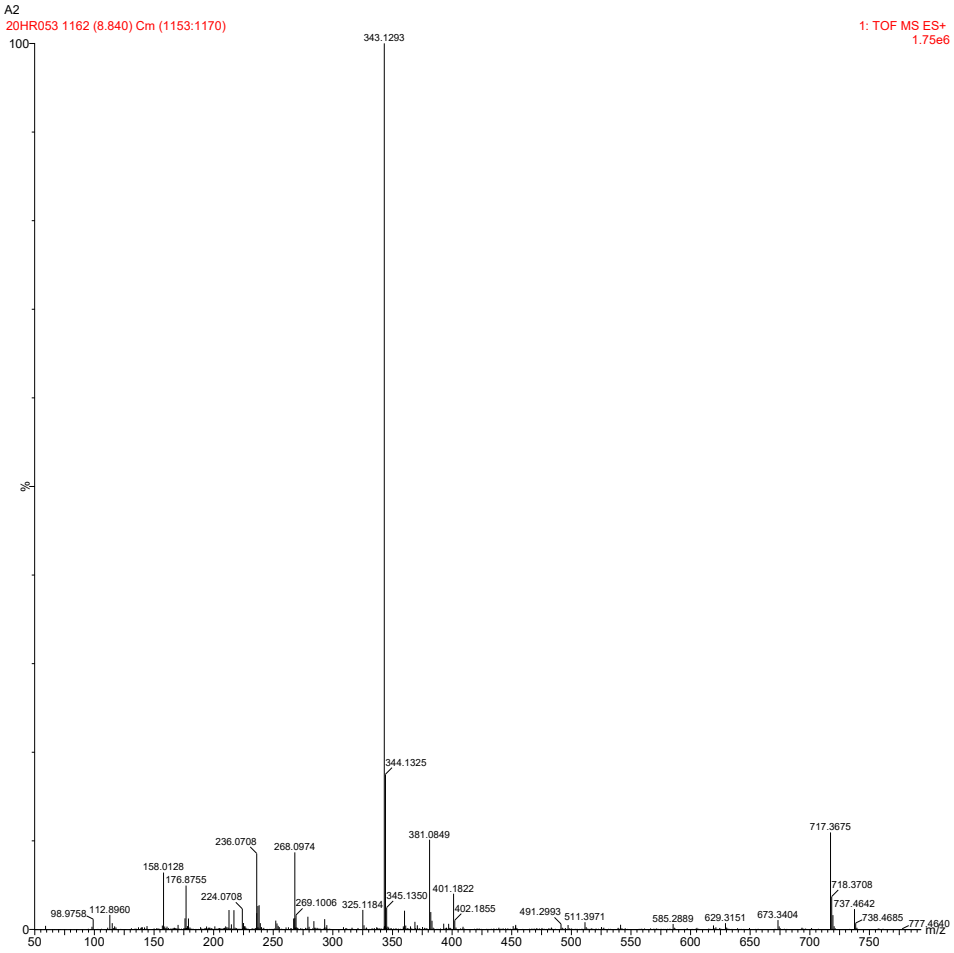

Fraction A2, RT=8.84 min

Elemental Composition Report, Single Mass Analysis

Tolerance = 5.0 PPM / DBE: min = -1.5, max = 50.0 / Element prediction: Off

Number of isotope peaks used for i-FIT = 3

Monoisotopic Mass, Even Electron Ions

Mass	Calc. Mass	mDa	PPM	DBE	i-FIT	Norm	Conf(%)	Formula
343.1293	343.1294	-0.1	-0.3	10.5	1822.6	0.002	99.77	C18 H19 N2 O5
	343.1310	-1.7	-5.0	11.5	1828.7	6.081	0.23	C21 H20 O3 Na

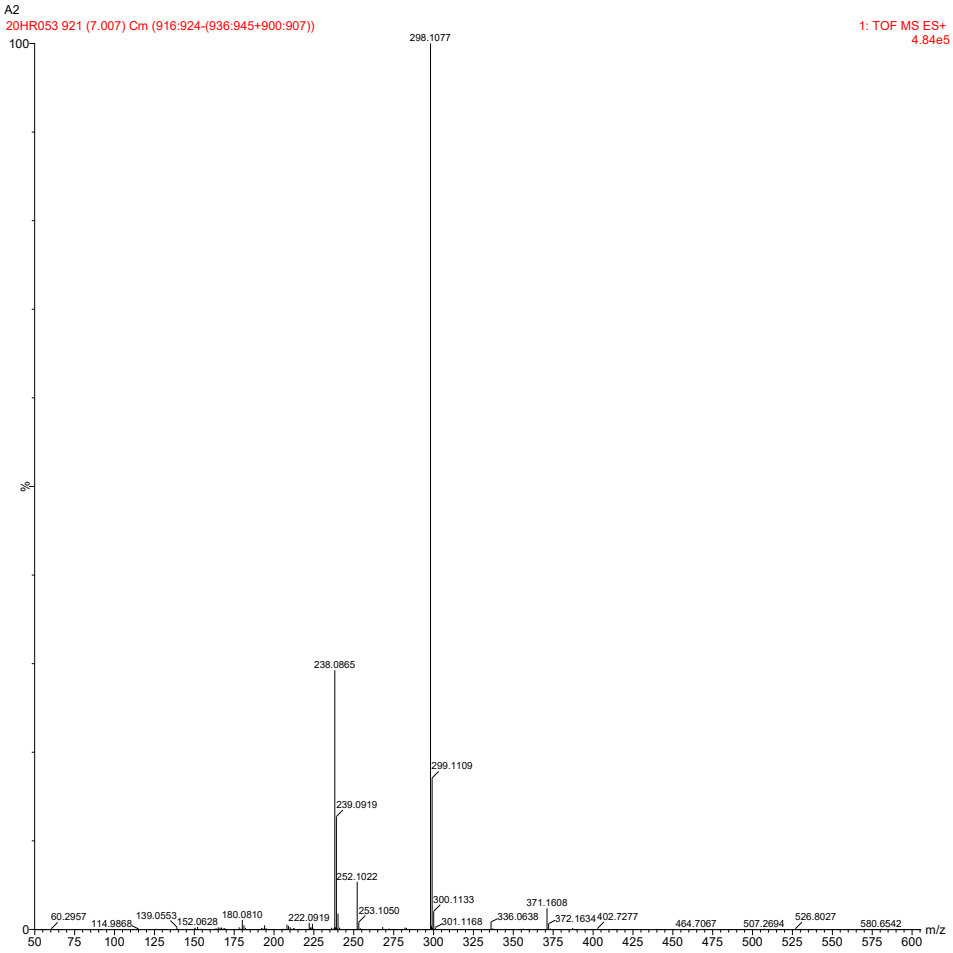

Mass	Calc. Mass	mDa	PPM	DBE	i-FIT	Norm	Conf(%)	Formula
298.1077	298.1079	-0.2	-0.7	10.5	1111.7	n/a	n/a	C17 H16 N O4

Fraction A3

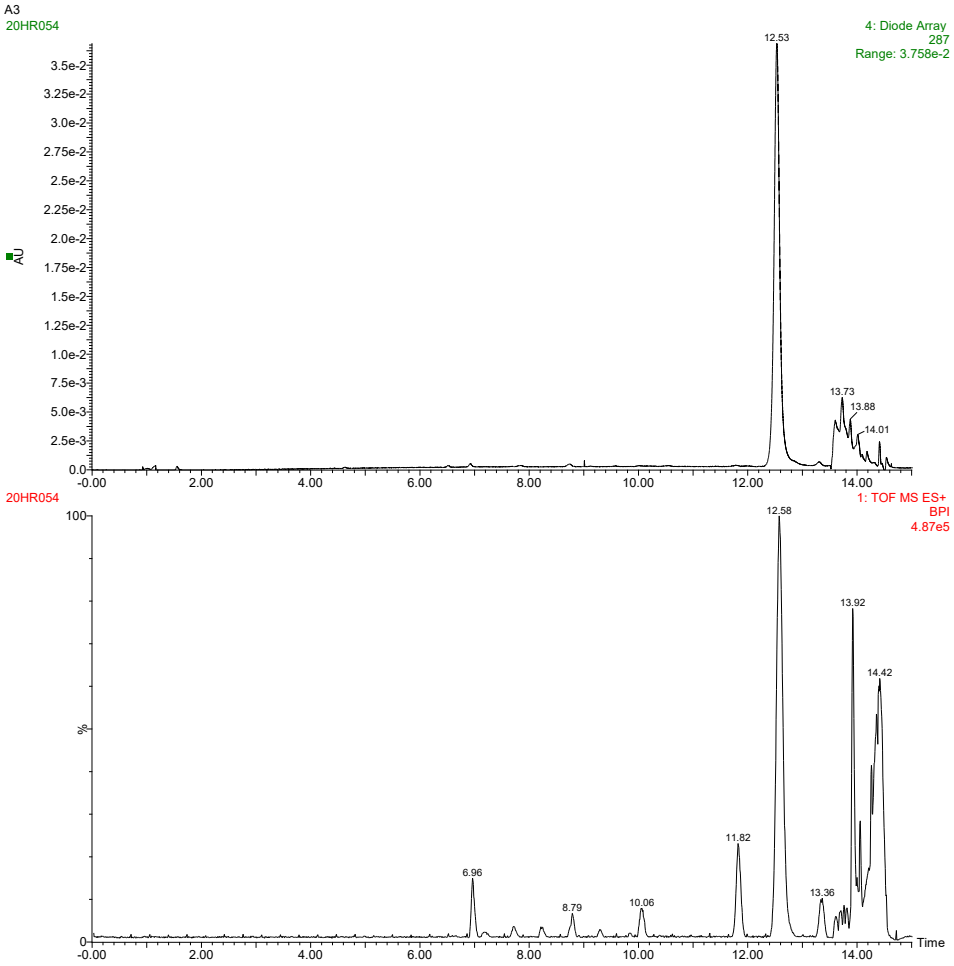
A3
20HR054
4: Diode Array
287
Range: 3.758e-2
AU
12.53
13.73
13.88
14.01
20HR054
1: TOF MS ES+
BPI
4.87e5
%
12.58
13.92
14.42
11.82
6.96
8.79
10.06
13.36
Time

Fraction A4

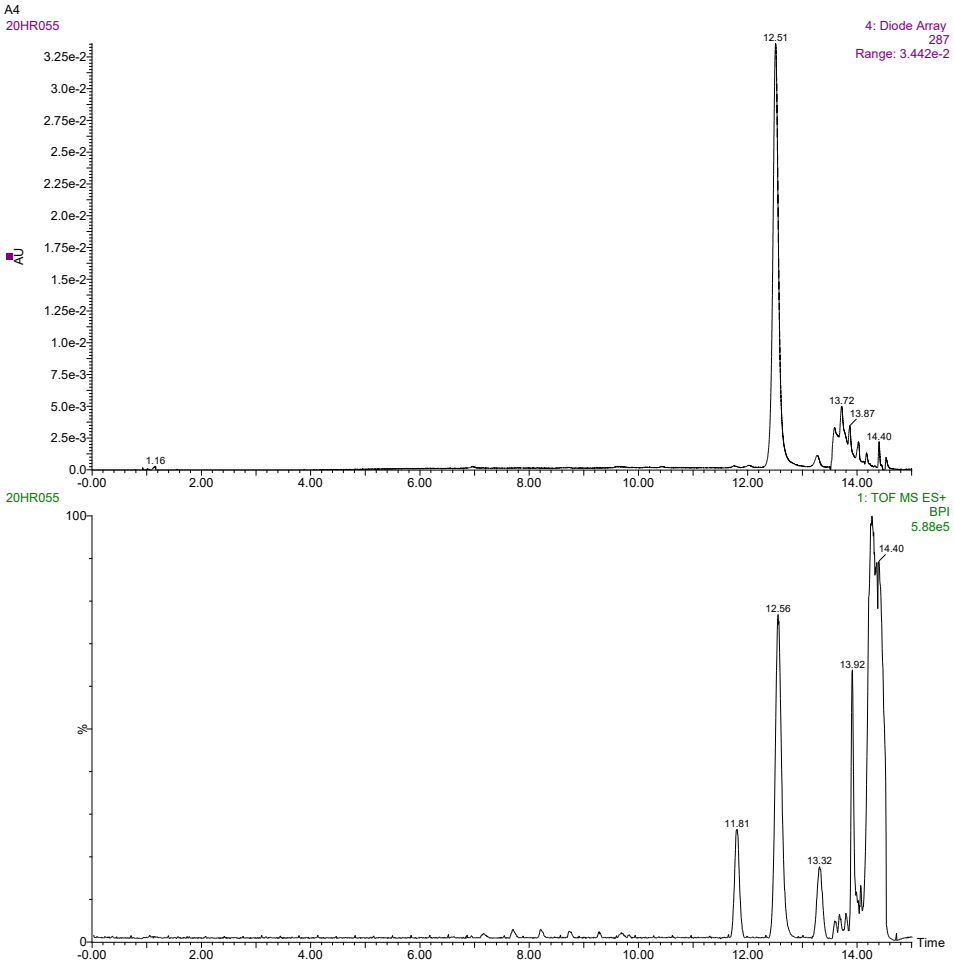
A4
20HR055
4: Diode Array
287
Range: 3.442e-2
12.51
13.72
13.87
14.40
1.16
AU
3.25e-2
3.0e-2
2.75e-2
2.5e-2
2.25e-2
2.0e-2
1.75e-2
1.5e-2
1.25e-2
1.0e-2
7.5e-3
5.0e-3
2.5e-3
0.0
-0.00
2.00
4.00
6.00
8.00
10.00
12.00
14.00
20HR055
1: TOF MS ES+
BPI
5.88e5
100
%
0
14.40
12.56
13.92
11.81
13.32
Time

Fraction A5

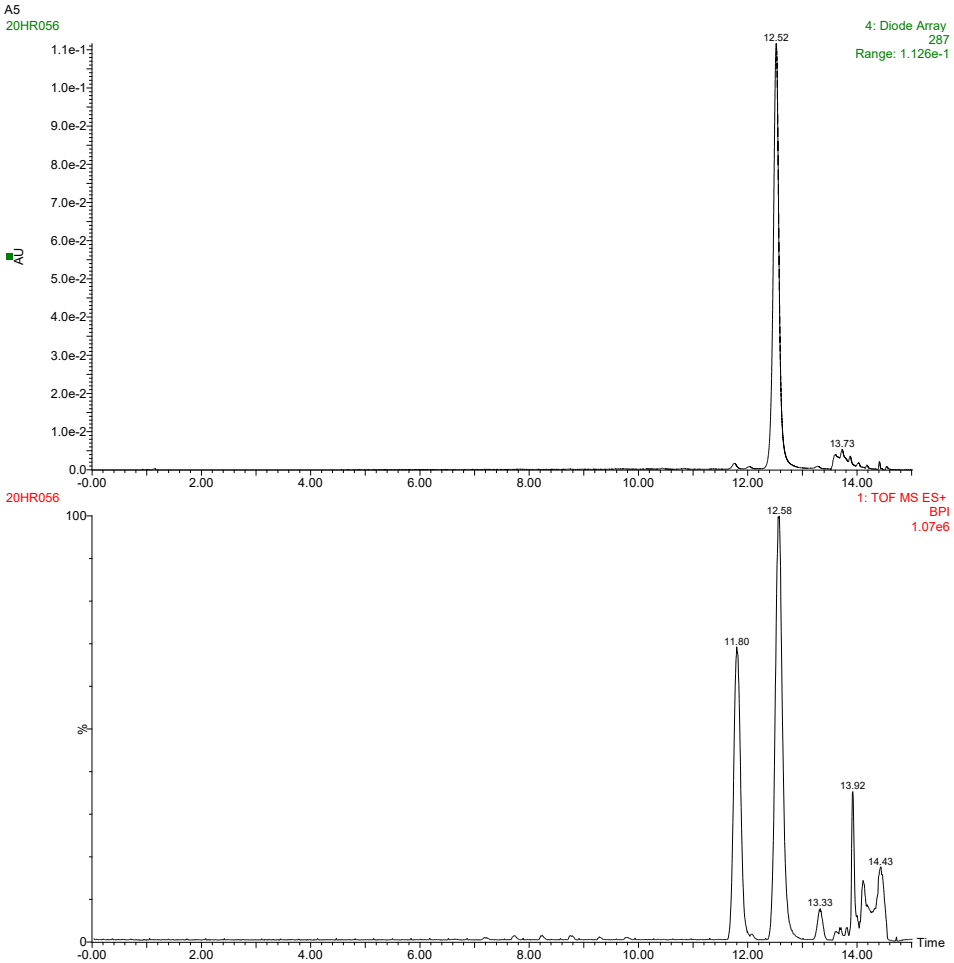
A5
20HR056
4: Diode Array
287
Range: 1.126e-1
12.52
13.73
AU
1.1e-1
1.0e-1
9.0e-2
8.0e-2
7.0e-2
6.0e-2
5.0e-2
4.0e-2
3.0e-2
2.0e-2
1.0e-2
0.0
-0.00
2.00
4.00
6.00
8.00
10.00
12.00
14.00
20HR056
1: TOF MS ES+
BPI
1.07e6
12.58
11.80
13.92
14.43
13.33
%
100
0
Time

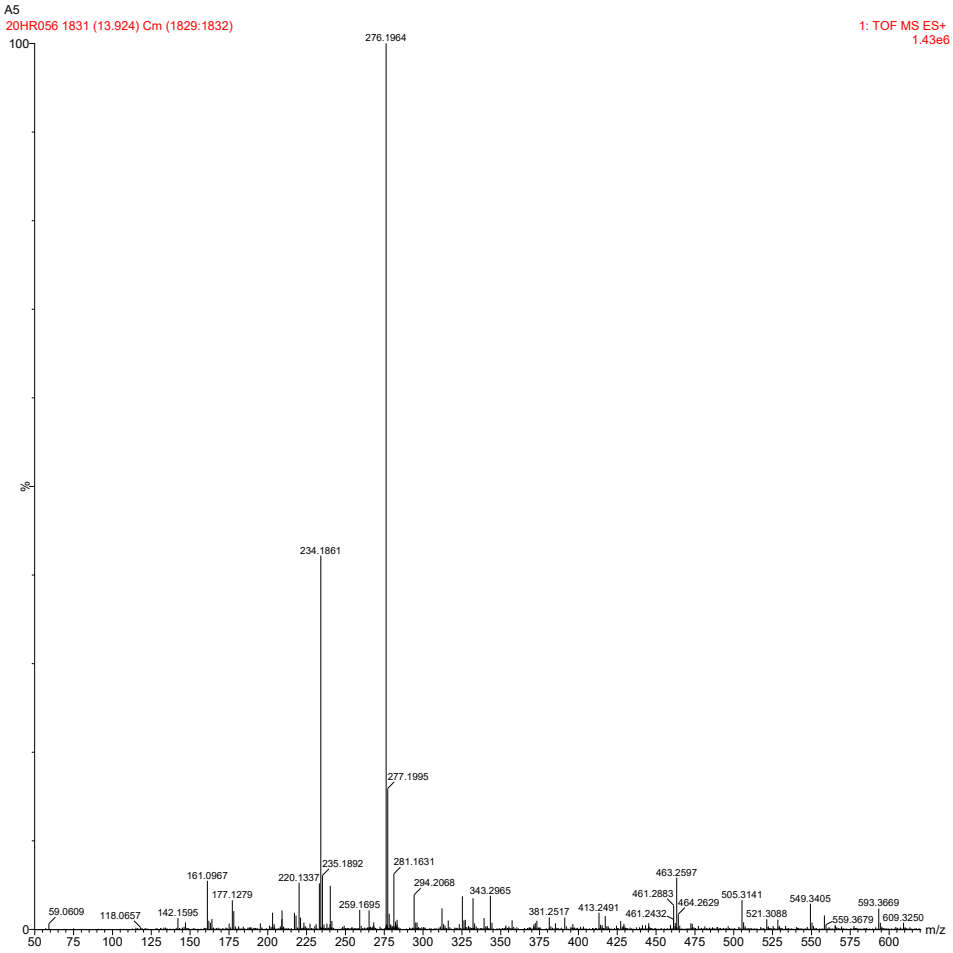

Fraction A5, RT = 13.92 min

Mass	Calc. Mass	mDa	PPM	DBE	i-FIT	Norm	Conf(%)	Formula
276.1964	276.1964	0.0	0.0	5.5	1613.1	n/a	n/a	C17 H26 N O2

Fraction A6

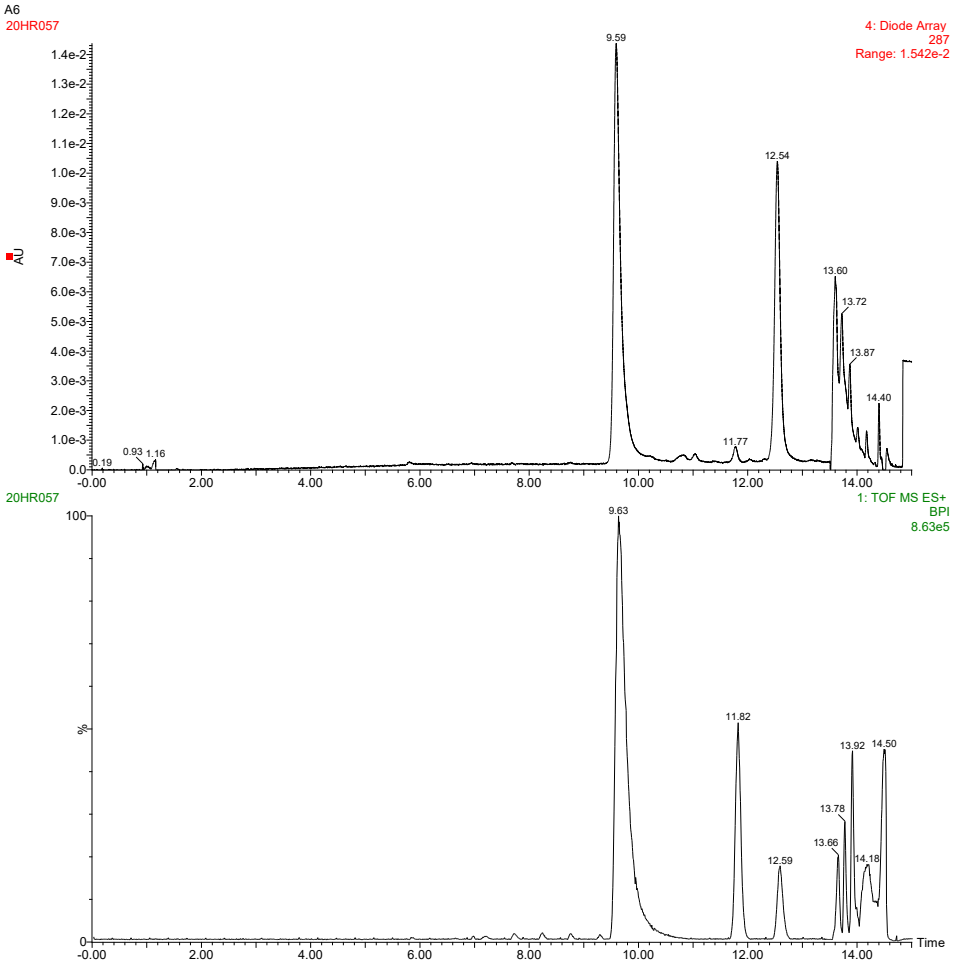
A6
20HR057
4: Diode Array
287
Range: 1.542e-2
AU
9.59
12.54
13.60
13.72
13.87
14.40
11.77
0.19
0.93
1.16
20HR057
1: TOF MS ES+
BPI
8.63e5
%
9.63
11.82
13.92
14.50
13.78
13.66
12.59
14.18
Time

Fraction A7

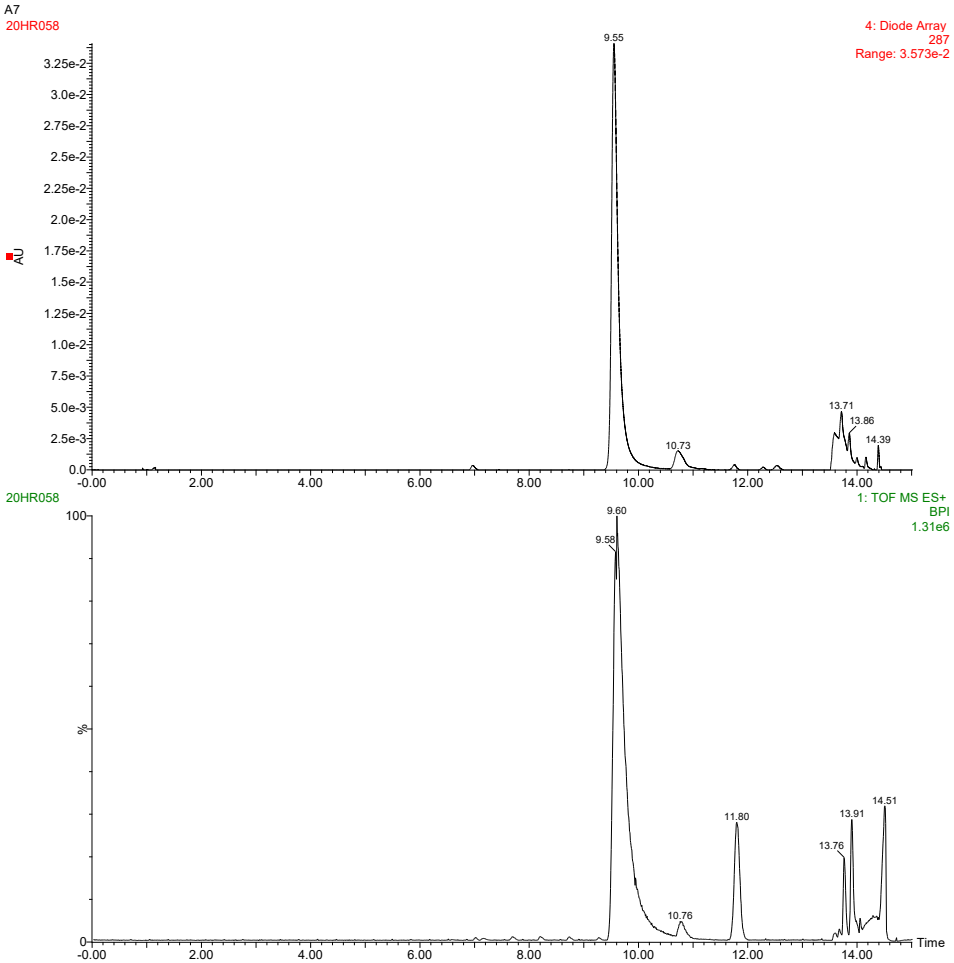
A7
20HR058
4: Diode Array
287
Range: 3.573e-2
AU
9.55
10.73
13.71
13.86
14.39
20HR058
1: TOF MS ES+
BPI
1.31e6
%
9.60
9.58
11.80
10.76
13.76
13.91
14.51
Time

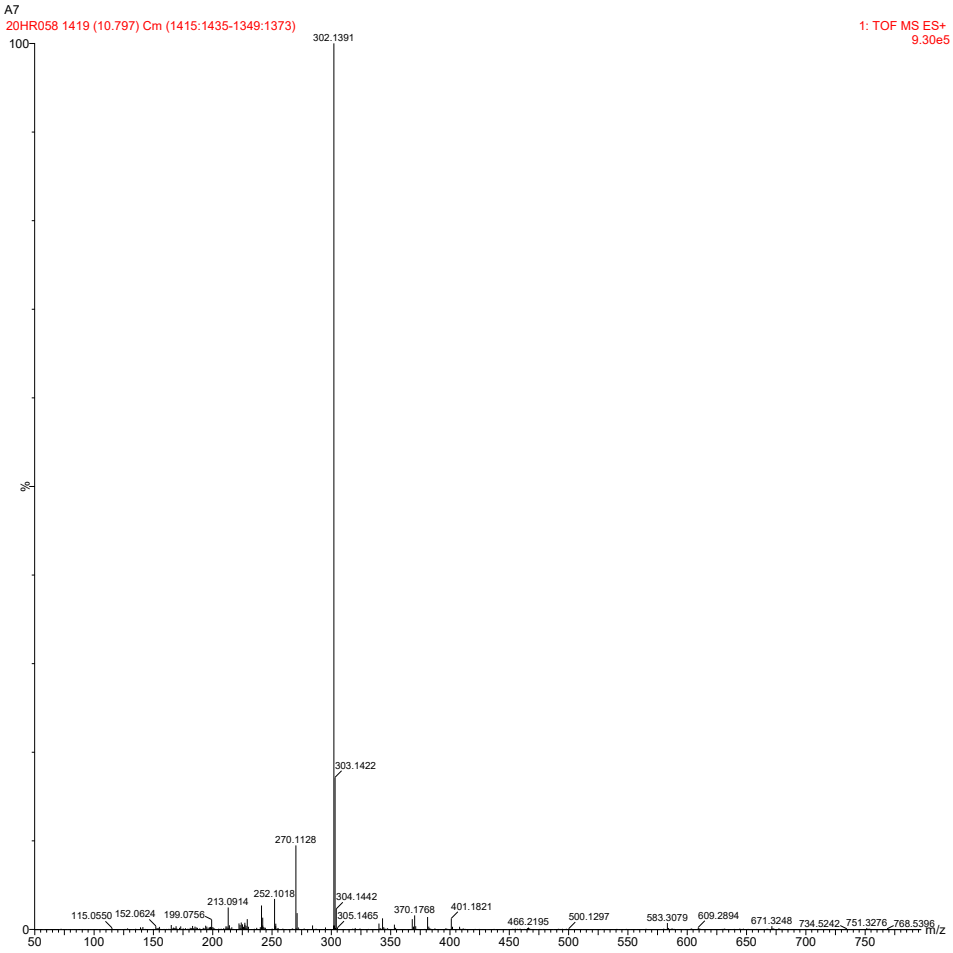

Fraction A7, RT = 10.98 min

Elemental Composition Report

Single Mass Analysis

Tolerance = 5.0 PPM / DBE: min = -1.5, max = 50.0 / Element prediction: Off

Number of isotope peaks used for i-FIT = 3

Monoisotopic Mass, Even Electron Ions

Mass	Calc. Mass	mDa	PPM	DBE	i-FIT	Norm	Conf(%)	Formula
302.1391	302.1392	-0.1	-0.3	8.5	1455.6	n/a	n/a	C17 H20 N O4

Fraction A8

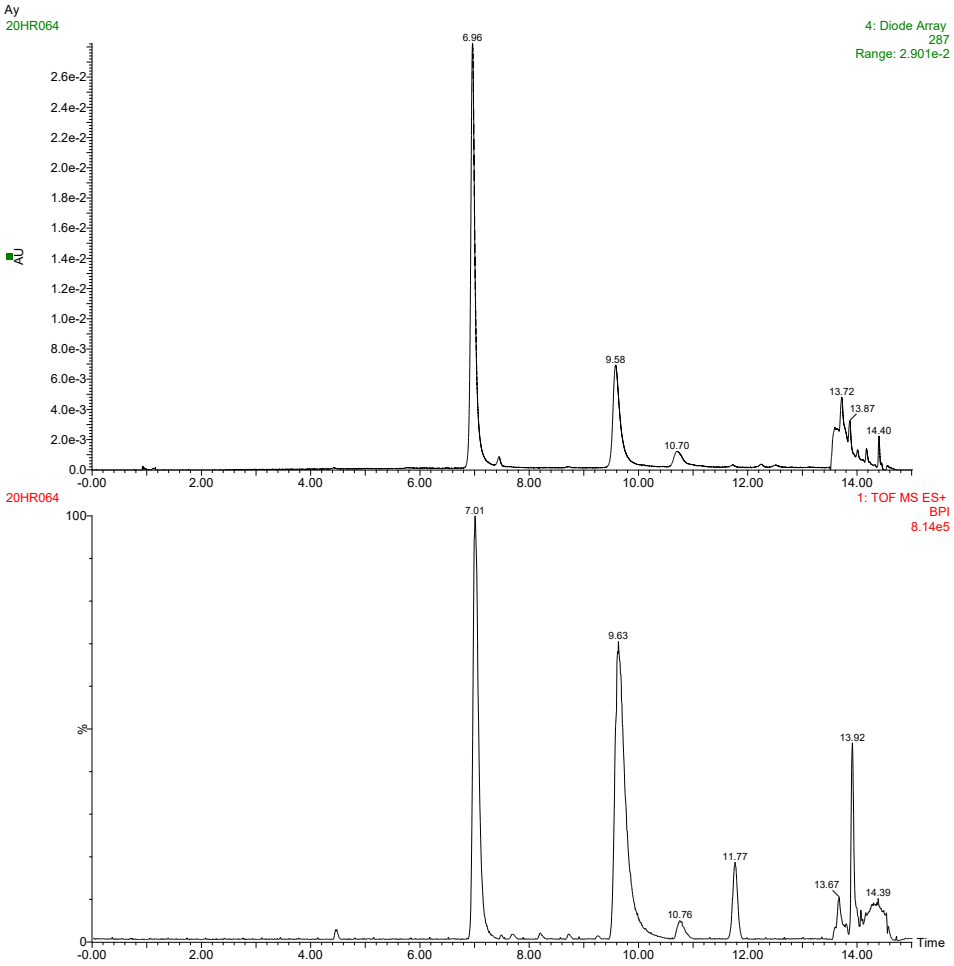
Ay
20HR064
4: Diode Array
287
Range: 2.901e-2
AU
6.96
9.58
10.70
13.72
13.87
14.40
20HR064
1: TOF MS ES+
BPI
8.14e5
%
7.01
9.63
10.76
11.77
13.67
13.92
14.39
Time

Fraction A9

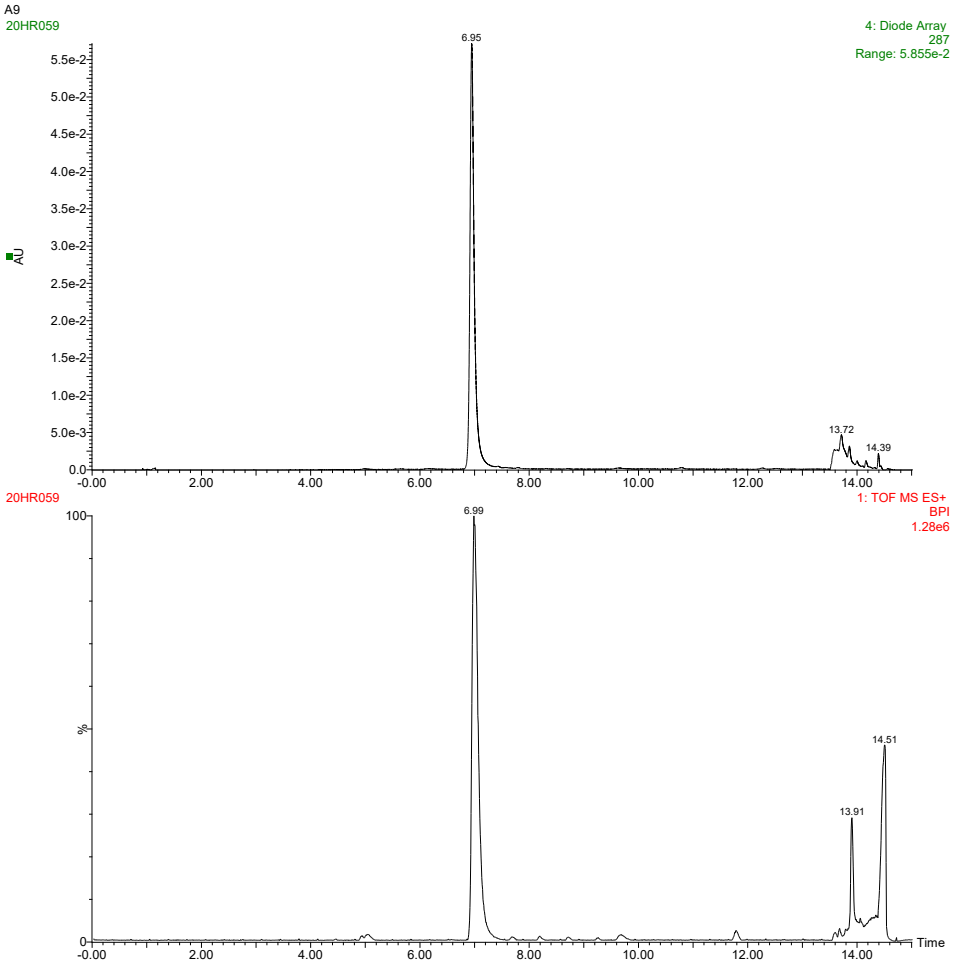
A9
20HR059
4: Diode Array
287
Range: 5.855e-2
6.95
13.72
14.39
AU
5.5e-2
5.0e-2
4.5e-2
4.0e-2
3.5e-2
3.0e-2
2.5e-2
2.0e-2
1.5e-2
1.0e-2
5.0e-3
0.0
-0.00
2.00
4.00
6.00
8.00
10.00
12.00
14.00
20HR059
1: TOF MS ES+
BPI
1.28e6
6.99
14.51
13.91
%
100
0
Time

Fraction A10

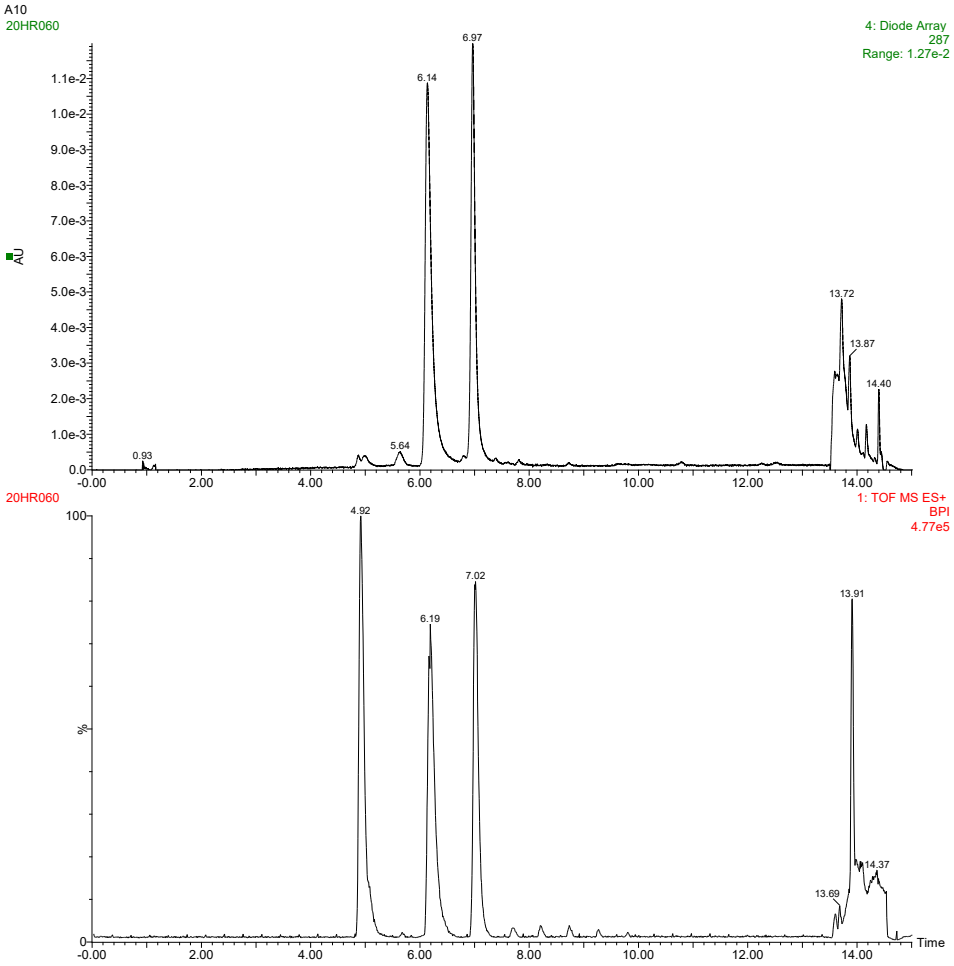

Fraction A11

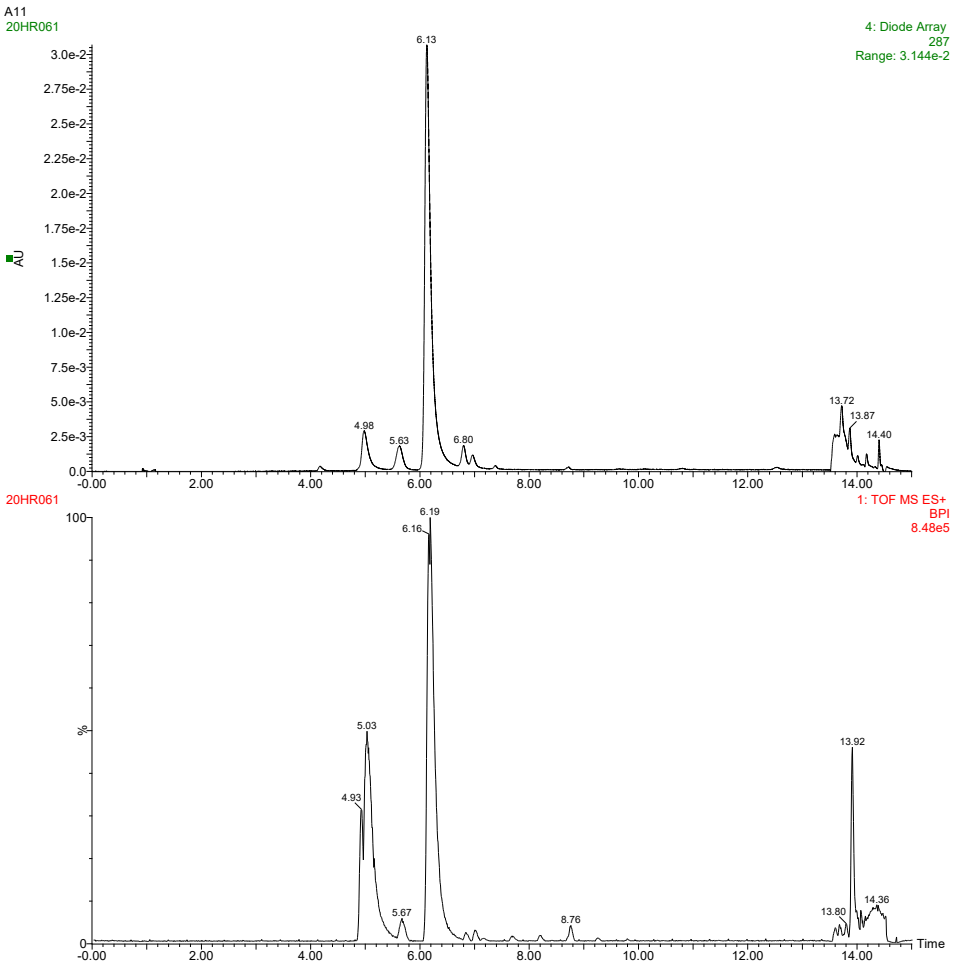

Fraction A12

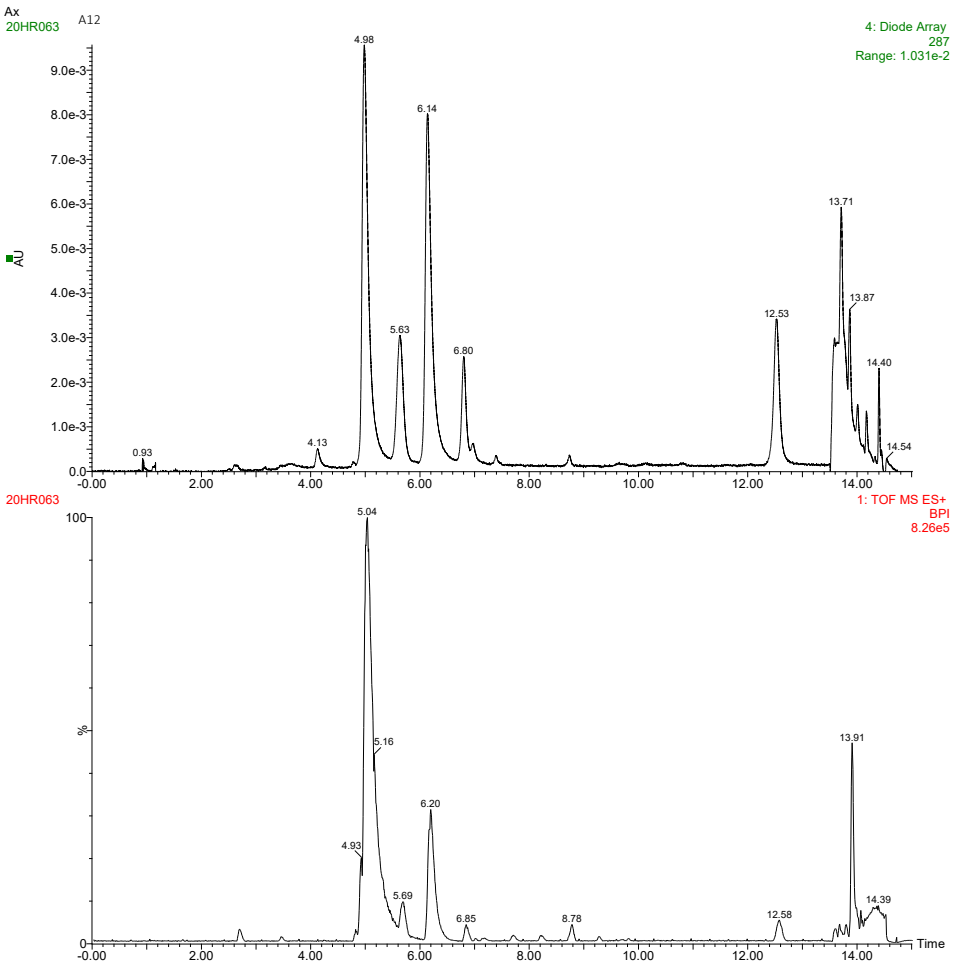

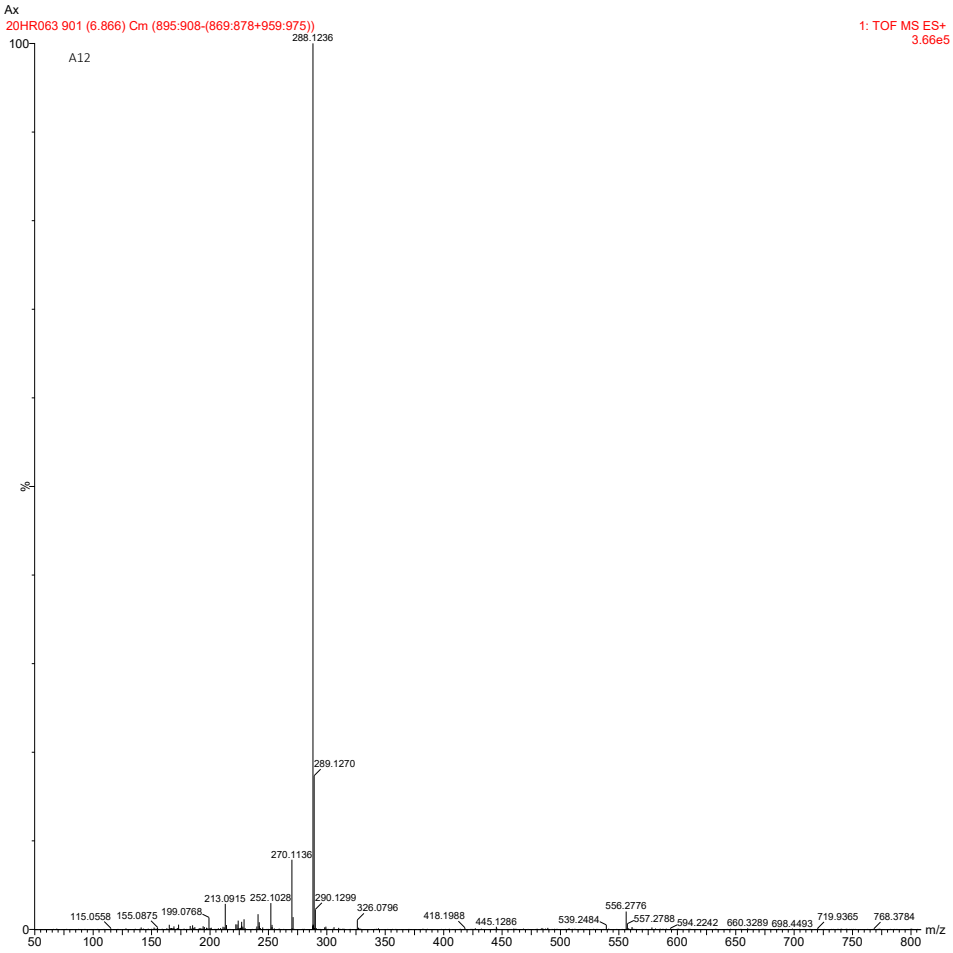

Fraction A12, RT = 6.87 min

Maximum:		5.0	5.0	50.0				
Mass	Calc. Mass	mDa	PPM	DBE	i-FIT	Norm	Conf(%)	Formula
288.1236	288.1236	0.0	0.0	8.5	987.5	n/a	n/a	C16 H18 N O4

Fraction A13

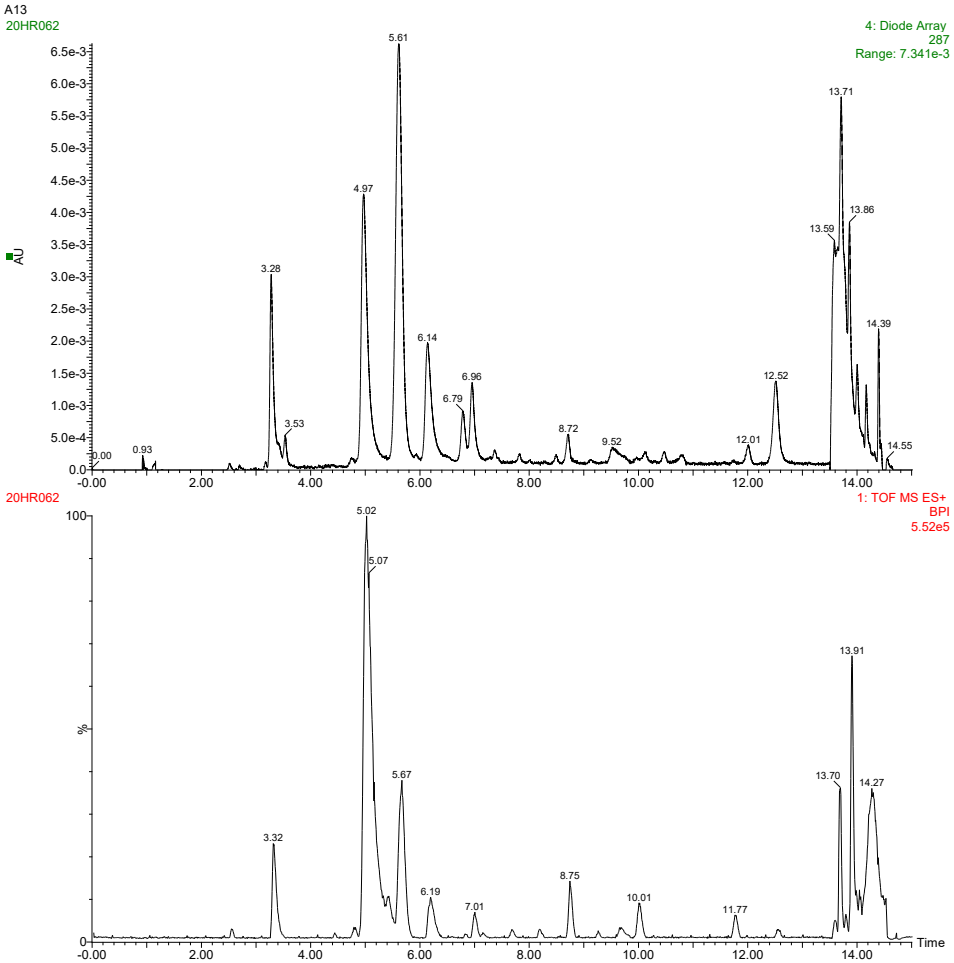

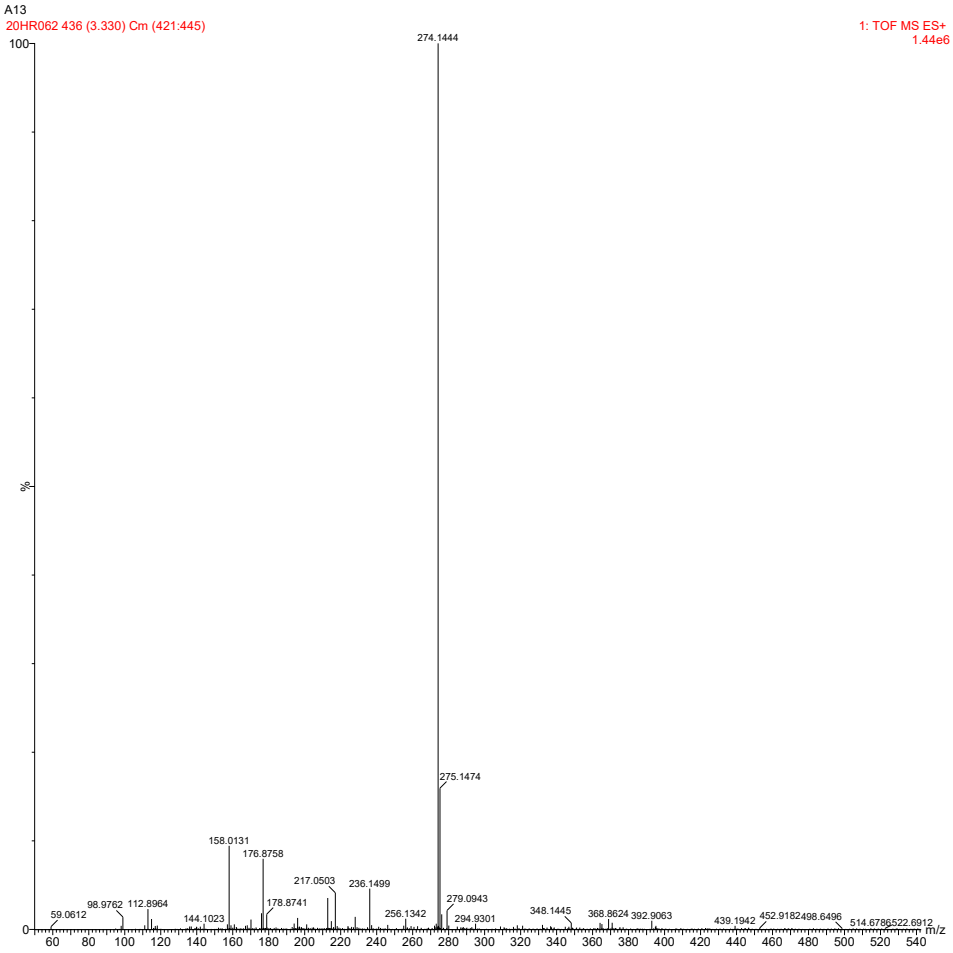

Fraction A13, RT = 3.30 min

Mass	Calc. Mass	mDa	PPM	DBE	i-FIT	Norm	Conf(%)	Formula
274.1444	274.1443	0.1	0.4	7.5	1706.2	n/a	n/a	C16 H20 N O3